CHAPTER 6

Classic Sinus Surgery for Inflammatory Diseases, Tumors, and Tumor-Like Conditions

Peter M. Som, William Lawson, and Margaret S. Brandwein

GENERAL CONSIDERATIONS REGARDING IMAGING

For the best interpretation of a postoperative imaging study, the radiologist should be aware of the specific operation that was performed, when it occurred, and what disease prompted surgery. Unfortunately, this information is often not available at the time of interpreting the imaging study. However, in order to minimize errors in interpretation, the radiologist should be familiar with the various surgical procedures so as to know which bone(s) may have been removed, what soft-tissue defects may have been created, and whether or not soft tissue and/or foreign material was placed to repair a surgical defect. This knowledge might prevent the misdiagnosis of a surgical defect as a site of bone erosion, or a muscle–fascia graft as a tumor recurrence.

The interval between the surgery and the time of imaging helps the radiologist determine the type of soft-tissue reaction to expect. For recent surgery, the primary healing reaction is active inflammation, edema, and possible hemorrhage. However, if the surgery was performed months to years ago, the primary expected healing reaction is mature granulation tissue, or vascularized scar, with varying degrees of fibrosis. In some patients, reactive bony sclerosis may occur following procedures that denude mucosa. Such a reaction requires time to produce bone thickening, which may reduce the sinus cavity size. Although this is a reactive process to the surgery that mimics the sclerosis associated with chronic inflammation, there is no evidence of active disease or pain in the majority of these patients. In some patients, recurrent sinusitis can coexist with the reactive postoperative changes. In these cases, the radiologist cannot determine whether the bone changes are attributable to the active chronic inflammation, the postoperative reaction, or both.

Knowledge of the disease process that initially prompted the surgery allows the radiologist to anticipate the types of imaging changes found. Thus, if the initial disease was chronic infection, recurrent sinus mucosal thickening, reactive bone sclerosis and thickening, and possible nasal polyposis are expected. If the initial disease was a granulomatous process, one may expect sinus mucosal thickening, nasal mucosal changes, septal erosions, and bone erosions intermixed with areas of reactive bone. If the initial disease was a tumor, the concern will be to characterize any nodular or localized soft-tissue disease, differentiate recurrent tumor from infection, and observe the presence of progressive bone erosion or soft-tissue extension to areas not normally involved by the surgery.

The best and most efficacious way to interpret a postoperative imaging study, especially of a patient with a malignancy, is to compare it with a prior examination. Initially, this is best accomplished by comparing a followup study to a baseline postoperative computed tomography (CT), magnetic resonance (MR) imaging, or positron emission tomography (PET)/CT examination. This baseline study provides an anatomic reference point for the new postoperative appearance of the patient to which all future examinations can be compared. If this baseline study is obtained too close to the time of surgery, the imaging findings are dominated by changes of hemorrhage, edema, and inflammation. This may give a false impression of what the eventual stable postoperative appearance will be. However, if one waits too long after surgery, recurrent disease may be present. The best compromise is a waiting period of 4 to 6 weeks after surgery. This interval allows most of the hemorrhage and edema to resolve, whereas few if any tumors (or chronic inflammatory diseases) will recur within this period.[1,2] Although the baseline study is less important in patients with inflammatory disease, it provides a reference standard against which future imaging studies can be compared.

On subsequent followup imaging studies on cancer patients, any progressive soft-tissue resolution can be interpreted as a further reduction of postoperative edema and inflammation. However, the appearance of any new soft-tissue changes, or sites of bone erosion, must be considered recurrent disease until proven otherwise. Patients who have been operated on for inflammatory disease usually do not need periodic followup scans and are only imaged if symptoms reappear. By comparison, those patients who have been operated on for tumors should have scheduled periodic followup scans if early tumor recurrences are to be diagnosed. The time interval between these examinations usually is 4 months for the first 2 postoperative years, 6 months for the next 2 years, and then yearly (see Chapter 44).[1,2]

CT and MR imaging are the examinations of choice for monitoring the postoperative course of patients. CT allows the detailed evaluation of bone and a fairly accurate assessment of the soft tissues. The use of contrast is desirable in a patient who had a tumor as it provides some distinction between inflammatory tissue, tumor, and scar.

MR imaging offers the best possibility of differentiating recurrent tumors from sites of active infection. However, even when contrast is used, the distinction between vascularized scar and tumor may be impossible to make and early bone erosions may go undetected.[3] However, perineural extension and tumor invasion into marrow-containing bone like the central skull base is usually detected earlier on MR imaging than on CT (see Chapters 4 and 14).

Ultimately the examination of choice depends on the surgical procedure and the disease. In general, recurrent inflammatory disease is best followed on CT. The appearance of mucosal thickening is easily identified, and interval changes can be assessed by comparison to a previous CT study.

The radiologist is presented with more serious diagnostic problems when following a patient with a tumor, as the distinction between inflammatory disease, scar, and tumor is of critical importance. On CT, inflammatory secretions and reactions tend to have lower attenuation than most sinonasal tumors. On contrast-enhanced CT, active inflammatory changes tend to enhance more than most tumors. However, variations in this pattern commonly exist, and in most cases vascularized scar tissue cannot be differentiated with confidence from either inflammation or tumor.

On MR imaging, inflammatory tissues have low to intermediate T1-weighted and a high T2-weighted signal intensity. Approximately 95% of sinonasal tumors have intermediate signal intensity on all imaging sequences. Thus, in most cases, the best distinction between tumor and adjacent inflammation is made using the T2-weighted images.[4] On contrast-enhanced MR imaging, inflammatory tissues enhance intensely, and they tend to follow the contour of the sinus cavity wall fairly smoothly. Tumors, on the other hand, usually enhance only moderately and have a distinctly nodular configuration. As mentioned, the vascularized scar tissue that often develops in the postoperative sinonasal cavities has the identical imaging characteristics as tumor, on both CT and MR imaging. Ultimately, the distinction between these tissues is made either by comparing the imaging findings on serial studies, or by biopsy of any suspicious nodular regions. In general, MR imaging is the preferred modality to follow patients with sinonasal tumors. With fluorodeoxyglucose (FDG)-PET/CT, an area of increased activity may represent recurrent tumor, but if a discrete mass in not associated with the area of increased activity, the PET findings likely represent granulations and inflammatory tissues. Either biopsy or serial imaging may be used to resolve the issue.

OPERATIVE PROCEDURES

Chapter 5 discusses endoscopic sinus surgery. This chapter describes the more classic surgical procedures, some of which are still performed for refractory inflammatory disease. These operations are also used for the surgical treatment of sinonasal tumors. As these procedures are still performed, it is incumbent on the radiologist to be familiar with the imaging appearances described.

NASAL SURGERY

Although surgery on the external nose is primarily cosmetic, developmental and posttraumatic airway reconstruction accounts for many procedures. Surgery confined to the nasal or septal cartilages is rarely identified on imaging. However, during a rhinoplasty, the use of chisels and files to remove and recontour bone can leave contour irregularities of the nasal bones. If the nasal bones were purposely fractured during a rhinoplasty, such iatrogenic fractures may mimic a posttraumatic fracture and only the patient's history may resolve any confusion. After 6 to 12 months, the sharp edges of all nasal fractures become smooth, and the fracture lines are less sharply identified. Old fractures also can prove confusing when evaluating recent nasal trauma. The soft tissues overlying the nasal bones can be helpful in assessing how recent any trauma may have been. Acutely, these soft tissues tend to be thickened, with possible edema of the soft tissues of the adjacent ipsilateral cheek and preseptal region. Chronically, there rarely is any overlying soft tissue fullness (see Chapter 7).

In more severe nasal injuries in which the nasal bones have been crushed, or in cases of tumors involving the nasal soft tissues, cartilage or bone grafts may have been used to reconstruct the nasal contour. Once identified, these implants allow the imager to identify that previous reconstructive surgery was performed (Figs. 6-1 to 6-4). Rarely can degenerative changes occur at the margins of the implant site (Fig. 6-4A). Piercing of the soft tissues of the nose is clinically obvious, as well as easily identified on imaging (Fig. 6-4B).

Rhinectomy

Malignant tumors (principally basal cell and squamous cell carcinomas) arising from the integument and vestibular lining of the nose have the capacity to invade and destroy large segments of the external nose and even extend to the adjacent facial skeleton. Surgical resection may entail a limited (partial rhinectomy) or total rhinectomy. Reconstruction of the defect may require the transposition of local or regional flaps, often in combination with the placement of cartilage and bone grafts. With extensive tissue loss, or in patients who are poor surgical risks, or who are unwilling to undergo additional surgery, the defect may be camouflaged with a maxillofacial prosthesis (see Figs. 6-4C and D and 6-5). In addition, some patients may have undergone pre- or postoperative radiation, further distorting the tissues, or compromising reconstruction.

FRONTAL SINUS SURGERY

Trephination

Purulent acute frontal sinusitis refractory to conservative or endoscopic management usually requires an incision and drainage type procedure, by trephination or some other decompression surgery. A slightly curved incision is made just below the medial eye brow. A small bur is used to enter the sinus, through its floor at the junction of the medial and superior orbital walls. After the sinus is entered and drained (the sinus mucosa is not stripped), one or two tubes are placed in the sinus for 7 to 10 days.[5] If two tubes are placed, one tube is used for irrigation, the other for drainage. If one tube is placed, it is a drainage tube (Fig. 6-6A). The small trephination defect is often not appreciated on CT images unless the scan passes directly through the defect and/or the radiologist specifically looks for the defect (Fig. 6-6B and C). If the scan is performed while a drain is in place, the drain can be followed to its exit point from the sinus.[6]

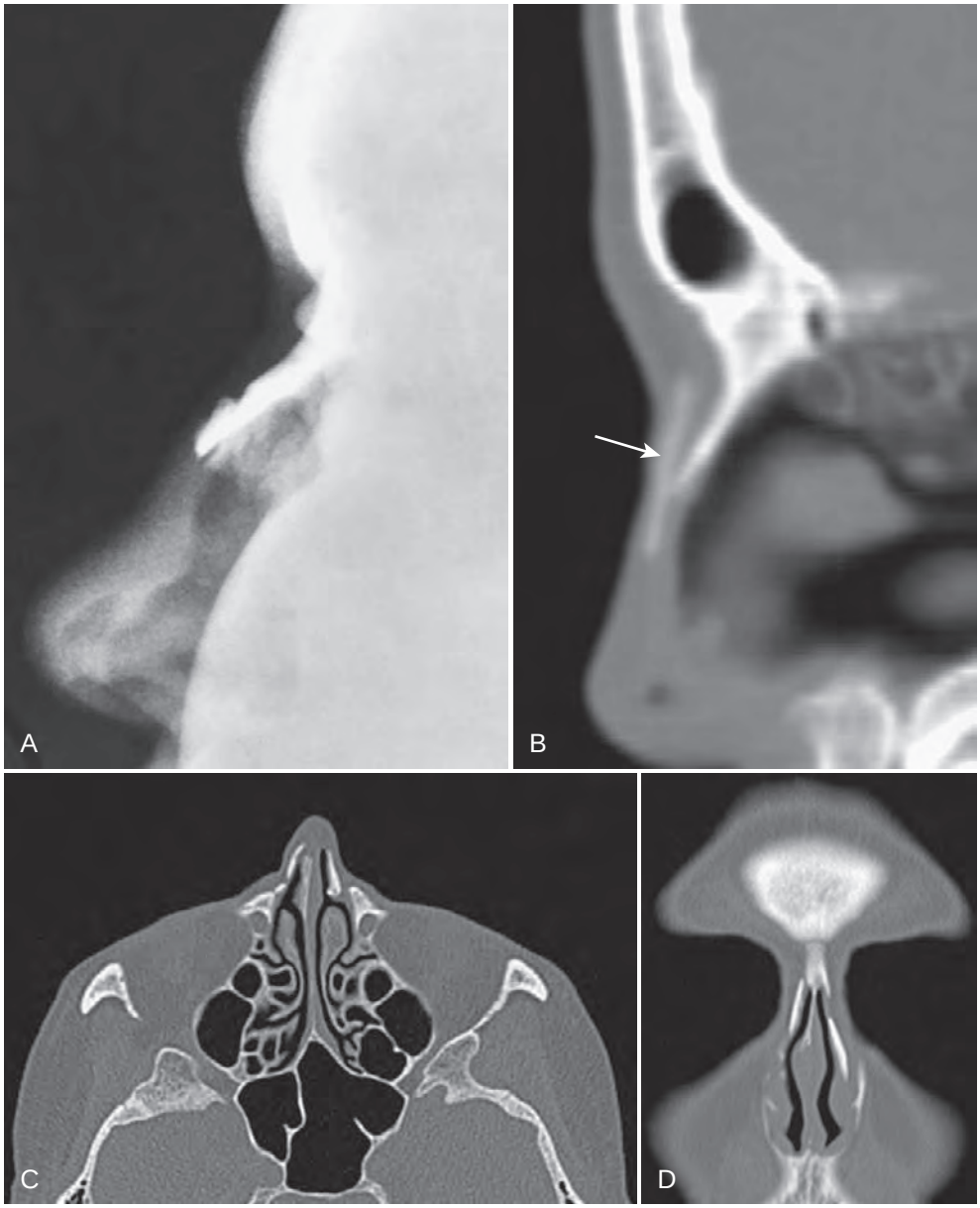

FIGURE 6-1 Lateral plain film (**A**) shows a patient who has had a prior rhinoplasty. The irregularity of the nasal bone contour is postsurgical in etiology. Sagittal CT reconstruction (**B**) shows a cartilage graft (*arrow*) placed in the midline of a rhinoplasty patient. Axial (**C**) and coronal (**D**) CT scans on a different patient show displaced and repositioned nasal bones with no overlying soft tissue swelling. Although a similar appearance could be secondary to old trauma, this patient had had a rhinoplasty many years earlier.

Currently, in patients with chronic inflammatory frontal sinus disease, either an endoscopic nonobliterative approach or an obliterative osteoplastic flap procedure is performed. Although rarely performed today, there are external frontal sinus procedures that may be encountered on imaging in older patients. These operations are the Lynch and Riedel procedures.

Lynch's Procedure

Lynch's procedure is an external ethmoidectomy approach used primarily for disease in the ethmoid sinuses and supraorbital ethmoid cells. However, it also provides good entrance into a small to moderate-size frontal sinus. Lynch's incision is placed on the lateral nasal wall and the superomedial orbital margin. The frontal sinus is entered from below and behind the orbital rim, and the region of the nasofrontal duct is exposed by a lateral (external) ethmoidectomy. The diseased mucosa from the frontal and ethmoid sinuses is removed, and a tube is placed that runs from the frontal sinus through the ethmoids into the nasal cavity. This tube is sutured in placed and remains for 6 to 8 weeks or less. It is then removed intranasally (Figs. 6-7 to 6-9).

If the frontal sinus is too large for all of its diseased mucosa to be effectively removed via the standard Lynch procedure, an extended Lynch incision can be used, where the incision is extended laterally over more of the orbital superior rim allowing greater entry into the frontal sinus. For the most part, such

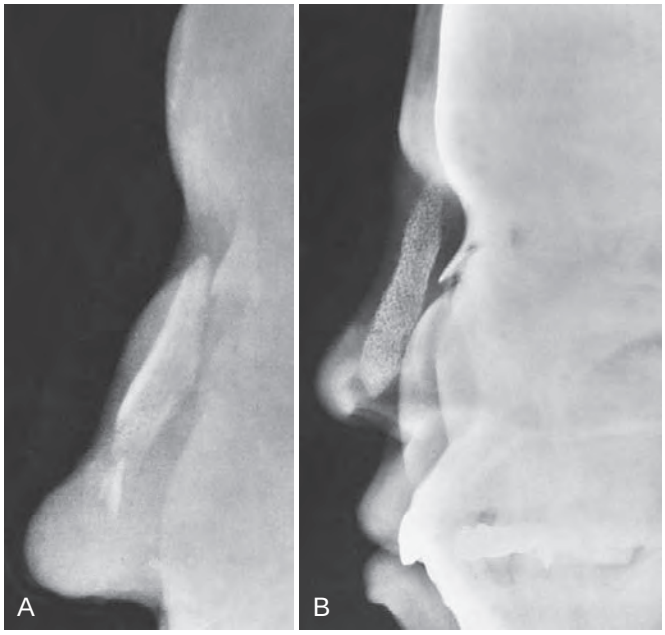

FIGURE 6-2 Lateral plain film (**A**) shows a patient with a rib nasal graft replacing badly fractured nasal bones. Lateral plain film (**B**) shows a patient with a partially calcified cartilage graft replacing crushed nasal bones.

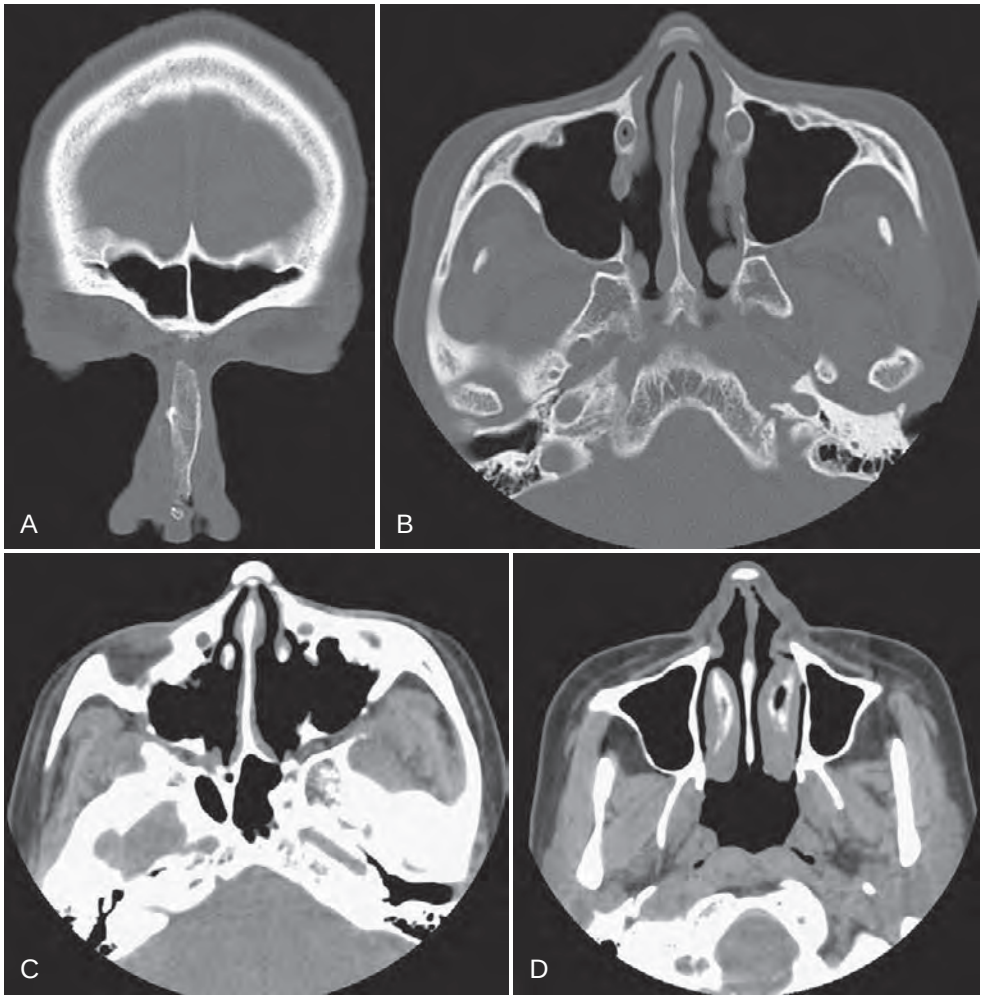

FIGURE 6-3 Coronal CT scan (**A**) shows a rib graft replacing the nasal bones. Axial CT scans (**B**) bone windowed and (**C** and **D**) soft tissue windowed scans show various nasal rib reconstructions on three different patients.

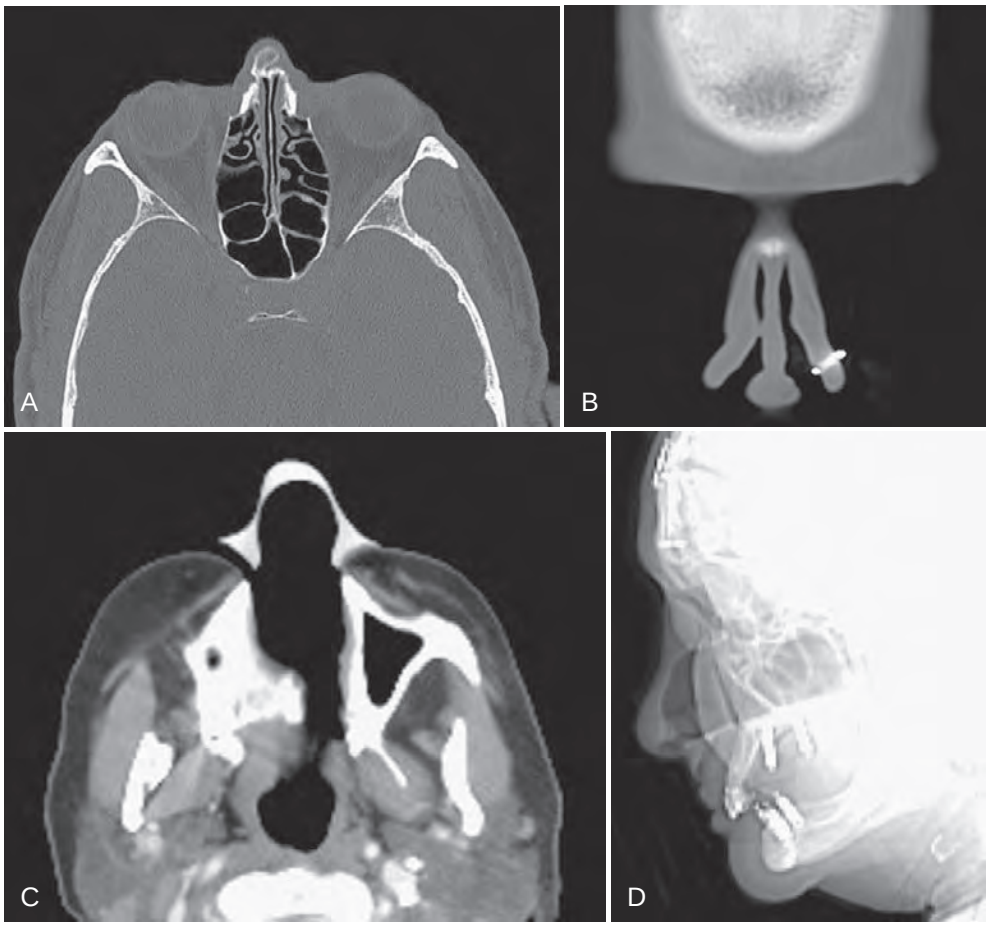

FIGURE 6-4 Axial CT scan (**A**) shows degenerative productive changes at the superior margin of a nasal graft. This can cause facial cosmetic deformity. Coronal CT scan (**B**) shows a metal stud piercing the left nasal alar lobule. This is a typical and easily identified imaging appearance. Axial CT scan (**C**) and lateral soft tissue plain film (**D**) of a patient who has a nasal prosthesis.

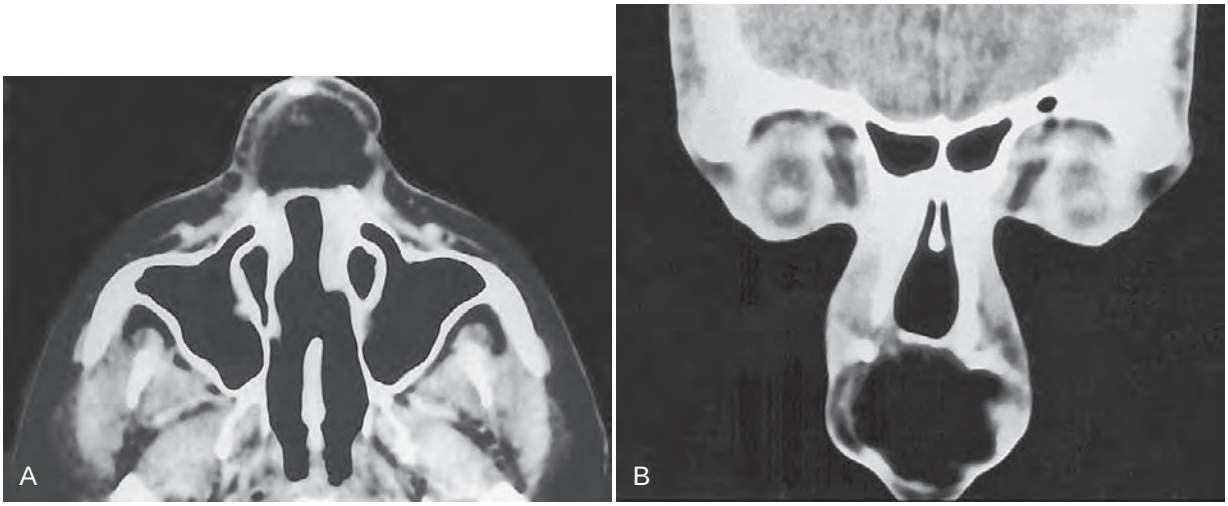

FIGURE 6-5 Axial (**A**) and coronal (**B**) CT scans show a free-flap reconstruction of the lower nose after a rhinectomy. The bulk of the graft is fatty.

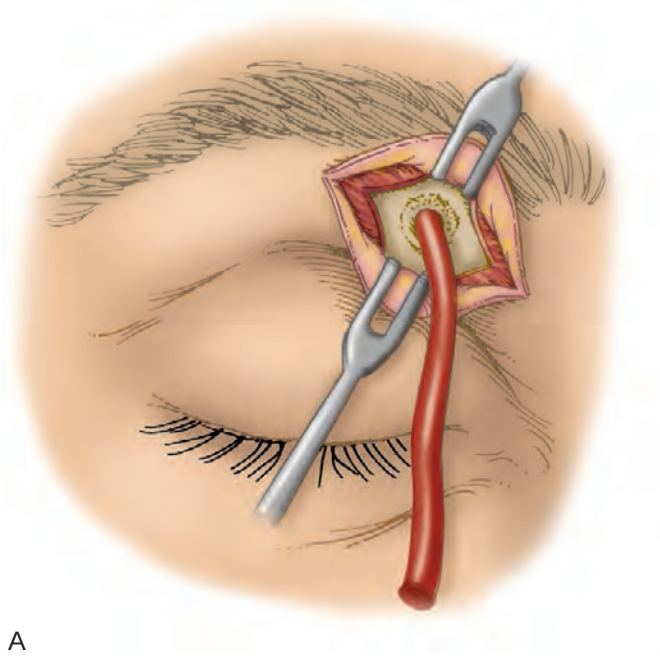

A

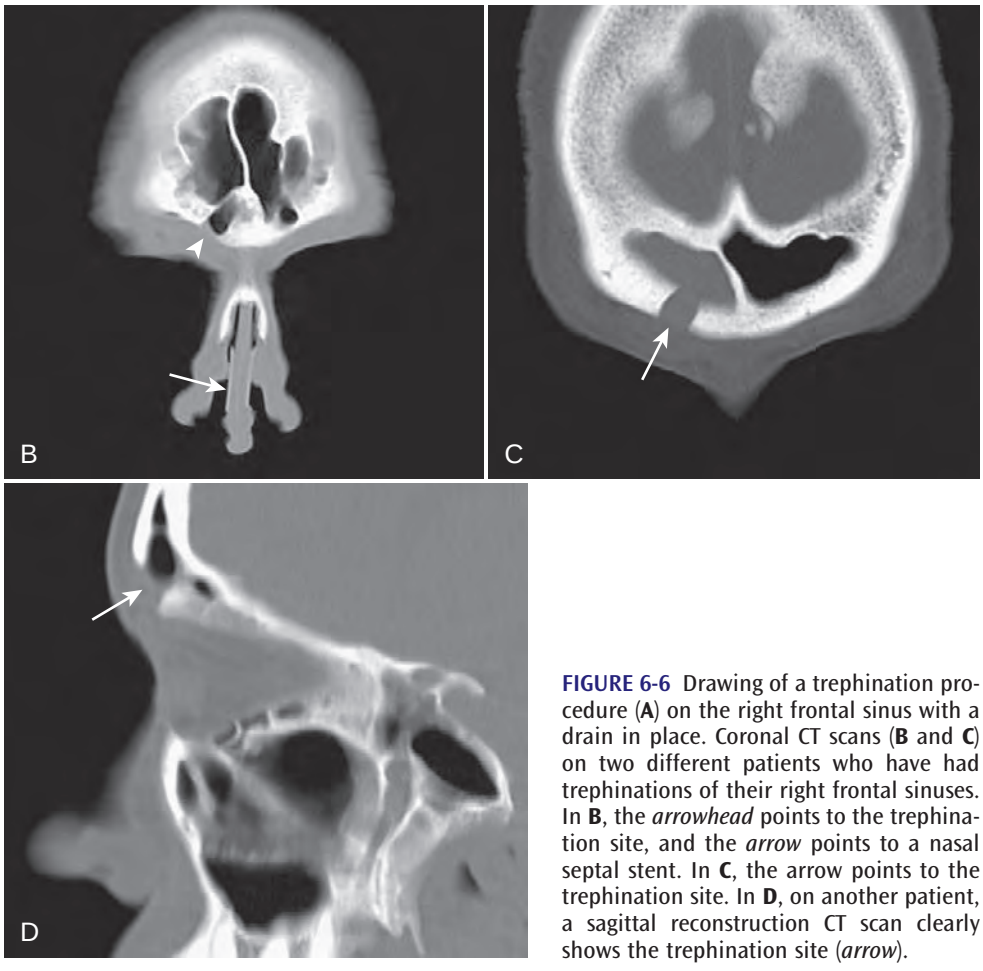

FIGURE 6-6 Drawing of a trephination procedure (**A**) on the right frontal sinus with a drain in place. Coronal CT scans (**B** and **C**) on two different patients who have had trephinations of their right frontal sinuses. In **B**, the *arrowhead* points to the trephination site, and the *arrow* points to a nasal septal stent. In **C**, the arrow points to the trephination site. In **D**, on another patient, a sagittal reconstruction CT scan clearly shows the trephination site (*arrow*).

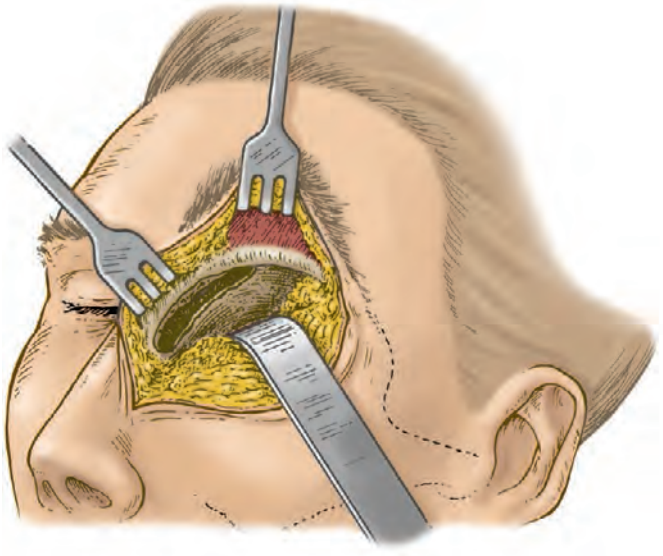

FIGURE 6-7 Diagram of a Lynch procedure performed on the left side. The ethmoid sinuses, supraorbital ethmoid cells, and small frontal sinuses can be approached by this procedure. The incision is buried in the creases of the lateral nose and the superomedial orbital rim.

FIGURE 6-8 Axial CT scan (**A**) shows an air-filled tube (*arrow*) in the left frontal sinus. The sinus is partially filled with secretions. Axial CT scan (**B**) through the ethmoid sinuses shows the drainage tube (*arrow*) extending down into the nose. There has been an external ethmoidectomy, and the anterior lamina papyracea has been removed. The left ethmoid cavity and the left sphenoid sinus have inflammatory changes.

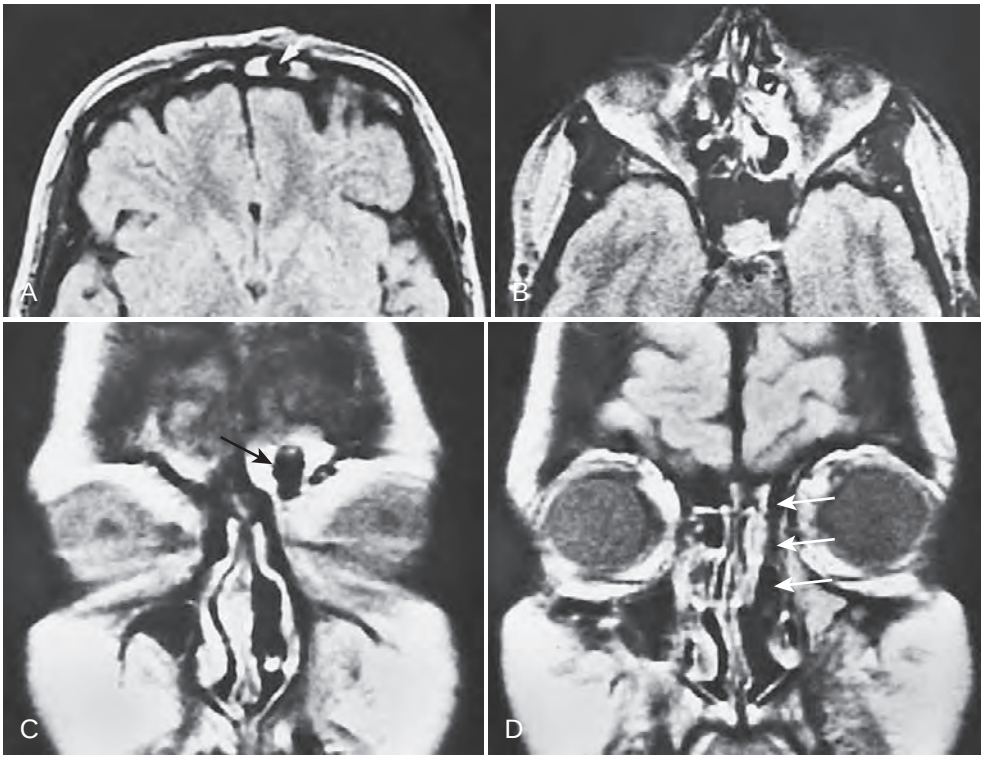

FIGURE 6-9 Axial proton density MR images (**A** and **B**) show a drainage lube in the left frontal sinus (**A**) (*arrow*) and sinus secretions. In **B**, the drainage tube can barely be seen in the left ethmoid sinuses, and inflammatory changes are present as well. On the MR images, it is almost impossible to appreciate that an external ethmoidectomy has been performed. Coronal proton density MR images (**C** and **D**) show the tube in the left frontal sinus (*black arrow*) and the drainage tube extending through the ethmoid sinuses into the nasal fossa (*arrows*).

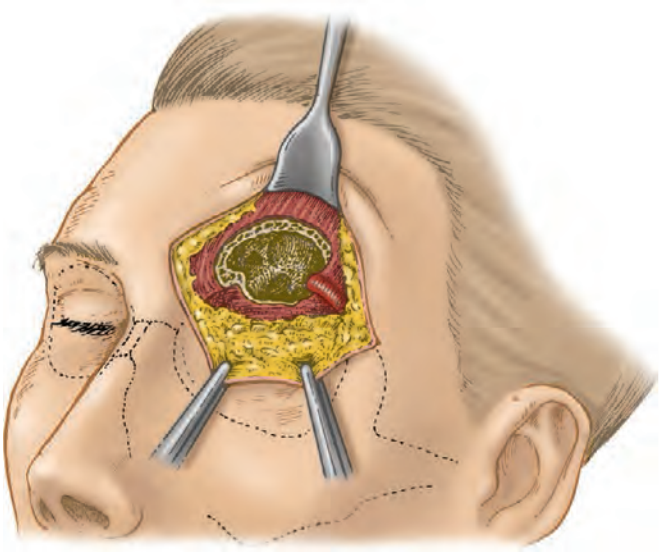

FIGURE 6-10 Diagram of Riedel's procedure performed on the left side in which the superior orbital rim has been removed. Because this operation causes a large deformity of the forehead, it is mostly abandoned. However, it is now occasionally used as the first operative stage in a reconstruction of a patient who had an infected osteoplastic flap which had to be removed.

large frontal sinuses today are approached with an osteoplastic flap.

Riedel's Procedure

Reidel's operation is a collapse procedure to obliterate the frontal sinus. This procedure is reserved for the management of chronic osteomyelitis refractory to medical treatment. It accomplishes this by the removal of the anterior table of the frontal sinus and the supraorbital ridge (Fig. 6-10). At the completion of the procedure the soft tissues of the forehead are laid on the posterior frontal sinus wall, which was denuded of its mucosa. This effectively obliterates the upper sinus cavity but creates a cosmetically undesirable soft-tissue defect in the forehead. The nasofrontal duct is obliterated with soft tissue.[5,7] A cranioplasty may be subsequently performed to correct the frontal contour deformity.[8,9]

Osteoplastic Flap Procedure

Patients with recurrent inflammatory disease, tumors, and complex fractures are candidates for the cosmetically nondeforming osteoplastic flap, generally performed with sinus cavity obliteration. The osteoplastic flap incision is performed through a curved coronal scalp incision hidden in the scalp hair, or through a brow incision that extends above the eyebrows, crossing the intervening skin at the root of the nose. Once the periosteum over the frontal bone is exposed, a template made from a Caldwell view is used to trace the frontal sinus contour on the bone and periosteum. This template should come from a film taken on either a dedicated head unit such as the Franklin head unit, which has a magnification factor of only 3.4%, or from a standard 40-inch posteroanterior Caldwell film with a magnification factor of 10.3%.[10] The template is made by marking the sinus contours and the contour of the upper orbits on this film and cutting them out. The resulting template is then sterilized. The orbital contours are used to position the template on the patient, and then the sinus outline is traced on the patient's exposed frontal bone with its intact periosteum.

The periosteum is incised on all except its inferior margin, and the frontal sinus contour is marked by sawing into the anterior frontal sinus table. The osteotomy line is beveled medially and downward into the sinus to help ensure that the frontal sinus and not the anterior cranial fossa is entered. The inferior margin of this anterior wall is not drilled, but outfractured with its overlying periosteum intact. This technique yields a viable osteoperiosteal flap. The sinus mucosa is then drilled out, and the sinus cavity is obliterated with fat that is usually taken from the abdominal wall. The anterior sinus wall is then replaced, the periosteum sutured, and the skin closed, leaving almost no cosmetic deformity (Fig. 6-11).[6]

The fat progressively and gradually undergoes fibrosis and throughout the process of fibrosis no volume loss occurs so that the sinus remains airless and obliterated.

The most common complications of the osteoplastic flap are reinfection of the frontal sinus from an infected adjacent ethmoid air cell and mucocele formation from microscopic retained mucosal remnants.

Infection of the bone with or without associated osteomyelitis, and infection of the obliterating fat are rare complications of the osteoplastic flap procedure. If the infection cannot be controlled with antibiotic treatment, reoperation is necessary. This often necessitates the removal of the anterior sinus wall bone flap, with some resulting inward prolapse of the forehead soft tissues (Riedel's procedure).

If the osteoplastic flap procedure was performed to obliterate a mucocele that thinned or destroyed a portion of the posterior or anterior sinus tables, these defects also will be visualized on subsequent imaging studies.

On CT the bone flap may go unnoticed if only narrow window images are available. Similarly, the bone flap may go unnoticed on MR images. At wide window CT settings, the bone flap should have a normal osseous texture with trabeculations in the medullary cavity (Figs. 6-12 to 6-18). However, the edges of the flap and the adjacent frontal bone occasionally have a ragged, irregular appearance that reflects the beveled drilling of the surgery. Without any associated clinical or soft-tissue changes of infection, such irregular bone at the margins of the bone flap should not elicit a diagnosis of osteomyelitis. Frank osteomyelitis appears as areas of bone demineralization, erosion, and/or sequestration accompanied by swelling and cellulitis of the overlying forehead soft tissues and the obliterating fat within the sinus.

The bone flap should be in a normal alignment with the adjacent frontal bone contour, that is, the flap should not be either depressed into the sinus or elevated over the adjacent frontal bone. When the flap is elevated, infection of the underlying obliterating fat must be considered. The obliterated sinus is best examined at both narrow and wide windows. The entire sinus cavity should be airless and filled with fat that has randomly scattered strands of soft-tissue-dense fibrous tissue. If no fat density is seen or there is new air within the obliterated sinus, infection should be considered, especially if there is also elevation of the bone flap (Figs. 6-19 to 6-25). In these cases the intracranial compartment should also be examined for evidence of spread of the infection.

Text continued on page 454

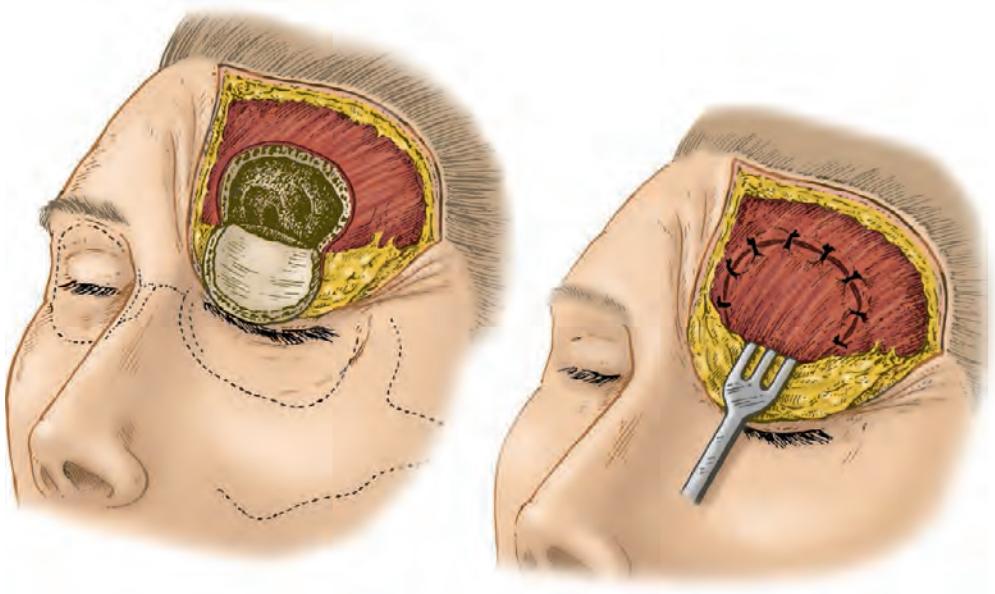

FIGURE 6-11 Diagram of an osteoplastic flap procedure performed on the left side. The anterior sinus wall is flipped down, with the inferior periosteum left intact. After the sinus mucosa and disease are removed, the sinus is obliterated with fat and the flap is replaced. This procedure leaves almost no cosmetic deformity. This operation may be performed as either a unilateral or bilateral procedure.

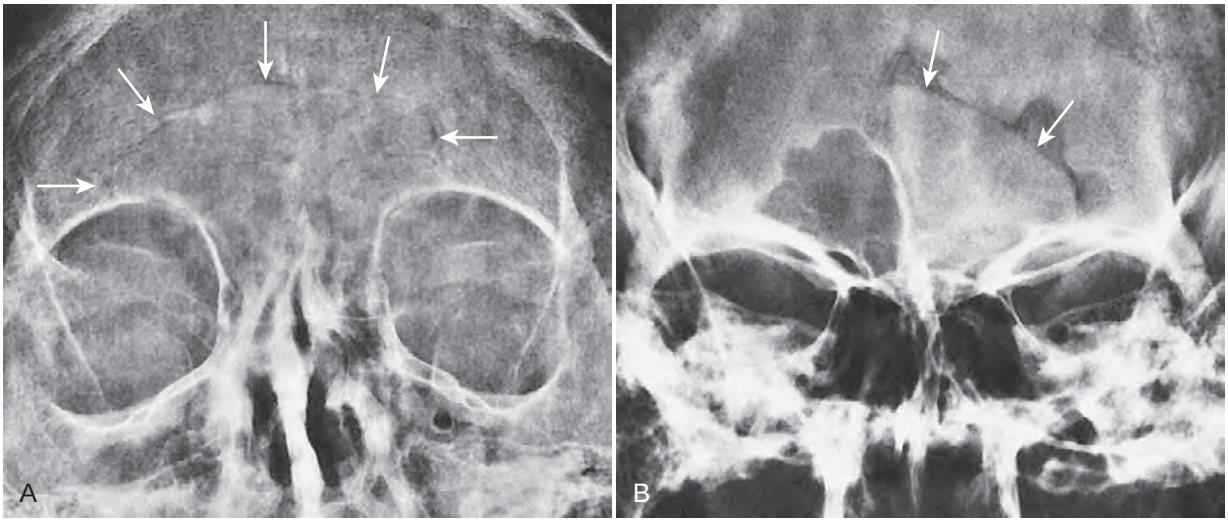

FIGURE 6-12 Waters view (**A**) shows a patient after bilateral osteoplastic flap surgery. The flap margins can barely be identified (*arrows*). Caldwell view (**B**) on a different patient after left osteoplastic flap surgery. The margins of the flap are well seen (*arrows*). The space between the flap and the calvarium is a normal postoperative finding resulting from the bone removal that occurs during surgery.

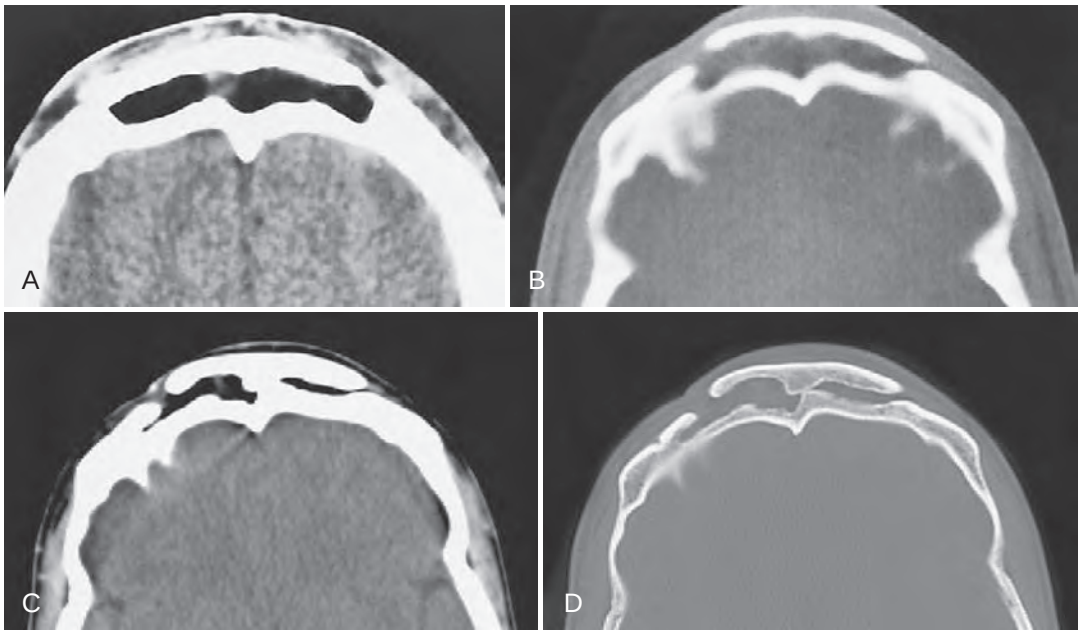

FIGURE 6-13 Axial CT scans at narrow (**A**) and wide (**B**) window settings. The patient has had an osteoplastic flap procedure. The sinus is filled with fat, and the flap is clearly seen in a good position. In **A**, the presence of the flap can be easily overlooked. Axial CT scans at narrow (**C**) and wide (**D**) window settings on another patient who also has had an osteoplastic flap procedure. The sinus is filled with fat; however, the bone flap appears elevated. This is secondary to the residual sinus septum abutting on the flap bone. This will be the new normal frontal sinus appearance for this patient and demonstrates why baseline postoperative scans should be obtained.

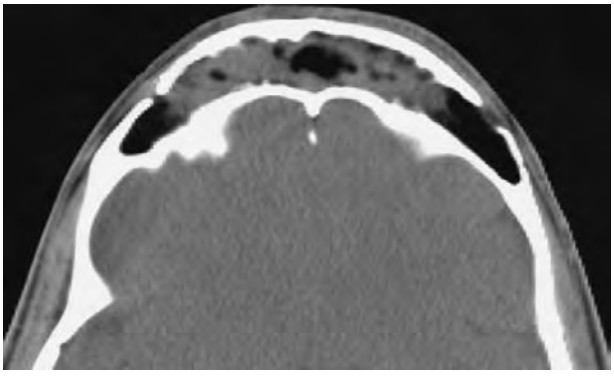

FIGURE 6-14 Axial CT scan shows an osteoplastic flap. Although more than half of the fat has soft tissue rather than fat attenuation, the bone flap is in a good position and there are no inflammatory changes in the overlying soft tissues. This is a normal imaging variant of this procedure.

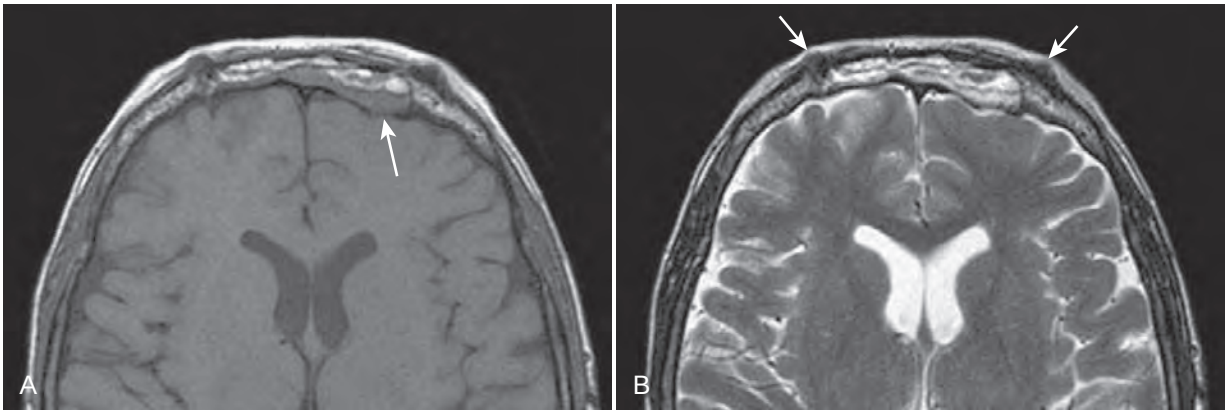

FIGURE 6-15 Axial T1-weighted (**A**) and T2-weighted (**B**) MR images of a patient who has had a bilateral osteoplastic procedure. This sinus cavity is filled with fat and fibrous tissues. The thinning of the left posterior sinus table is secondary to remodeling that occurred from a mucocele (*arrow*). It is always helpful to see a preoperative imaging study to better assess any such bone changes. In this patient, the bone flap is secured by wire sutures (*small arrows*).

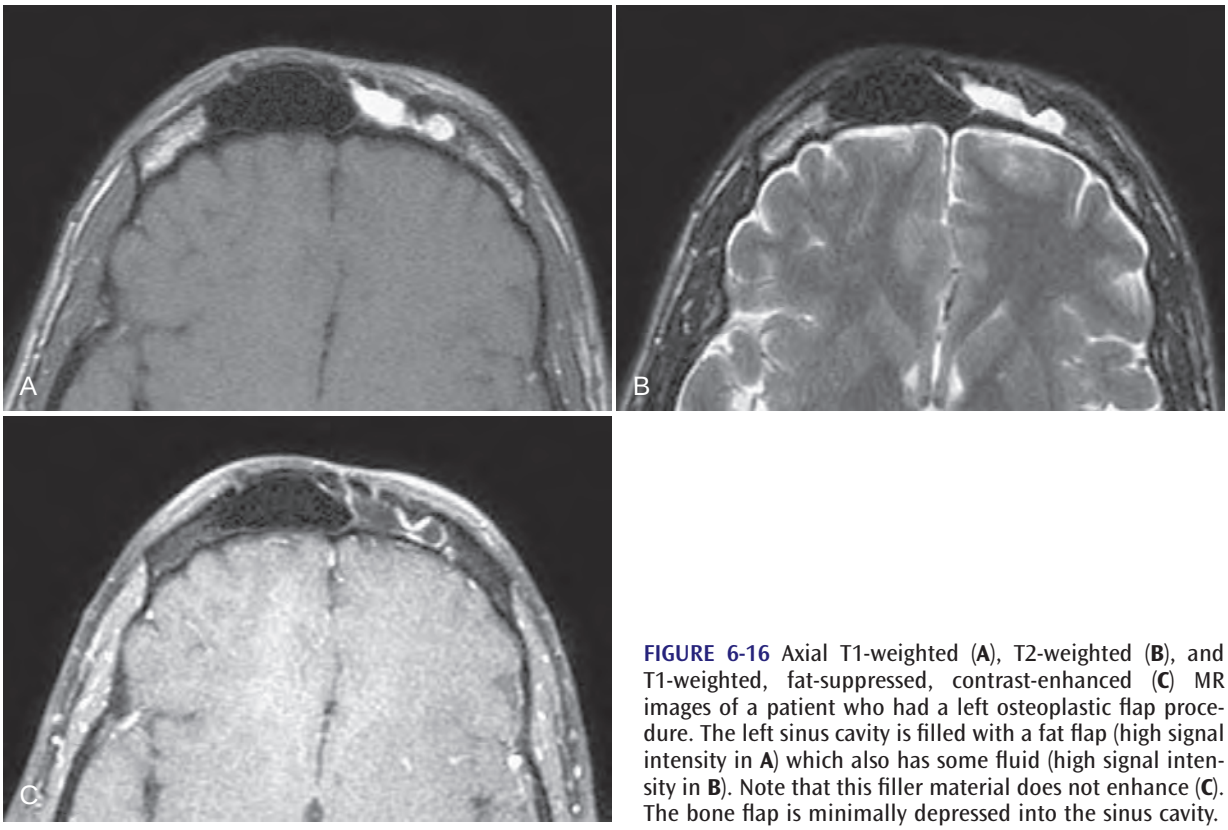

FIGURE 6-16 Axial T1-weighted (**A**), T2-weighted (**B**), and T1-weighted, fat-suppressed, contrast-enhanced (**C**) MR images of a patient who had a left osteoplastic flap procedure. The left sinus cavity is filled with a fat flap (high signal intensity in **A**) which also has some fluid (high signal intensity in **B**). Note that this filler material does not enhance (**C**). The bone flap is minimally depressed into the sinus cavity.

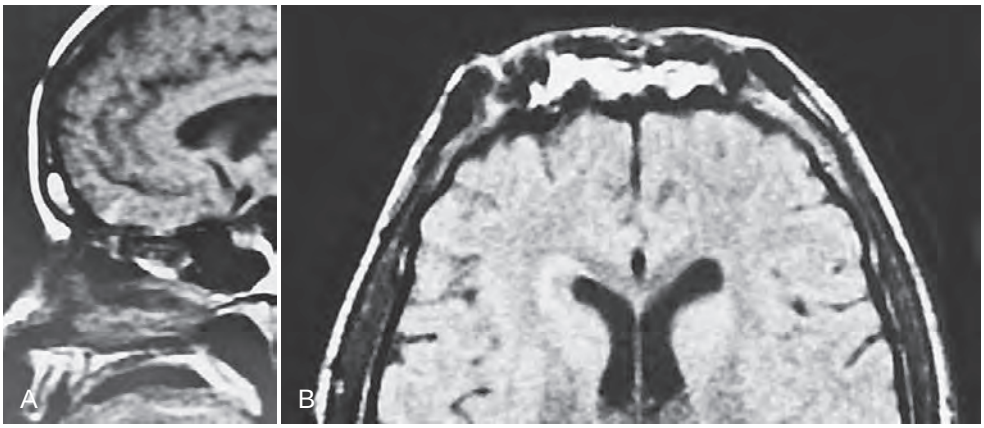

FIGURE 6-17 Sagittal T1-weighted (**A**) and axial proton-density (**B**) MR images show high signal intensity material (fat) within the obliterated sinus. The bone flap, which is often hard to identify on MR images, is in a good position. This can be a normal MR imaging appearance after this procedure.

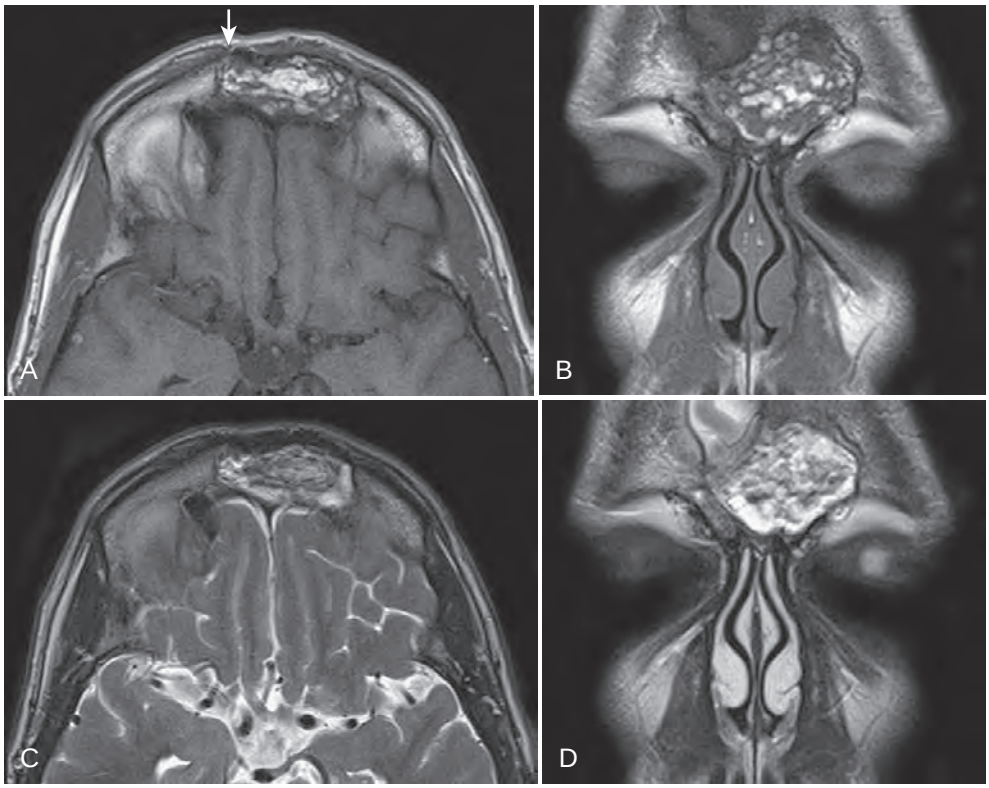

FIGURE 6-18 Axial (**A**) and coronal (**B**) T1-weighted and axial (**C**) and coronal (**D**) T2-weighted MR images of a patient who had a left osteoplastic flap. There is both fat (from the obliterating graft) and fluid within the sinus cavity, however, there is no elevation of the bone flap and there are no inflammatory changes in the forehead or intracranial soft tissues. This is a normal postoperative appearance.

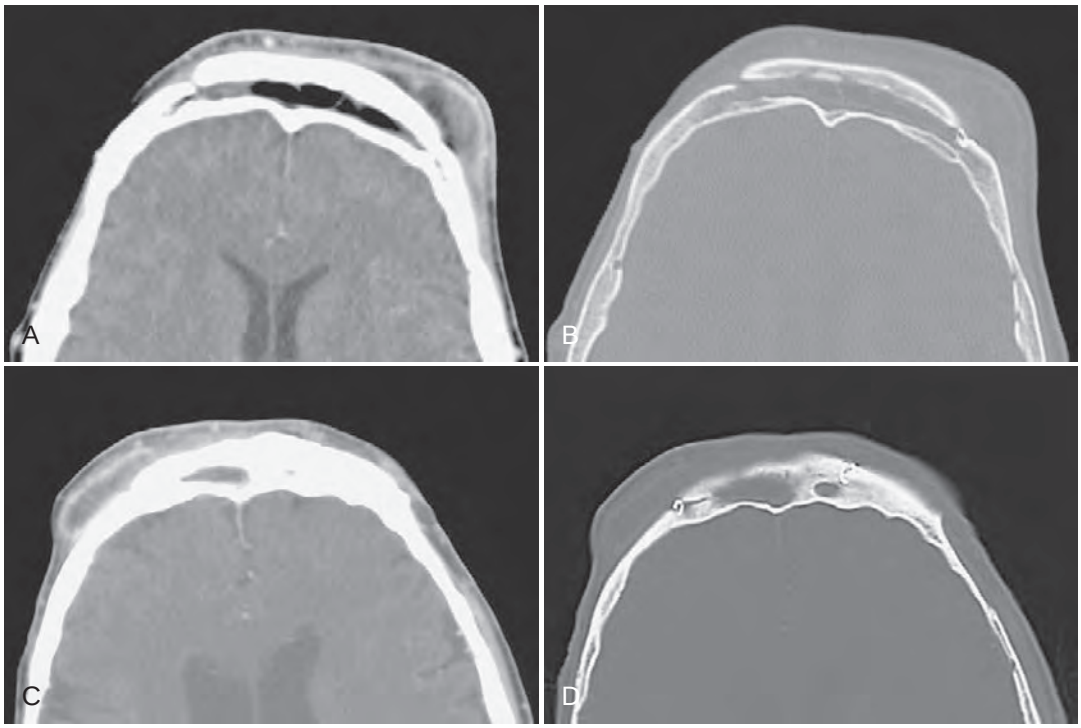

FIGURE 6-19 Axial CT scans at narrow (**A**) and wide (**B**) window settings. The patient has had an osteoplastic flap procedure. Despite the presence of primarily fat attenuation within the sinus, the right side of the bone flap is elevated, there is an abscess at the left margin of the flap, and there is swelling of the forehead soft tissues. This was an infected flap. Axial CT scans at narrow (**C**) and wide (**D**) window settings on another patient. In **C**, an abscess is seen in the forehead soft tissues. Although it lies at the right margin of an osteoplastic flap, the bony flap cannot be seen clearly. In **D**, the bony flap is clearly seen. This was an early abscess, developing after local head trauma to the region. The flap is otherwise normal on imaging.

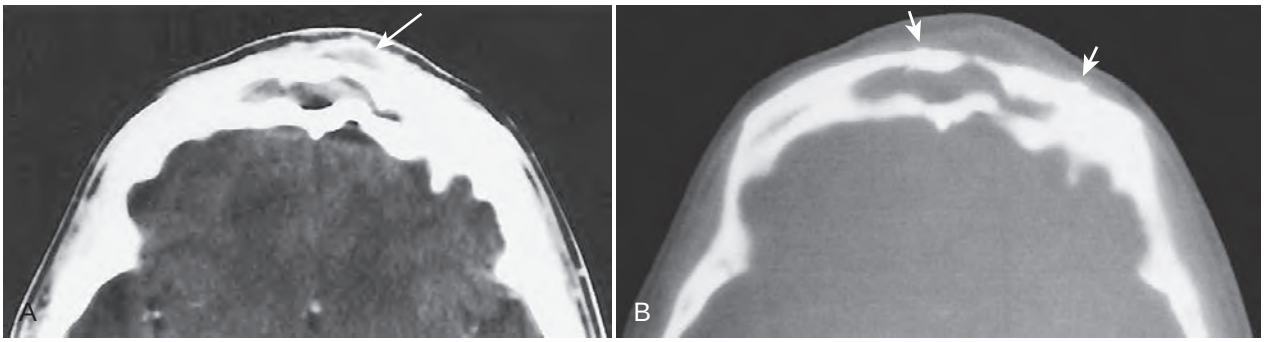

FIGURE 6-20 Axial CT scans at soft tissue (**A**) and bone (**B**) window settings show a patient who had a left osteoplastic flap. The small wire sutures stabilizing the flap can barely be seen in **B** (*arrows*). There is erosion of the midanterior bone flap, and an abscess is present in the forehead (*arrow* in **A**). The fat used to obliterate the sinus is also dense, reflecting infection.

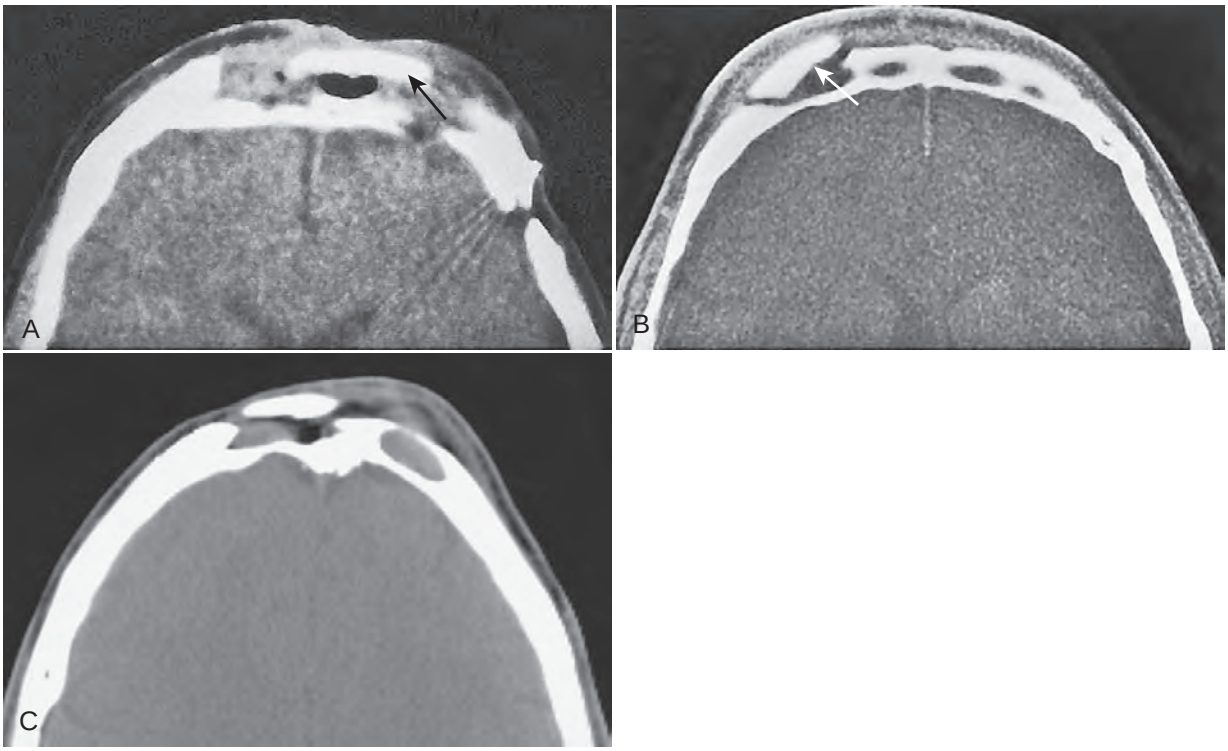

FIGURE 6-21 Axial CT scan (**A**) shows an infected osteoplastic flap. There is swelling of the overlying forehead soft tissues, and the bone flap (*arrow*) has been partially eroded. In addition, just behind the flap there is air, which should not be present in an obliterated sinus. The defect in the left posterior sinus table and the more lateral calvarium were related to the surgery. Axial contrast CT scan (**B**) on a different patient who had a right osteoplastic flap procedure. Although the obliterating fat is only slightly denser than expected, there is elevation and rotation of the bone flap (*arrow*) and swelling of the forehead soft tissues. This was an infected flap. Axial CT scan (**C**) on a third patient who had a right osteoplastic flap procedure. There is an ovoid soft-tissue density within the right sinus. The bone flap is elevated, and there is thickening of the forehead soft tissues. In addition, the left frontal sinus is opacified, and there is a soft-tissue mass in the overlying forehead with thinning of the intervening anterior frontal sinus bone. This patient had a recurrent mucopyocele in the right frontal sinus. There was a mucocele in the nonoperated left frontal sinus.

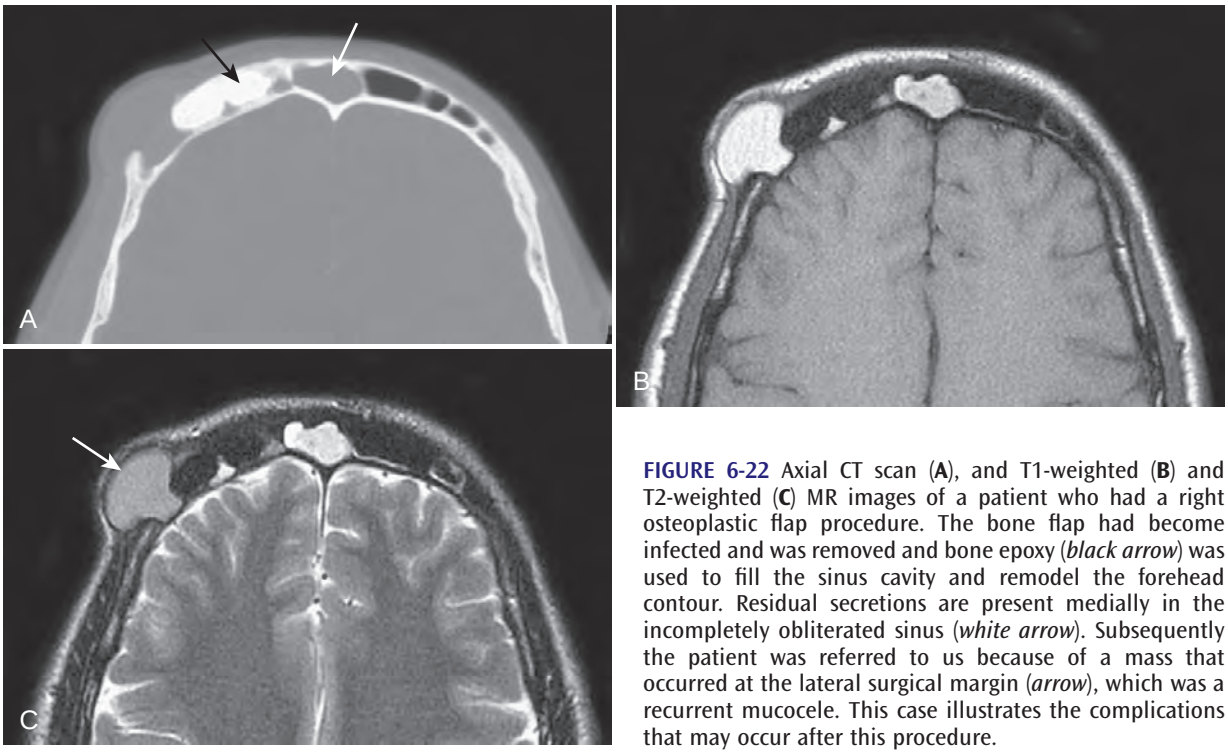

FIGURE 6-22 Axial CT scan (**A**), and T1-weighted (**B**) and T2-weighted (**C**) MR images of a patient who had a right osteoplastic flap procedure. The bone flap had become infected and was removed and bone epoxy (*black arrow*) was used to fill the sinus cavity and remodel the forehead contour. Residual secretions are present medially in the incompletely obliterated sinus (*white arrow*). Subsequently the patient was referred to us because of a mass that occurred at the lateral surgical margin (*arrow*), which was a recurrent mucocele. This case illustrates the complications that may occur after this procedure.

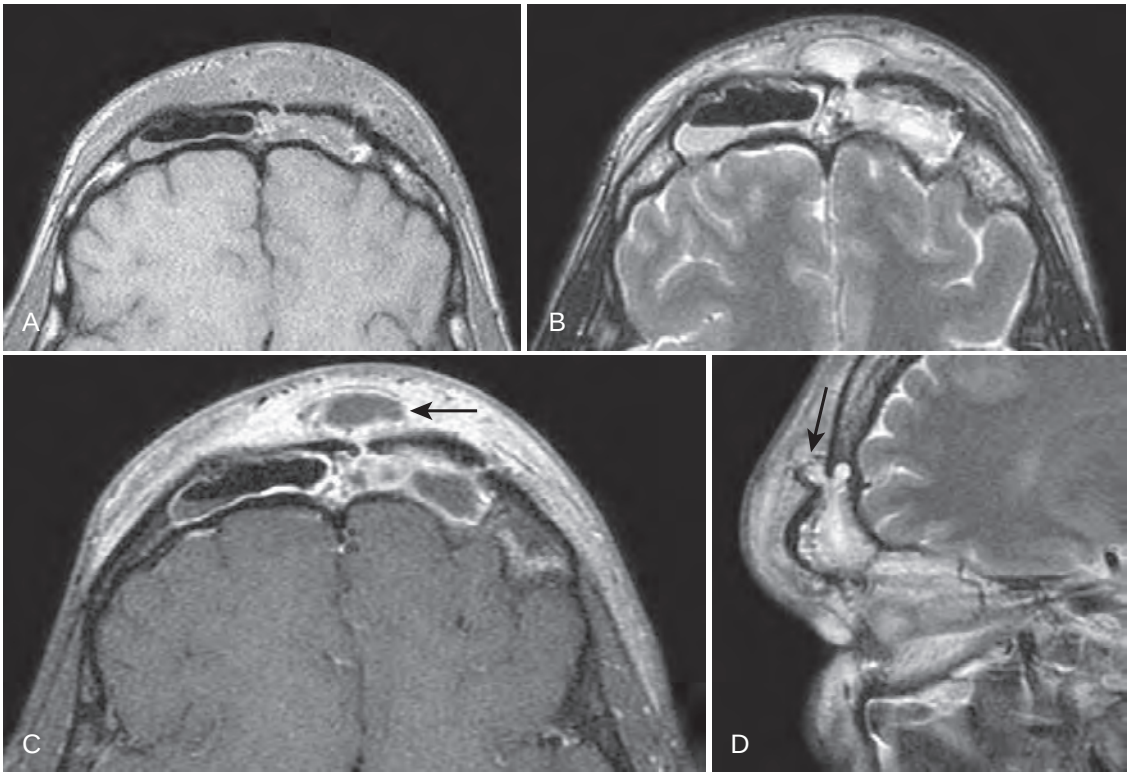

FIGURE 6-23 Axial T1-weighted (**A**), T2-weighted (**B**), and axial (**C**) and sagittal (**D**) T1-weighted, fat-suppressed, contrast-enhanced (**C**) MR images of a patient who had a left osteoplastic flap procedure. Inflammatory mucosal thickening and secretions are present in the right frontal sinus. The left sinus obliterating fat has become infected and as it expanded it extruded along the medial bone flap margin into the forehead (*arrows*).

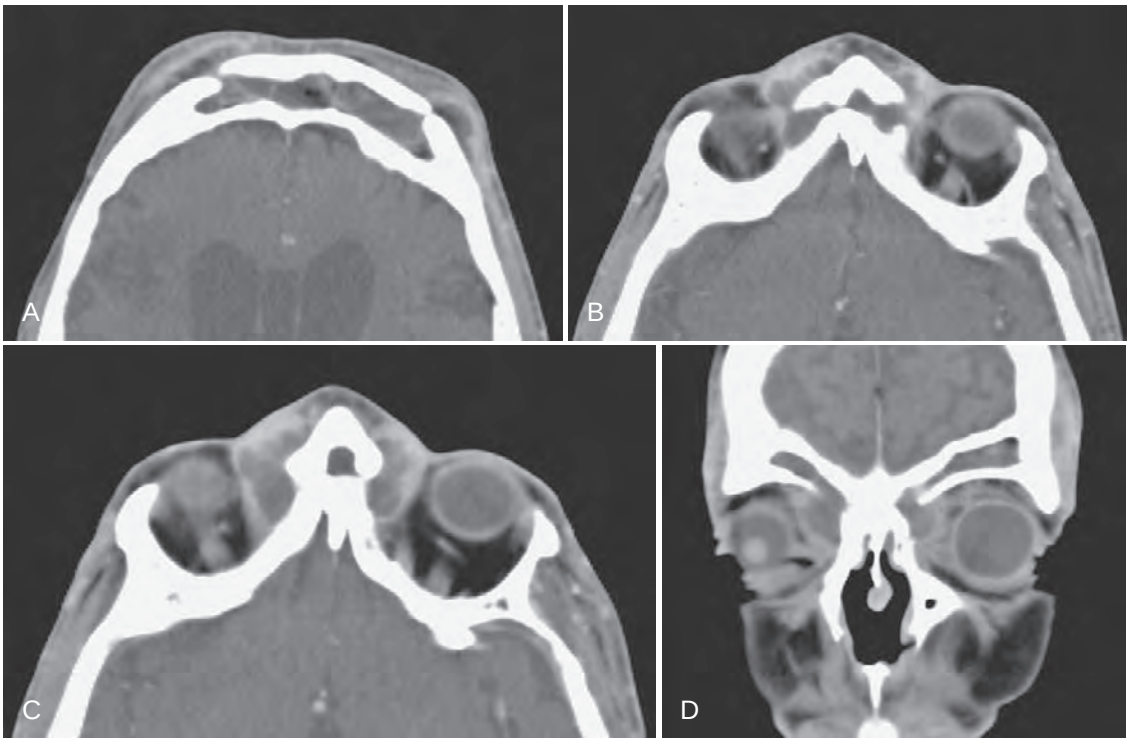

FIGURE 6-24 Serial axial CT scan from cranial (**A**) to caudal (**C**) and coronal CT scan (**D**) show a patient who has had an osteoplastic flap procedure. The fat is dense and swollen, and there is elevation of the flap. Along the left and right margins of the upper flap there are small abscesses. In addition, there is an abscess extending from the lower flap margin into the upper medial aspect of each orbit. There is unrelated ventricular dilatation.

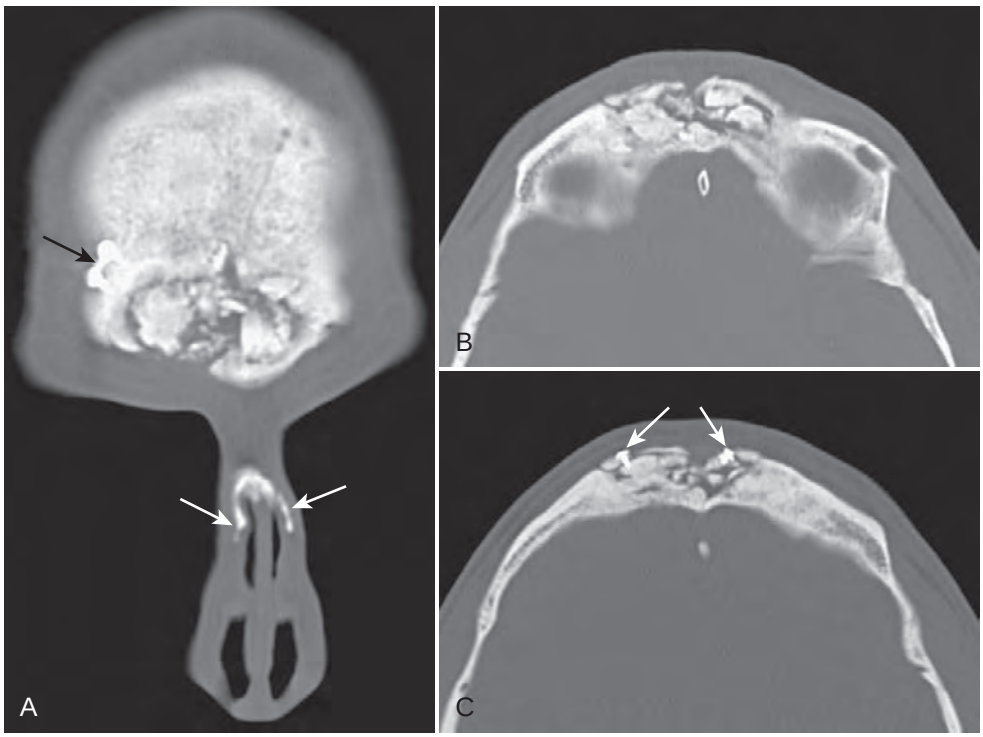

FIGURE 6-25 Coronal (**A**) and serial axial (**B** and **C**) CT scans of a patient who had a bilateral osteoplastic flap procedure. Subsequently, he was in a car accident and suffered extensive fractures of the bone flap and his nose (*white arrows* in **A**). Osteosynthesis plates and screws used to secure the bone flap are also seen (*black arrow* in **A** and *white arrows* in **C**).

Occasionally the osteoplastic bone flap fractures during surgery; however, as long as the overlying periosteum remains intact, the segments usually remain viable. The imager should verify that the bony pieces have a normal texture, that there are no sites of osteomyelitis, and that the bone fragments are not elevated. In rare instances, after many years some calcification can occur in the obliterating fat; this should be considered a normal postoperative variant.

On MR imaging the signal intensities in the normal postosteoplastic flap sinus reflect the obliterating fat. Thus, there is a high T1-weighted and an intermediate T2-weighted signal intensity. Although infection in the fat will produce a high T2-weighted signal intensity, occasionally areas of high T2-weighted signal intensity are seen in noninfected sinuses (see Figs. 6-16 to 6-18). The precise cause of this is unclear.[11] Thus, the mere presence of a high T2-weighted signal intensity within the obliterating fat should not warrant a diagnosis of postoperative infection. Infection should be considered if there is high T2-weighted signal intensity in the obliterating fat, elevation of the bony flap, and evidence of swelling and inflammation in the surrounding forehead soft tissues. Pain in the frontal region after an osteoplastic flap does not necessarily imply infection. Although the exact cause remains unclear, neuralgia from injury to the supraorbital nerve during surgery is considered a likely possibility.

If the bone flap is irreparably infected or fractured, "bone epoxy" products are being used to obliterate the sinus cavity and contour the forehead shape. These materials are quite dense and should not cause a diagnostic problem in their identification (Figs. 6-26 and 6-27).

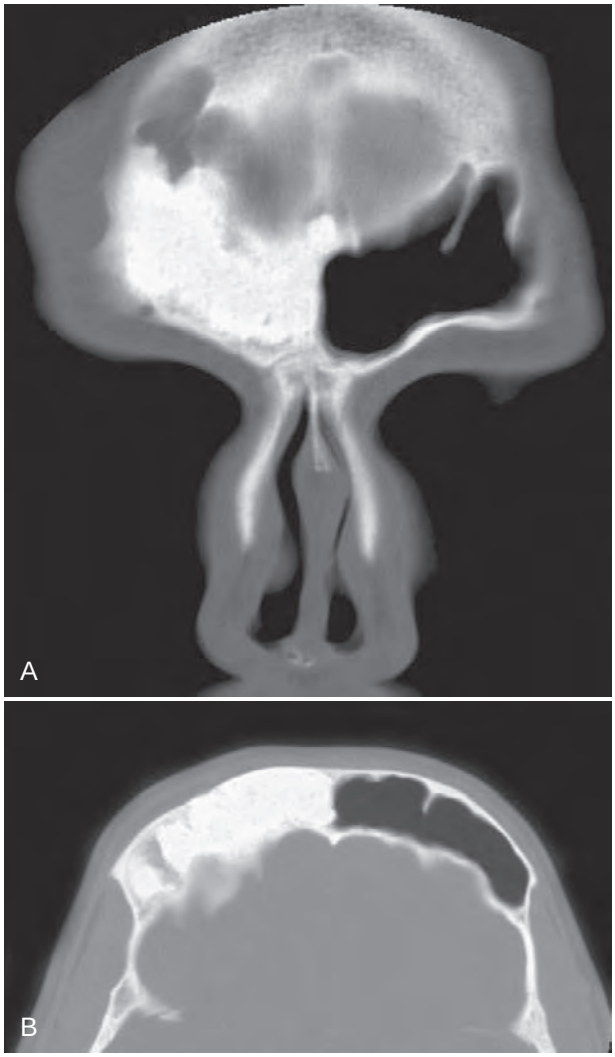

FIGURE 6-26 Coronal (**A**) and axial (**B**) CT scans of a patient who had a right osteoplastic flap procedure. The sinus cavity was filled with bony epoxy.

ETHMOID SINUS SURGERY

Although today the ethmoid sinuses are most often approached endoscopically, the ethmoid complex has been partially resected via three major approaches: the external, the internal (intranasal), and the transmaxillary (transantral) (Fig. 6-28). These procedures are performed for inflammatory disease, and the aim is to progressively remove the disease from each cell until all of the pathologic material is extirpated. The primary areas of complication are entrance into the floor of the anterior cranial fossa and damage to the orbital contents.[1,2,10] Imaging of the postethmoidectomy patient is shown in Figures 6-29 to 6-35.

External Ethmoidectomy

The external approach provides the best overall access and visualization of the ethmoid cells. After Lynch's incision, the periorbita is elevated, the lacrimal sac retracted and the surface of the lamina papyracea is viewed to identify prior fractures and any areas of dehiscence or erosion. The anterior and posterior ethmoidal canals are exposed. A line connecting these canals lies just below the floor of the anterior cranial fossa, and if the surgeon stays caudal to this line, entrance into the anterior cranial fossa should not occur. The surgical field can be enlarged to access the frontal sinus, supraorbital cells, sphenoid sinus and base of the skull. In an external ethmoidectomy, the anterior cells are first entered through the lamina papyracea, and then the posterior cells are progressively opened as needed. The nasofrontal outflow can be opened and the opening into the nasal cavity stented with a Silastic tube.

Internal Ethmoidectomy

The internal ethmoidectomy is an endoscopic approach and may include resection of the middle turbinate to provide better access to the ethmoid and sphenoid cells (see Chapter 5). The ethmoid complex is usually entered via the uncinate process or bulla ethmoidalis; the anterior cells are resected and then the more posterior cells are opened. Although in experienced hands the lamina papyracea is not violated in this procedure, dehiscence of the lamina papyracea or presence of a prior external ethmoidectomy is a contributing factor to inadvertent entrance into the orbit. The internal ethmoidectomy approach is used for isolated ethmoid sinus disease, or as part of total sphenoethmoidectomy for multisinus disease. Today, the classic nonendoscopic internal ethmoidectomy is rarely performed.

Transantral Ethmoidectomy

Because of the advent of the endoscope, the transantral approach for extirpating ethmoid sinus disease is rarely

Text continued on page 459

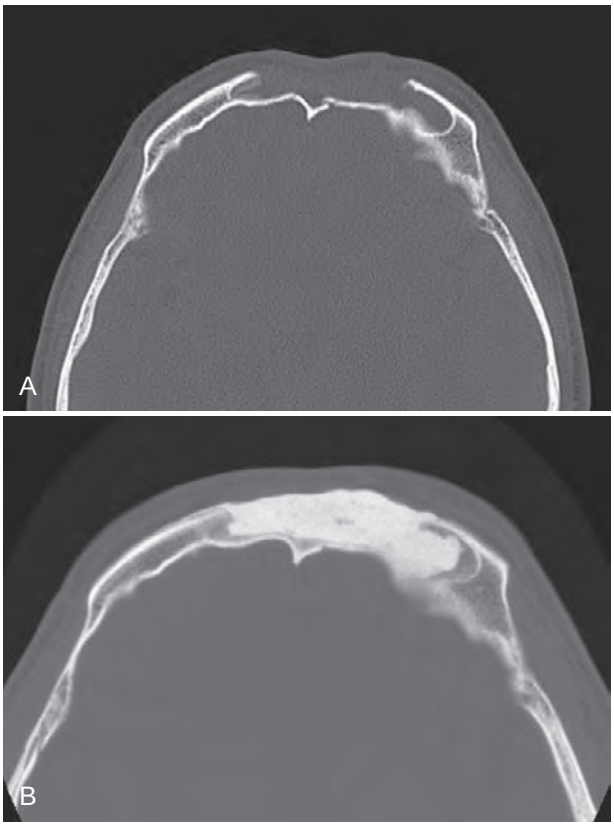

FIGURE 6-27 Axial bone windowed (**A**) and soft tissue (**B**) windowed CT scans of a patient who had a bilateral osteoplastic flap procedure.. The sinus cavities were filled with bony epoxy.

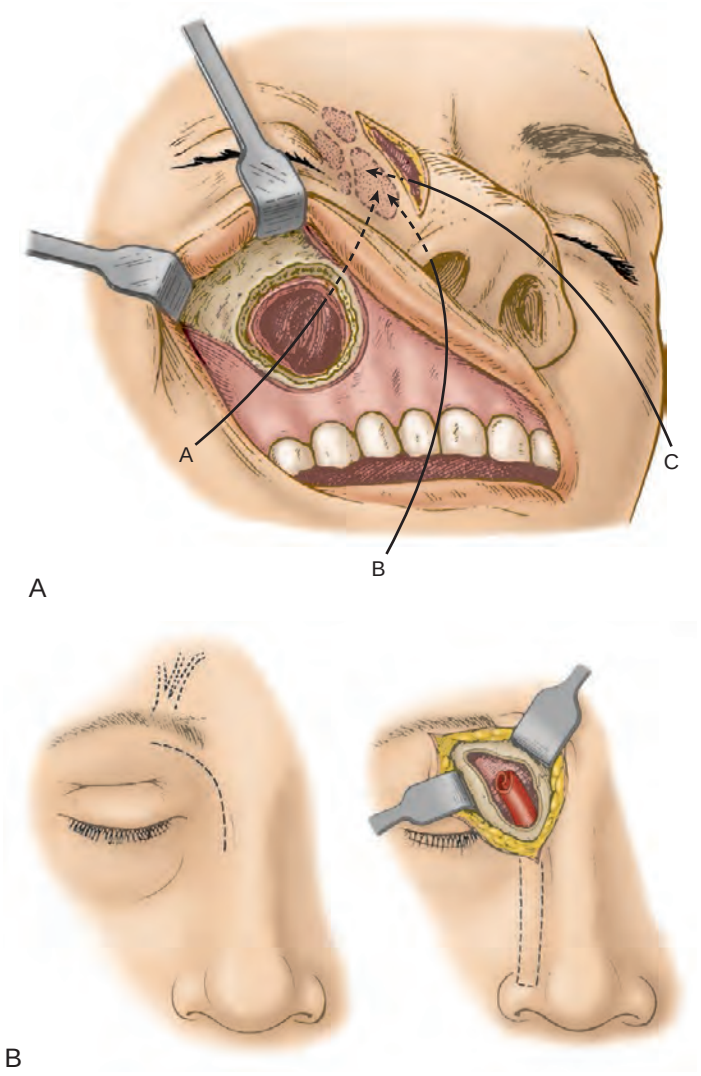

FIGURE 6-28 Diagram (**A**) of the three major surgical approaches to the right ethmoid sinuses. *A*, Transmaxillary or transantral. *B*, Internal or intranasal. *C*, External (Lynch). Diagram (**B**) shows Lynch's incision into the right ethmoid and lower frontal sinuses. A drainage tube is placed from the frontal sinus through the ethmoid complex into the nasal cavity.

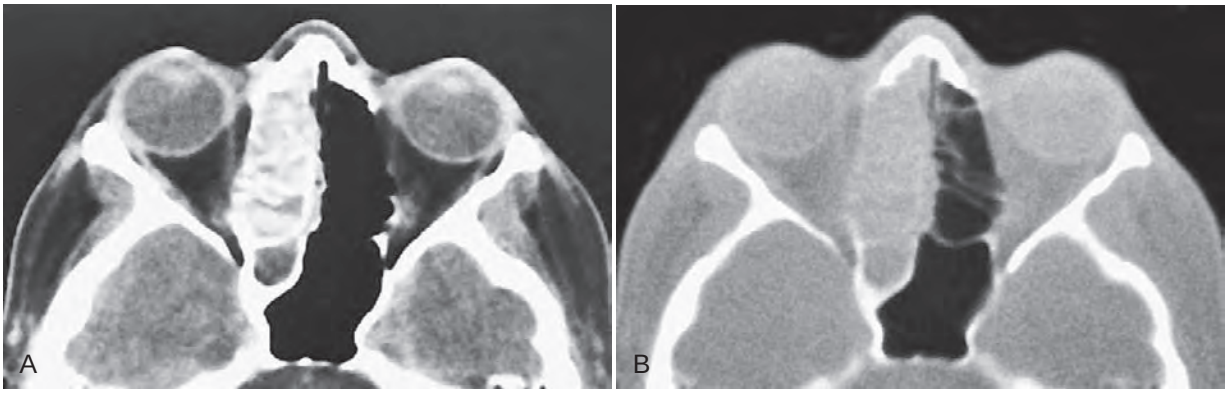

FIGURE 6-29 Axial CT scans at narrow (**A**) and wide (**B**) window settings show inflammatory disease in the right ethmoid and sphenoid sinuses. In **A**, there appears to have been a left sphenoethmoidectomy, as the septations are not seen. However, in **B**, the left ethmoid septa and the anterior sphenoid sinus wall are intact, indicating that no surgery was performed. To avoid such mistakes, these cases should always be viewed at wide window settings.

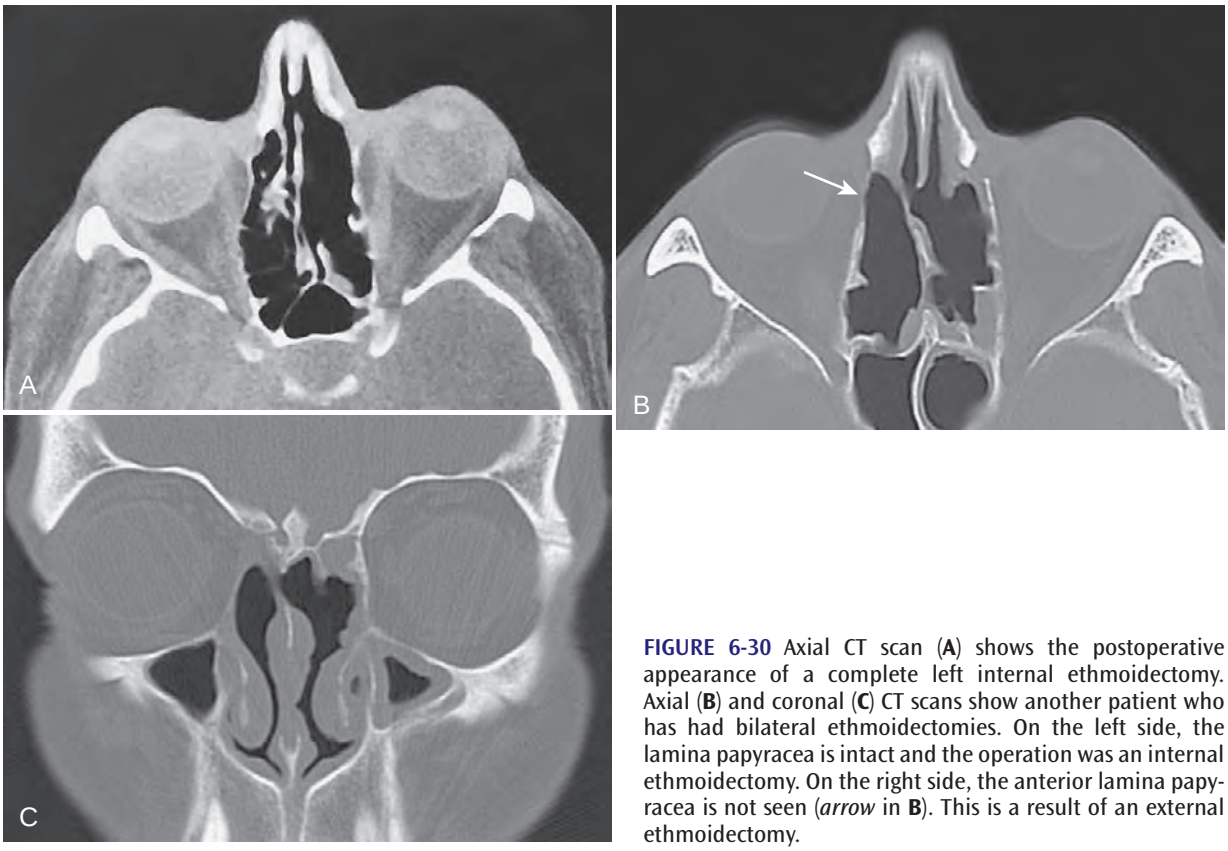

FIGURE 6-30 Axial CT scan (**A**) shows the postoperative appearance of a complete left internal ethmoidectomy. Axial (**B**) and coronal (**C**) CT scans show another patient who has had bilateral ethmoidectomies. On the left side, the lamina papyracea is intact and the operation was an internal ethmoidectomy. On the right side, the anterior lamina papyracea is not seen (*arrow* in **B**). This is a result of an external ethmoidectomy.

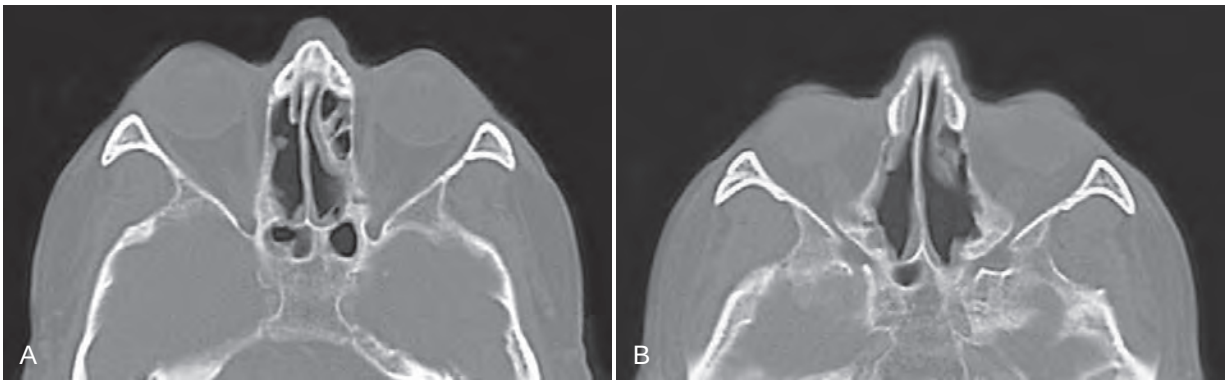

FIGURE 6-31 Axial CT scans at cranial (**A**) and caudal (**B**) levels of the ethmoid complex of a patient who has had bilateral internal ethmoidectomies. On the right side, almost all of the cells were removed. On the left side, the uppermost anterior cells remain. This appearance is typical of this operation, and the location of any remaining cells should be noted in the imaging reports of these cases.

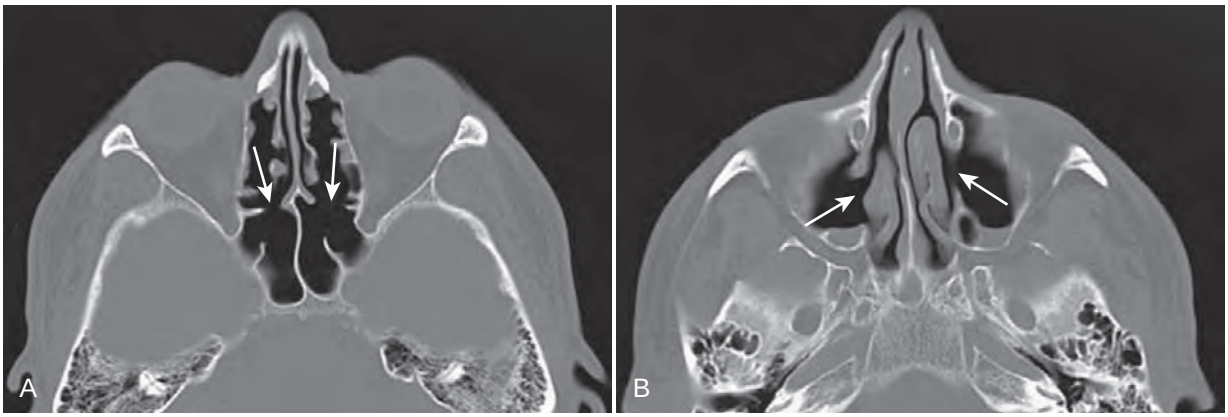

FIGURE 6-32 Axial CT scans through the ethmoid sinuses (**A**) and the upper maxillary sinuses (**B**) of a patient who had bilateral internal ethmoidectomies, bilateral sphenoid sinusotomies and bilateral antrostomies. Both lamina papyracea remain intact. The anterior walls of the sphenoid sinuses have partially been removed (*arrows* in **A**), and there are wide antrostomies (*arrows* in **B**). Small mucosal thickening is seen in the maxillary sinuses.

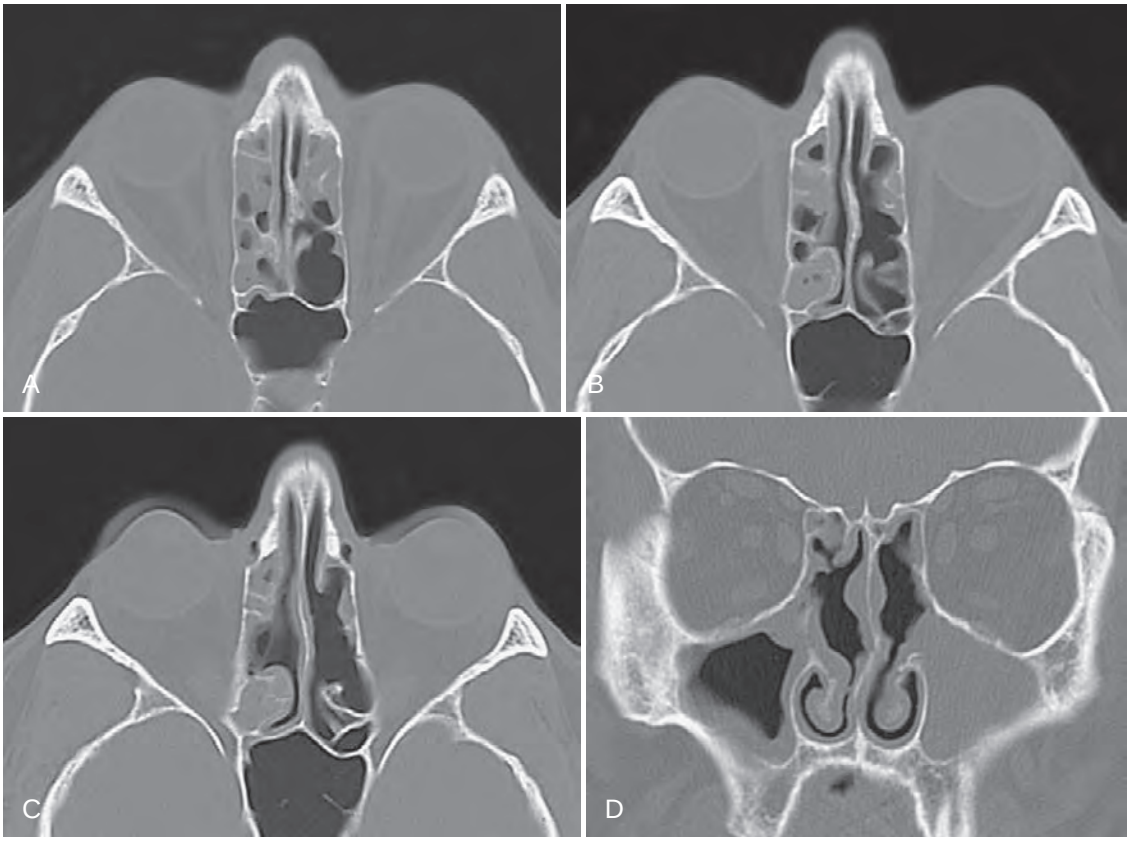

FIGURE 6-33 Serial axial CT scans from cranial (**A**) to caudal (**C**) and a coronal CT scan (**D**) on this patient who has had bilateral internal ethmoidectomies. The most superior cells remain anteriorly on both sides. The upper middle and posterior cells are also still present on the right side. Inflammatory disease is present in these remaining cells. Typically, the upper and posterior cells are not removed in internal ethmoidectomies because the surgeon does not want to enter the anterior cranial fossa inadvertently. The middle turbinates were removed at surgery, and inflammatory disease is present in both maxillary sinuses.

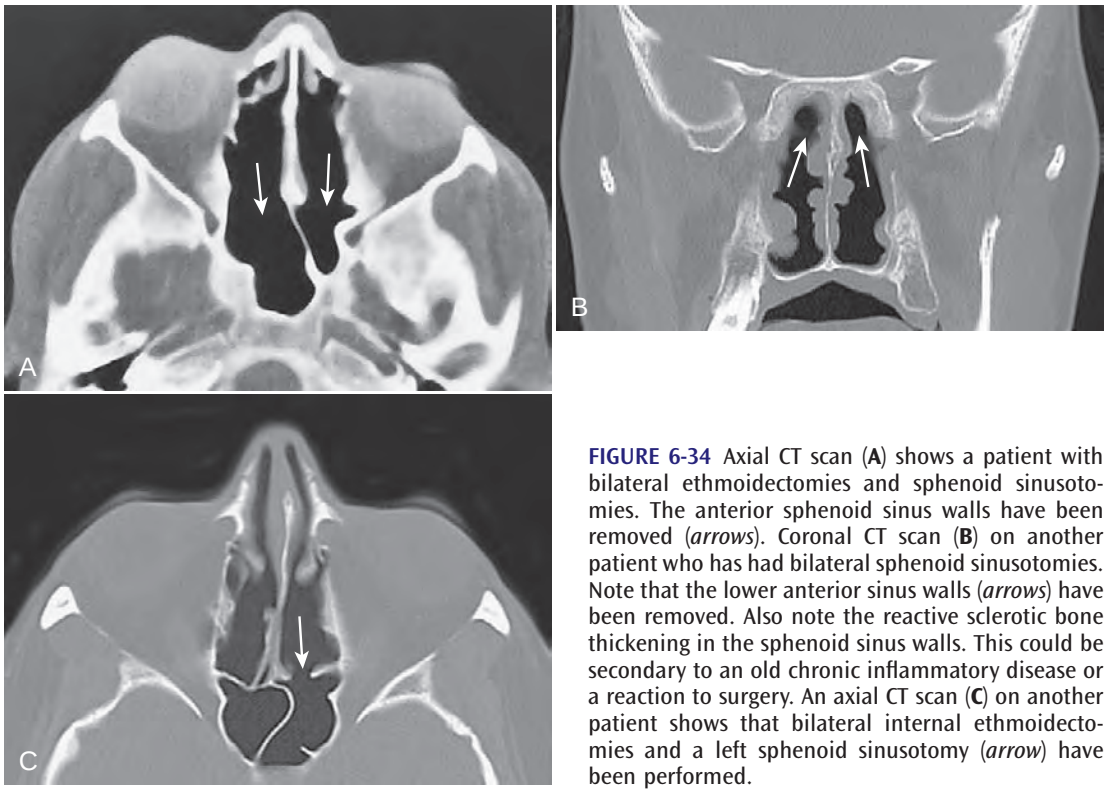

FIGURE 6-34 Axial CT scan (**A**) shows a patient with bilateral ethmoidectomies and sphenoid sinusotomies. The anterior sphenoid sinus walls have been removed (*arrows*). Coronal CT scan (**B**) on another patient who has had bilateral sphenoid sinusotomies. Note that the lower anterior sinus walls (*arrows*) have been removed. Also note the reactive sclerotic bone thickening in the sphenoid sinus walls. This could be secondary to an old chronic inflammatory disease or a reaction to surgery. An axial CT scan (**C**) on another patient shows that bilateral internal ethmoidectomies and a left sphenoid sinusotomy (*arrow*) have been performed.

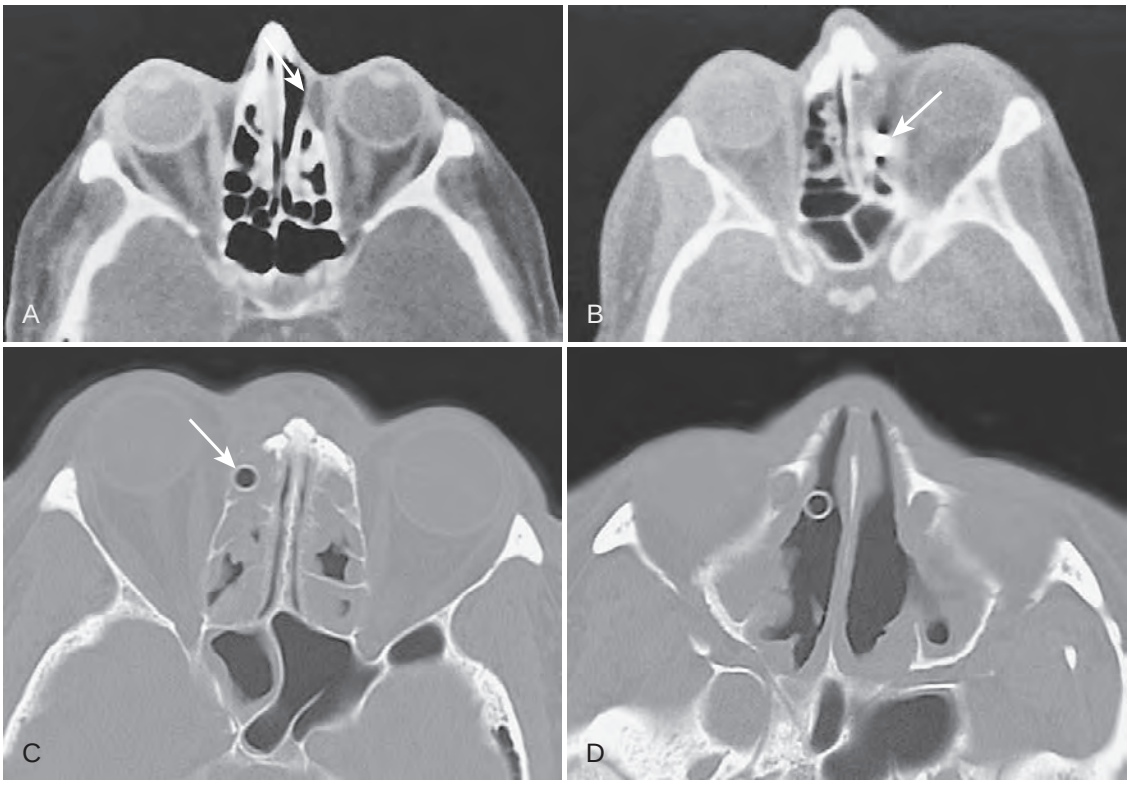

FIGURE 6-35 Axial CT scan (**A**) shows the postoperative appearance of a left external ethmoidectomy. The anterior lamina papyracea has been surgically removed and is replaced by fibrosis (*arrow*). Axial CT scan (**B**) shows a patient's status after a left external ethmoidectomy. The surgical clip (*arrow*) is used to control bleeding from the ethmoidal vessels. The soft tissue in the anterior ethmoid cavity was fibrosis and granulation tissue in this asymptomatic patient. Axial CT scans (**C** and **D**) on another patient show that a Lynch procedure was performed on the right side, and the drainage tube extends from the frontal sinus down through the ethmoid (*arrow* in **C**) sinus into the right nasal fossa (**D**).

performed today. The greatest application of this procedure is for radical orbital decompression for thyroid ophthalmopathy (Ogura-Sewell-Walsh procedure), in which the ethmoid labyrinth is extirpated through the medial antral wall, as well as the removal of the orbital floor.

To better define the borders of the ethmoid labyrinth and to more thoroughly extirpate the air cells, navigational guidance is used in which the tip of instruments can be localized in real time in the operating room. This is discussed in Chapter 5. Because disease can recur in any remaining cells, postoperative scans should be obtained if the patient's symptoms persist or recur.[1,2]

Because of the relatively small, box-like anatomy of the ethmoid complex, postoperative hemorrhage can fill some unresected cells and rather than resorb, on occasion the blood becomes fibrosed, or even ossified. Such en bloc fibrosis does not often occur after surgery in the other paranasal sinuses, but it is fairly common in the ethmoid complex. The imaging differentiation of recurrent disease from fibrosis can be difficult, as the attenuation values frequently are not sufficiently different to establish a definitive diagnosis. In general, on CT recurrent inflammation enhances and fibrosis does not.

Uncommonly, a dense fibrous scar develops within the postoperative ethmoid bed. This usually has low T1-weighted and T2-weighted signal intensity, and thus can be distinguished from active infection (which has a high signal intensity) on the T2-weighted scans. The denuded ethmoid bone may also develop a hyperostotic reaction that produces variable amounts of bone (Fig. 6-36). In some cases, a localized osteoma-like bone develops; in other cases, the entire postoperative cavity may be obliterated by the bone that often mimics the appearance of fibrous dysplasia. This type of bone reaction also occurs in the maxillary sinus and to a lesser degree in the sphenoid sinus. Uncommonly, reactive bone develops in the postoperative frontal sinus.

In addition to noting how extensive is the removal of the ethmoid septae, the imager should anticipate (1) an absent anterior third to half of the lamina papyracea from an external approach, (2) an absent medial ethmoid wall, upper antral wall and/or ostiomeatal complex and most often an abbreviated or absent middle turbinate from a partial turbinectomy associated with an internal approach, and (3) a Caldwell-Luc defect in the lower anterior antral wall, absent bone in the upper medial antral wall, resected ethmoid cells, and a defect from a partial turbinectomy associated with a transantral approach. Any residual soft tissues in the remaining ethmoid cells should be clearly noted by the imager for future reference.

If a postethmoidectomy cavity becomes obstructed after mucosal reepithelialization, a postoperative mucocele may develop (Fig. 6-37). This mucocele usually does not grow like a typical ethmoid mucocele, which tends to expand laterally into the orbit. Rather, this postoperative mucocele takes the course of least resistance and expands within the enlarged postoperative ethmoid cavity. It is only after the entire ethmoid cavity is filled that the mucocele bulges into the orbit. On imaging, characteristically there is a collection of entrapped secretions within the postoperative ethmoid.[12]

MAXILLARY SINUS SURGERY

Today, the most common diagnostic and therapeutic procedures performed on the antrum and the ostiomeatal complex are endoscopic, however, the Caldwell-Luc operation is still performed. Chapter 5 discusses the endoscopic techniques and their postoperative appearances.

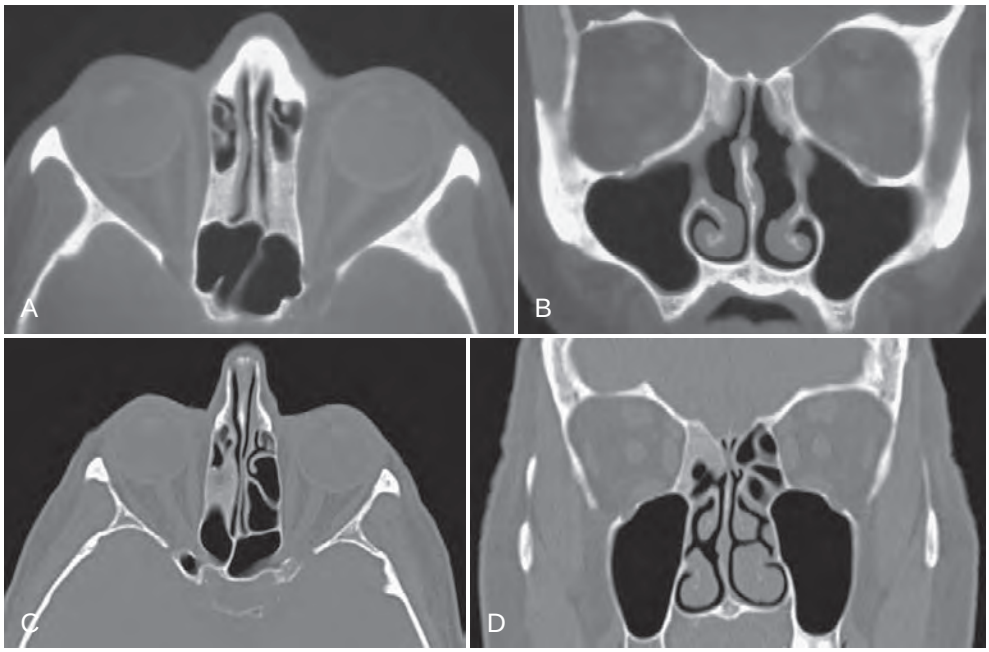

FIGURE 6-36 Axial (**A**) and coronal (**B**) CT scans of a patient who has had bilateral internal ethmoidectomies. "Ground glass"-appearing bone is present in the upper posterior and middle postoperative cavities, partially obliterating the postoperative ethmoid cavities. This is a normal postoperative bony reactive change and should not be misinterpreted as an abnormality. Axial (**C**) and coronal (**D**) CT scans on another patient who had a right internal ethmoidectomy. The thickened sclerotic bone in the upper post operative cavity is reactive bone, not fibroosseous disease, and is secondary to the surgery.

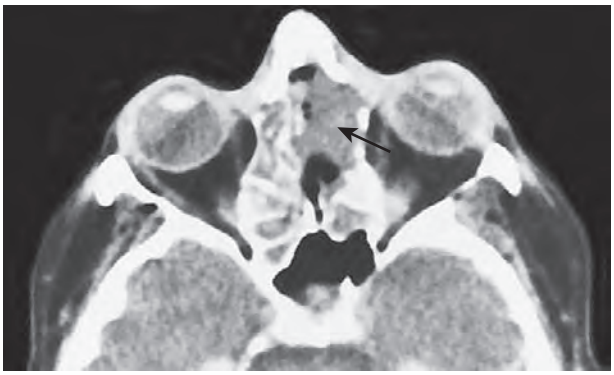

FIGURE 6-37 Axial CT scan shows the appearance of a left ethmoidectomy that has an accumulation of mucoid material within the postoperative cavity (*arrow*). Rather than extending into the left orbit as a typical ethmoid mucocele, the postoperative mucocele tends to fill the postethmoidectomy cavity first.

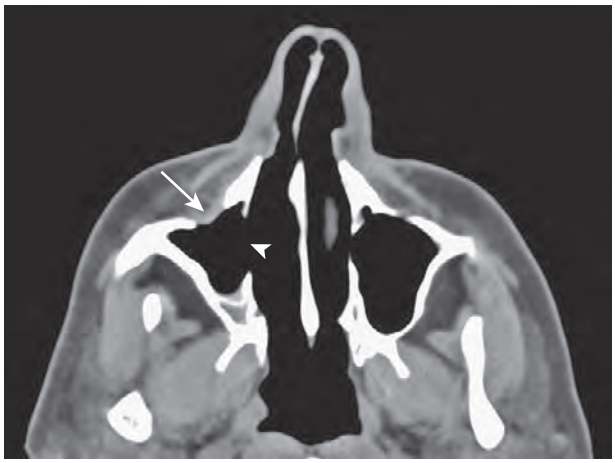

FIGURE 6-39 Axial CT scan of a patient who had a right Caldwell-Luc procedure. The approach defect in the anterior wall is closed by fibrous scar and the soft tissues of the cheek (*arrow*). The medial antrostomy defect is also seen (*arrowhead*).

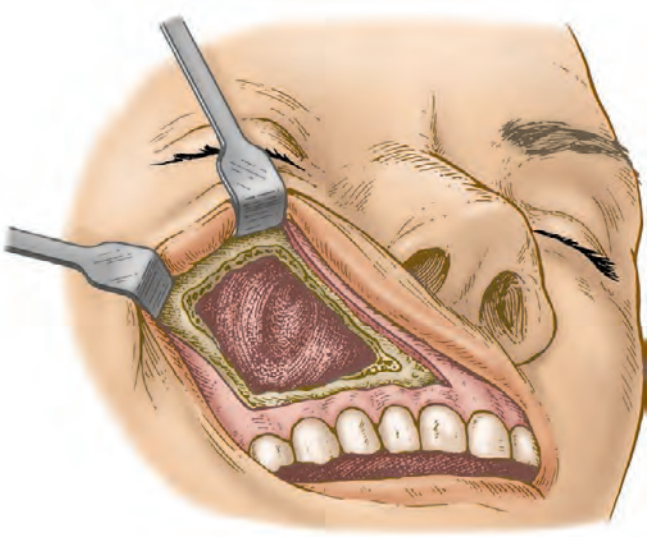

FIGURE 6-38 Diagram of the Caldwell-Luc approach to the right maxillary sinus. The maxillary sinus is entered anteriorly under the lip via the canine fossa. The hole in the sinus can be variable in size. A medial antrostomy is also performed.

Intranasal Antrostomy and the Caldwell-Luc Procedure

An intranasal antrostomy is generally performed in the middle meatus, with the membranous and bony wall removed to enhance mucociliary flow into the nasal cavity. Rarely, an antrostomy is made in the inferior meatus to create better gravity drainage for the sinus. In the Caldwell-Luc procedure, in addition to the intranasal antrostomy, the maxillary sinus is entered via the canine fossa region of the lower anterolateral antral wall. Because this entrance scar is intraoral, there is no facial scarring (Fig. 6-38). Once the sinus is entered, the diseased mucosa is removed. Initially the anterior wall bony defect is closed by a hematoma that eventually undergoes fibrosis (Figs. 6-39 and 6-40). However, this hematoma can occasionally become infected, and in rare instances an oroantral fistula may develop. If this complication occurs, it is usually within the first or second postoperative week.

Via the Caldwell-Luc approach, the bone of the posterior sinus wall can also be removed to provide access to the pterygopalatine fossa for internal maxillary artery ligation or to expose the vidian nerve, and pterygopalatine ganglion.[5] In such cases, a bony defect in the upper medial and posterior antral wall also can be seen on imaging.

In some patients, synechiae develop between the posterior maxillary sinus wall and the margins of the canine fossa/Caldwell-Luc defect in the anterior sinus wall. Such synechiae may form the basis for the development of a membrane that extends across the sinus between the anterior and posterior walls. Once formed, this membrane may obstruct the drainage of the lateral portion of the maxillary sinus and lead to the appearance of a postoperative antral mucocele. In these cases, the medial postoperative sinus cavity may remain aerated, while the lateral sinus cavity first becomes obstructed and then expands, as a mucocele develops. The imaging appearance of a laterally expanded mucoid mass in such a sinus signifies the presence of a postoperative mucocele (Figs. 6-41 and 6-42). Less often, a postoperative antral mucocele can occur in the tuberosity recess, or in the palatal recess.

As previously mentioned, once the sinus mucosa has been stripped from the sinus wall, a reaction may be elicited that results in reactive bone formation, thickening of the sinus wall, and reduction, or obliteration of the sinus cavity. Such a reaction is an expected consequence of the procedure and should not necessarily signify to the radiologist that active infection is present (see Figs. 6-40 and 6-43).[13]

Optic nerve compression and decreased visual acuity in patients with thyroid ophthalmopathy may be treated by surgical decompression of the orbit. The procedures most commonly employed are a lateral orbitotomy (Krönlein's procedure); an antral roof (orbital floor) decompression using a Caldwell-Luc approach; an ethmoid decompression using an external ethmoidectomy approach; and an orbital roof decompression accomplished via a craniotomy. Of these operations, the greatest degree of decompression from a single procedure is obtained from the orbital floor approach. However, this procedure must be performed bilaterally so that the visual axes are not made asymmetric, resulting in diplopia and cosmetic

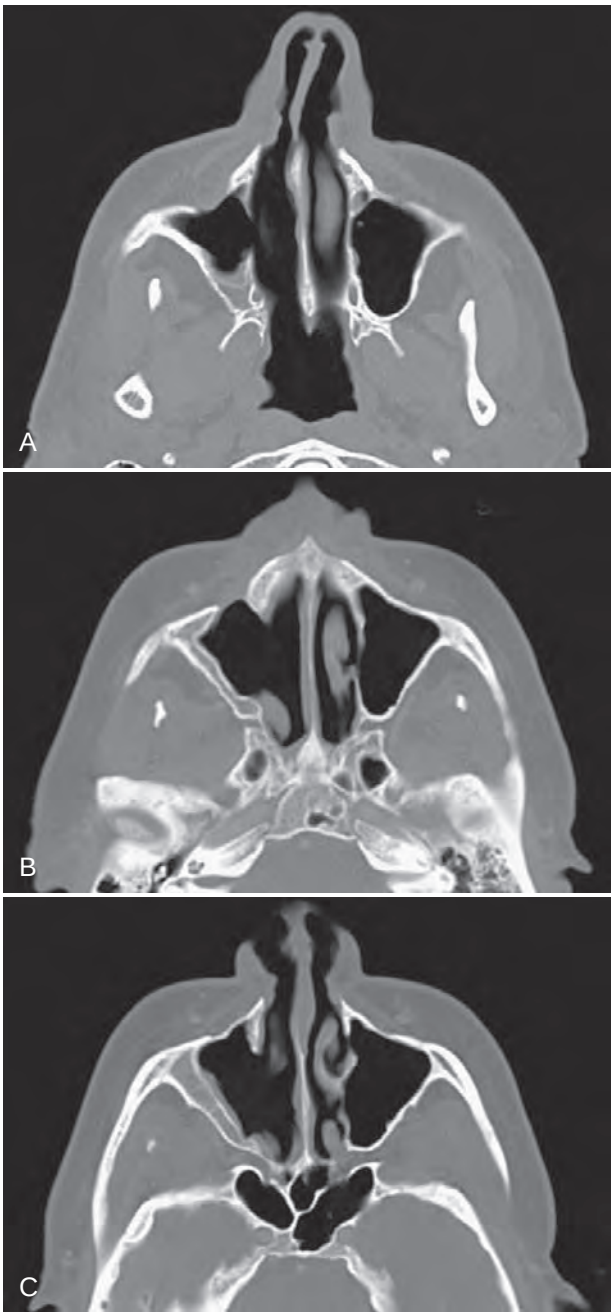

FIGURE 6-40 Axial CT scans (**A** to **C**) on three different patients who had Caldwell-Luc operations on the right side. In **A**, there is some sclerotic bone thickening along the posterolateral antral wall. In **B**, the reactive sclerosis and thickening of the posterolateral antral wall is more prominent than in **A**. In **C**, the wall thickening is even greater than in **B**. These are all normal postoperative findings from this operation.

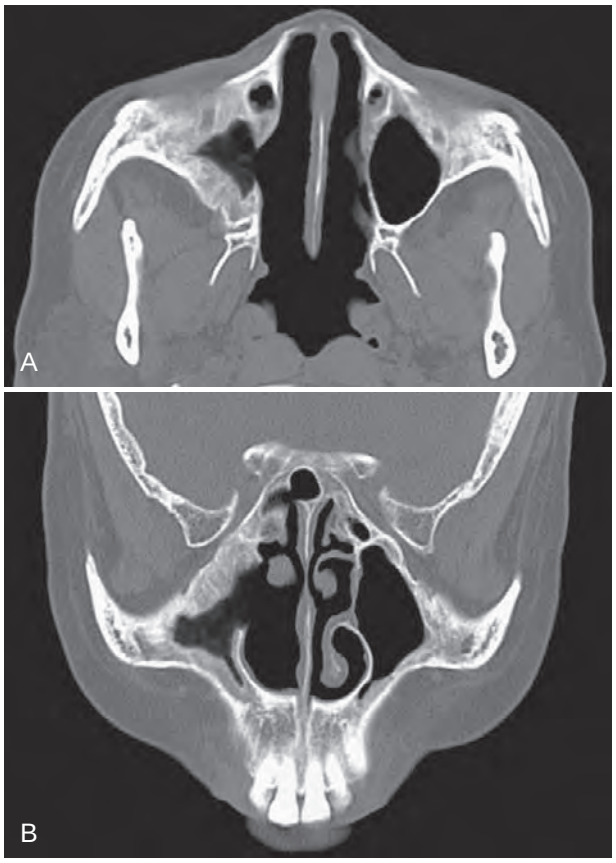

FIGURE 6-41 Axial (**A**) and coronal (**B**) CT scans of a patient who had a right medial antrostomy. There is marked sclerotic thickening of the remaining antral walls with resultant diminishing of the antral cavity. This appearance could be a result of prior chronic sinusitis, the operative procedure, or both. This is a normal postoperative appearance. This patient also had a right inferior turbinectomy and an internal ethmoidectomy.

deformity. The lateral and ethmoid decompressions can be combined with antral decompressions to achieve maximal relief of exophthalmos and a decrease in intraorbital pressure (Fig. 6-44). The orbital roof approach provides relatively little decompression, and because it is a more extensive surgical approach, it is reserved for the most severe cases. A decompression procedure has been developed that opens the posterior orbital wall as it is formed by the greater wing of the sphenoid bone. This approach, although not yet widely practiced, addresses the orbital apex relief more directly than the other approaches.[14,15]

On sectional imaging, the absence of the lateral portion of the orbital wall may at first elude detection, the imager's attention being drawn by pronounced proptosis with muscle enlargement. However, careful evaluation of the bony orbital walls will show that a Krönlein's procedure was performed. The ethmoid decompression has the same appearance as an external ethmoidectomy, with the orbital muscle findings of thyroid ophthalmopathy suggesting the diagnosis. The antral decompression reveals prolapse of the orbital fat and inferior muscles into the upper maxillary sinuses. Without a clinical history, axial scans are often suggestive of unusual antral disease. However, coronal scans reveal that most of the orbital floor bone is missing, a finding that differentiates this postoperative appearance from the rare event of bilateral orbital floor blowout fractures, in which the displaced fracture's segments can be identified.

FIGURE 6-42 Axial CT scan (**A**) of a patient who has had bilateral Caldwell-Luc procedures. On the right side, the defect is fibrosed over and the sinus cavity is opacified. On the left side, fibrous strands extend from the surgical defect to the posterior sinus wall. Axial CT scan (**B**) of a patient after a right Caldwell-Luc procedure. On this more cranial scan through the antrum, a septum has formed between the anterior and posterior sinus walls. If this septum completely obstructs the lateral portion of the sinus, a postoperative mucocele will develop.

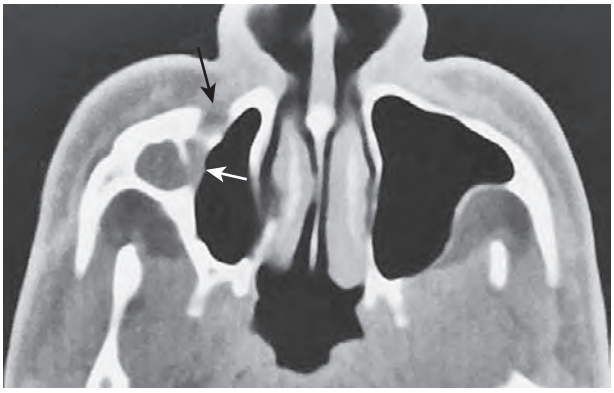

FIGURE 6-43 Axial CT scan shows an anterior Caldwell-Luc defect in the right maxillary sinus wall (*black arrow*). There is an expansile mass in the lateral portion of the right antrum (*white arrow*). This patient had a postoperative antral mucocele.

SPHENOID SINUS SURGERY

The sphenoid sinuses can be approached through the anterior sinus wall for biopsy, to improve sinus drainage, or to remove inflammatory tissue. The sphenoid sinusotomy opens the anterior wall of the sinus and creates a wide-open cavity that leads into the nasopharynx. Although sphenoid sinusotomies are today most often accomplished via an endoscopic surgical approach, the sinus can be reached by intranasal, transseptal, transmaxillary, or transethmoidal (transorbital) approaches.

In the transnasal approach, portions of the posterior middle turbinate, the superior turbinate, and some of the posterior ethmoid cells are removed to gain exposure. In the transseptal approach, portions of the cartilaginous and bony nasal septum (vomer) are removed. The transmaxillary approach is an extension of a Caldwell-Luc procedure in which a transmaxillary ethmoidectomy is extended to include the anterior sphenoid sinus wall. The transethmoidal approach is simply a posterior extension of an external ethmoidectomy procedure. Thus, depending on the approach used, in addition to a widened sphenoid sinus ostium, or absence of the anterior sphenoid sinus wall, the respective surgical defects just described should be observed on images.[5,7]

When a sphenoid sinusotomy is performed, care must be taken to avoid trauma to the carotid artery. In 17% of patients the bony wall separating the sinus and artery is so thin that it provides little if any protection from trauma, and carotid artery damage may lead to a posttraumatic aneurysm or a carotid–cavernous fistula.[16,17] Similarly, damage can occur to the cavernous sinus and to the vidian, maxillary, and optic nerves in those patients who have these nerves running within the sinus (see Chapters 2 and 5).

A transsphenoidal hypophysectomy can be performed as an extension of a sphenoid sinusotomy. Once the sphenoid sinus cavity is surgically exposed, portions of the anterior wall and the floor of the sella turcica can be removed and the pituitary fossa entered from below. Muscle, fat, cartilage, or bone may be used to seal the surgical defect. On sectional imaging, in addition to the site of surgical bone removal, occasionally sclerotic thickening of the remaining portions of the anterior wall and the floor of the sella turcica may be observed. Some postoperative prolapse of sellar contents can occur into the obliterated sphenoid sinus. Without benefit of the surgical history, the imaging picture can simulate that of a large pituitary tumor with extension into the sphenoid sinus.

In the preoperative evaluation of patients being considered for a transsphenoidal hypophysectomy, the imager must direct special attention to the thickness of the bone forming the anterior wall of the sella turcica. In nearly 99% of patients, the sphenoid sinus development extends back to within 1 mm of the anterior wall or under the sellar floor. However, in the 1% of patients in whom a thick margin of bone remains between the sinus and sella, the transsphenoidal approach is not desirable; instead, an intracranial approach is used.[18]

As the ostia of the sphenoid sinuses are quite small and often not clearly identified on axial imaging, whenever a large opening is seen in the anterior sphenoid sinus wall a sphenoid sinusotomy has probably been performed (see Figs. 6-32 and 6-34).

SURGERY FOR SINUS MALIGNANCY

The type of oncologic ablation operation performed on the maxillary sinus varies, depending upon the precise location of the primary neoplasm. A tumor affecting the lower portion of the antrum may require an infrastructure-type partial maxillectomy, whereas a nasal tumor may require a medial maxillectomy. More extensive tumor necessitates a total

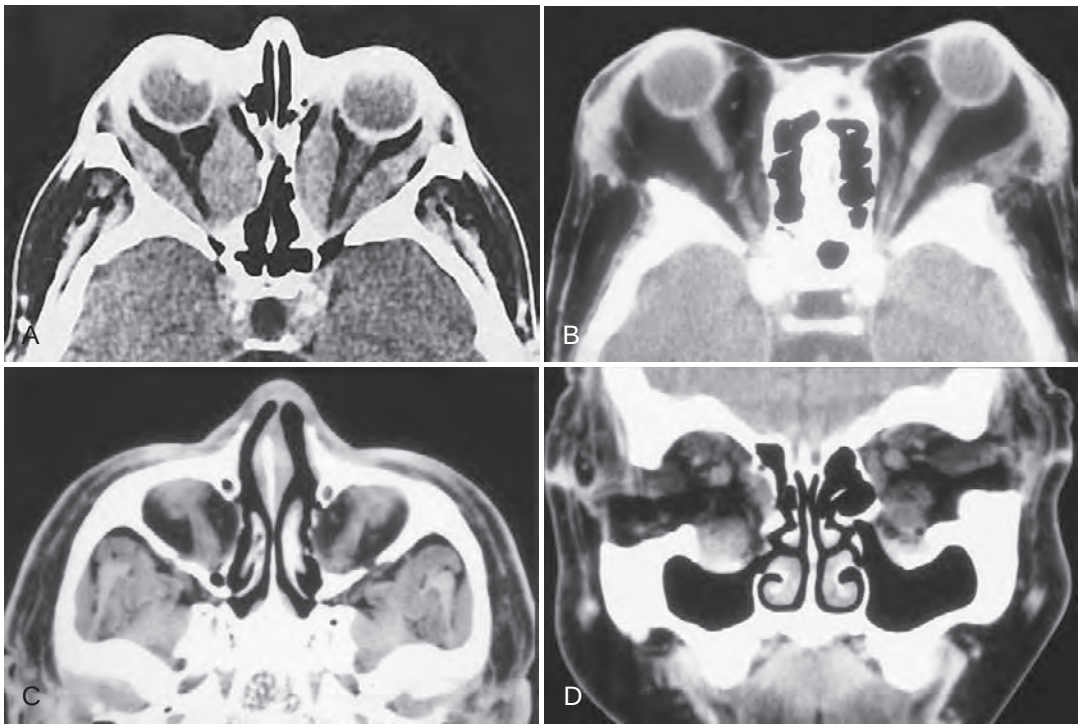

FIGURE 6-44 Axial CT scan (**A**) shows large muscle bellies in the extraocular muscles with tapering at the anterior tendon insertions. The ethmoid complexes have been collapsed by a decompression procedure to create more orbital volume. This patient had thyroid ophthalmopathy. Very-long-standing severe thyroid ophthalmopathy can also remodel the ethmoid walls and appear similar to the postoperative decompression appearance. Axial CT scan (**B**) on a different patient with thyroid ophthalmopathy. Lateral orbitotomies (Krönlein's procedures) have been performed bilaterally, allowing the orbital fat and contents to extend laterally in an attempt to decompress the orbit. The removal of the anterior lateral orbital walls makes any proptosis appear more extensive than it is. This approach is favored by ophthalmologists. Axial CT scan (**C**) on a third patient with thyroid ophthalmopathy shows the inferior orbital contents projecting down into the upper maxillary sinuses. This patient had orbital floor decompressions, which provide the most volume increase to the orbit. This approach is favored by otolaryngologists. Coronal CT scan (**D**) on another patient with bilateral thyroid ophthalmopathy, who had bilateral Krönlein procedures, bilateral orbital floor decompression procedures, and a medial right ethmoid decompression.

maxillectomy with or without removal of the pterygoid plates and adjacent structures. A partial or total ethmoidectomy is often combined with a maxillectomy for complete tumor extirpation (Figs. 6-45 to 6-47). Bone sections utilized in reconstructions are usually fixed together with osteosynthesis microplates or miniplates in a similar manner to the use of these plates in fracture repair cases (Fig. 6-48).

Medial Maxillectomy

For localized nasal tumors that only involve a portion of the medial antral wall, a partial or medial maxillectomy is performed, usually in association with a partial ethmoidectomy and resection of the nasal tumor. If the lower antral wall is involved, portions of the adjacent hard palate and maxillary alveolus may also be included in the resection (see Fig. 6-45). Thus, in a partial maxillectomy, the medial antral wall, the inferior turbinate, often the middle turbinate, the lower ethmoid cells, and, if appropriate, portions of the hard palate and alveolus are removed. The lateral portion of the antrum and its mucosa remain intact.

Total Maxillectomy

For more extensive tumors, a total maxillectomy is performed (see Figs. 6-46 and 6-47). In addition to resection of the maxilla, there is some variation as to what is included in the resection. Such surgery may include the body of the zygoma, the ipsilateral hard palate and alveolus, the inferior turbinate, and often the pterygoid plates and portions of the ethmoid sinuses.[19,20] Modifications are made to fit the specific tumor location. Thus the orbital floor may be left in place or it may be included along with an orbital exenteration. The latter is performed when there is gross tumor extension into the orbit.

Erosion of the bones lining the orbit may necessitate an orbital exenteration, and the degree of orbital involvement must be noted by the imager so as to aid the clinician in planning surgery. Gross orbital invasion almost always requires an orbital exenteration. However, erosion of bone, without gross penetration of the periorbita, may or may not necessitate an orbital exenteration. To some degree, this depends on the particular philosophy of the clinician, the tumor histology, and the patient's age and preferences.

Today, there is a tendency not to exenterate an orbit for minimal disease, especially if the periorbita remains intact. This is a less-aggressive approach than that of several decades ago, when exenteration was almost always performed. This is partly a result of better chemotherapy/radiation treatments and partly because of a change in philosophy based on statistics noting tumor recurrences.

For squamous cell carcinoma, the initial involvement of any orbital bone must be considered when surgery is performed, even if preoperative chemotherapy/radiation has shrunk the

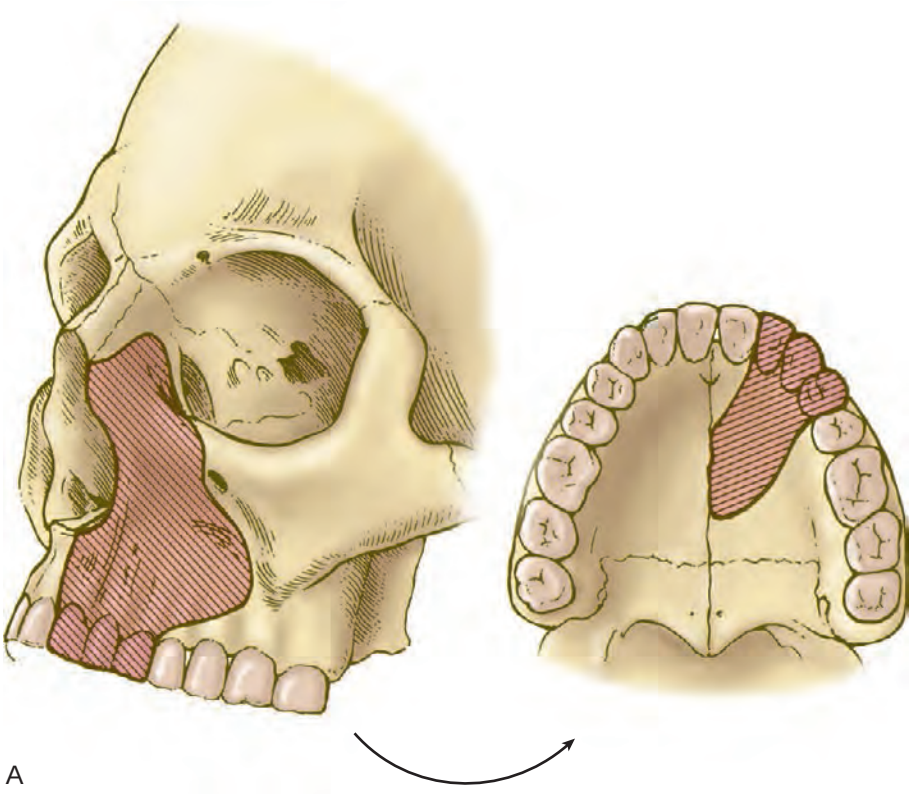

A

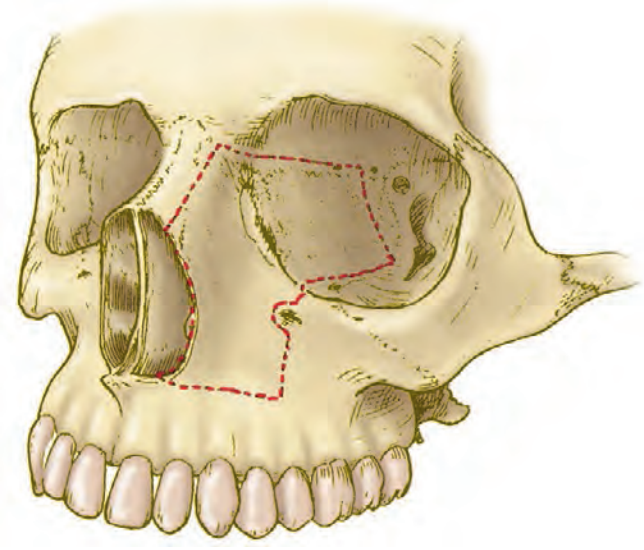

B

FIGURE 6-45 Diagram (**A**) of a typical medial maxillectomy resection. A portion of the palate is removed if needed to obtain a tumor-free margin. The medial antral wall and inferior turbinate are also included in the resection. Diagram (**B**) shows a typical variation of a medial maxillectomy operation.

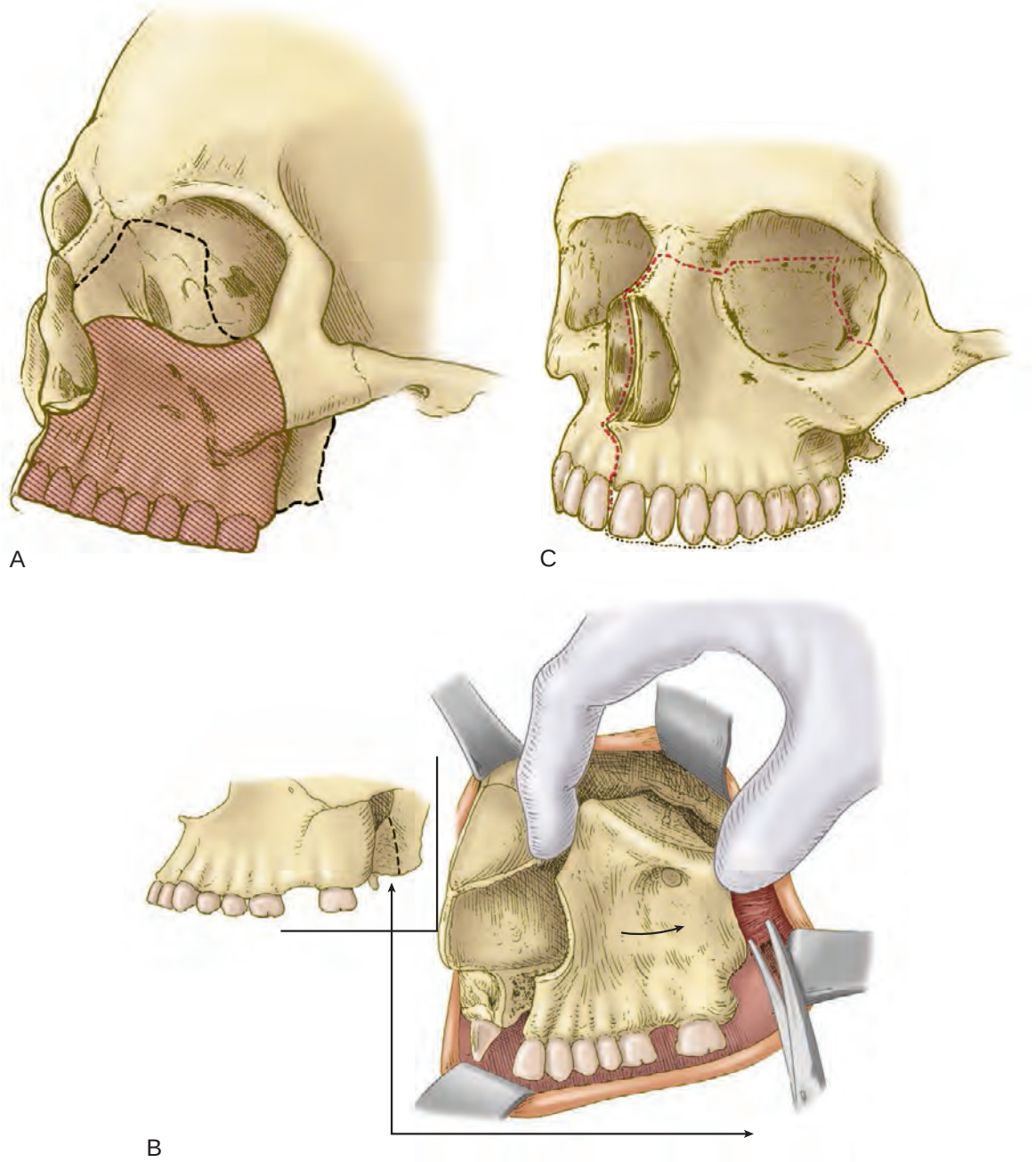

FIGURE 6-46 Diagram (**A**) of a typical total maxillectomy resection. Variable portions of the zygoma and pterygoid plates may be included in the resection. Similarly, the orbital floor may be taken in its entirety, and an ethmoid resection (*dotted line*) may also be included to obtain a tumor-free margin. Diagram (**B**) showing the technique of performing a total maxillectomy. Diagram (**C**) shows the variation of the margins of a radical maxillectomy.

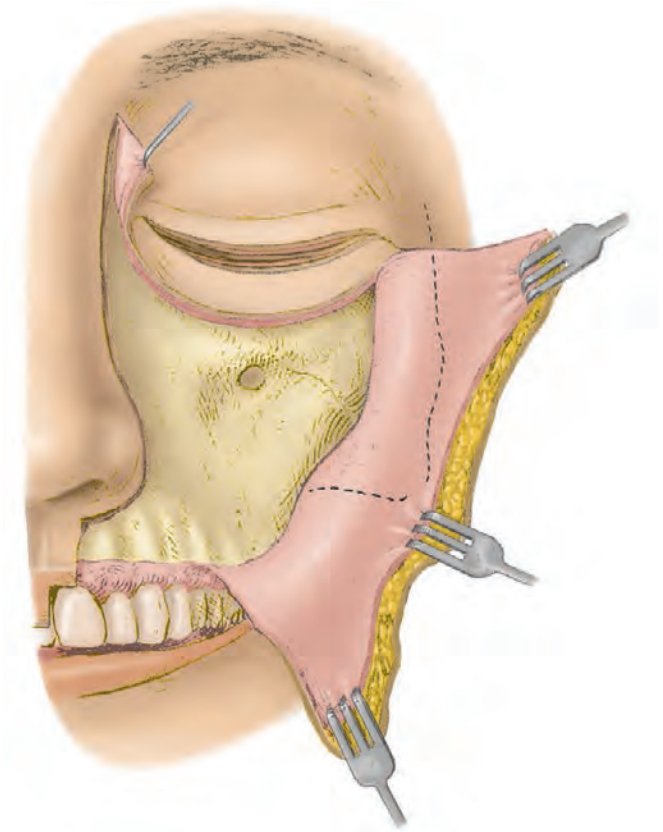

FIGURE 6-47 Drawing of a Weber-Fergusson incision to expose the maxilla. During this approach, the infraorbital nerve is transected and the exposure extends to the anterior zygomatic arch and the lateral canthal margin.

tumor away from the orbit. The rule is to include the original tumor margins in the resection. Failure to do so usually results in an orbital margin recurrence. With other tumors such as olfactory neuroblastomas, initial involvement of the orbital wall need not result in an exenteration. If there is a good preoperative tumor response to chemotherapy/radiation and the orbit becomes grossly free of tumor, tumor resection without an exenteration may be curative in most cases.

After the bone is resected, the postmaxillectomy cavity can be lined with a split-thickness skin graft to create an immediate epithelial surface. Today, there is a tendency to obliterate the postoperative maxillectomy cavity, with or without an ethmoidectomy, by using a pedicle or free flap. Such a flap brings skin, muscle, fat, and bone into an area in which they normally are not present, and recognition of such a flap will obviate difficulties in interpreting postoperative CT and MR images.

If the orbital floor was removed, various synthetic implants can be placed to help support the orbital contents. Similarly, bone and prosthetic material can be placed to support the anterior and lateral facial structure, and prostheses can be placed to fill the surgical defects created in the hard palate and alveolus. Such postoperative reconstructions can cause imaging problems, either because they may degrade the image quality or because they may simulate tumor. Eye prostheses also may cause degradation artifacts on scans.

The sinus cavity in a partial maxillectomy patient is lined by normal mucosa. The defect after a total maxillectomy can be lined either by a split-thickness skin graft or a myocutaneous flap. In any case, after a 4- to 6-week postoperative interval, nearly all of the operation-related edema and hemorrhage will have subsided and a baseline scan should be performed. This scan maps the patient's new anatomy and establishes the contour and thickness of the postoperative mucosal surfaces. The normal postoperative mucosa is smooth and moderately thin (Figs. 6-49 to 6-61). Any localized area of soft-tissue nodularity or mucosal–submucosal thickening must be suspected of representing recurrent tumor until proven otherwise (Figs. 6-62 to 6-65). If such an area develops that was not noted on the baseline scan, the imager should direct the clinician specifically to this site for biopsy. This approach has led to more positive biopsy specimens than are obtained from clinical assessment alone. The routine postoperative imaging followup of patients has also led to identification of small, early recurrences that were overlooked on routine clinical followup.[20] As with the Caldwell-Luc procedure, uncommonly, a mucocele may develop, often in a remaining zygomatic recess area (Figs. 6-66 and 6-67). As with all sinonasal malignancies, one must always look for perineural extension into the skull base and cavernous sinuses (Fig. 6-68).

EXTENSIVE NASOETHMOID SURGERY

The lateral rhinotomy provides access to the entire nasal cavity and the maxillary, ethmoid, and sphenoid sinuses. Modifications and extensions of this approach can be used to include access to the frontal sinuses. The typical incision extends from just below the medial end of one eyebrow, caudally between the nasal dorsum and medial canthus of the eye, down the nasofacial crease, and along the nasal alar rim. The incision can be extended down the upper lip if necessary. Following bony osteotomies, the nose is reflected to the opposite side, thereby exposing the pyriform aperture. This procedure gives access to the entire lateral nasal wall and nasal septum. The specimen usually includes the medial antral wall, the ethmoid cells, and the inferior and middle turbinates en bloc. The anterior sphenoid wall can be resected via this procedure, and the operation can be extended to include the entire nasal septum and contralateral nasal cavity structures, through a total rhinotomy. In general, the operation of choice for a unilateral nasal tumor is a medial maxillectomy with a lateral rhinotomy and ethmoidectomy. Despite the extent of the resection, the cosmetic and functional results are excellent. Regarding patient followup, as with the postmaxillectomy patient, the same general imaging rules apply, namely, one must suspect tumor at sites of soft-tissue nodularity and mucosal thickening (see Figs. 6-62 to 6-68).

CRANIOFACIAL RESECTION

This large composite operation was introduced in 1954, and is reserved for patients with tumors of the superior nasal cavity, ethmoid sinuses, frontal sinuses, anterior sphenoid sinuses, and orbits that extend to or through the floor of the anterior cranial fossa.[21] The operation essentially combines a frontal craniotomy with a resection of the midportion of the floor of the anterior cranial fossa and an extended lateral rhinotomy–maxillectomy. The surgery is often performed by a skull base team comprised of a neurosurgeon and an otolaryngologist.

Text continued on page 477

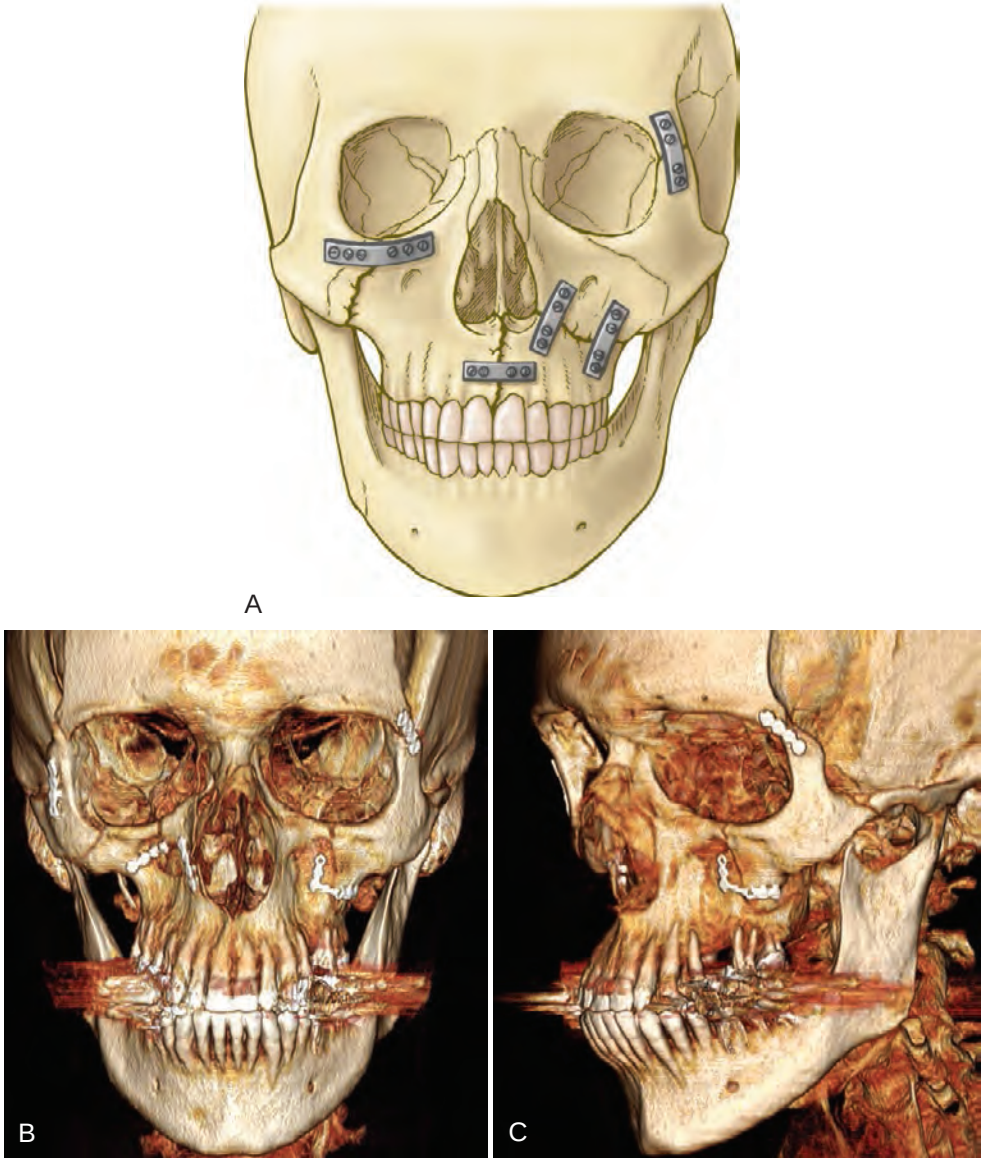

FIGURE 6-48 Frontal drawing (**A**) showing the use of osteosynthesis microplates and miniplates. These plates stabilize the adjacent bones in all directions. They are used to secure fracture segments as well as bone reconstructions in cancer surgery. Frontal (**B**) and left anterior oblique (**C**) 3D reconstruction showing the appearance of these osteosynthesis plates in this type of imaging reconstruction.

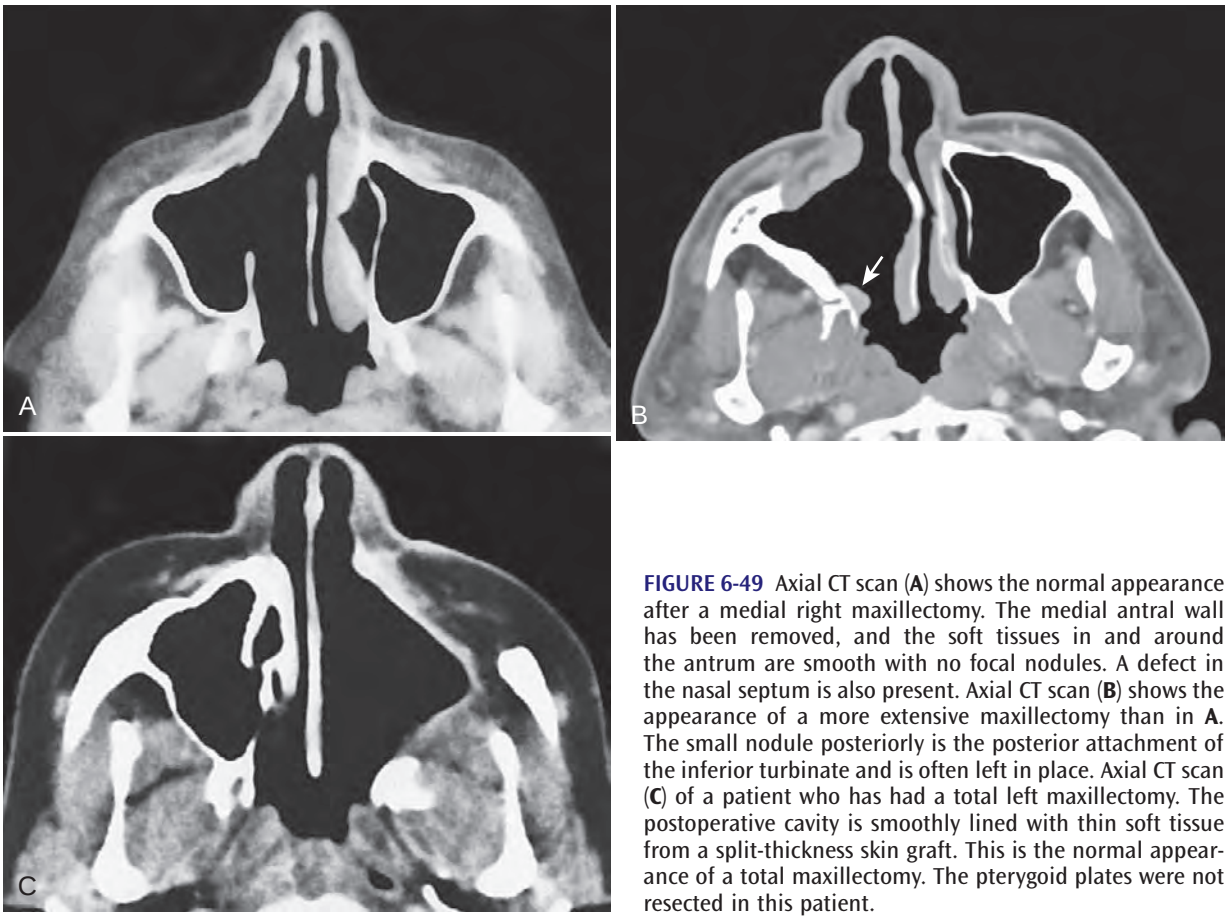

FIGURE 6-49 Axial CT scan (**A**) shows the normal appearance after a medial right maxillectomy. The medial antral wall has been removed, and the soft tissues in and around the antrum are smooth with no focal nodules. A defect in the nasal septum is also present. Axial CT scan (**B**) shows the appearance of a more extensive maxillectomy than in **A**. The small nodule posteriorly is the posterior attachment of the inferior turbinate and is often left in place. Axial CT scan (**C**) of a patient who has had a total left maxillectomy. The postoperative cavity is smoothly lined with thin soft tissue from a split-thickness skin graft. This is the normal appearance of a total maxillectomy. The pterygoid plates were not resected in this patient.

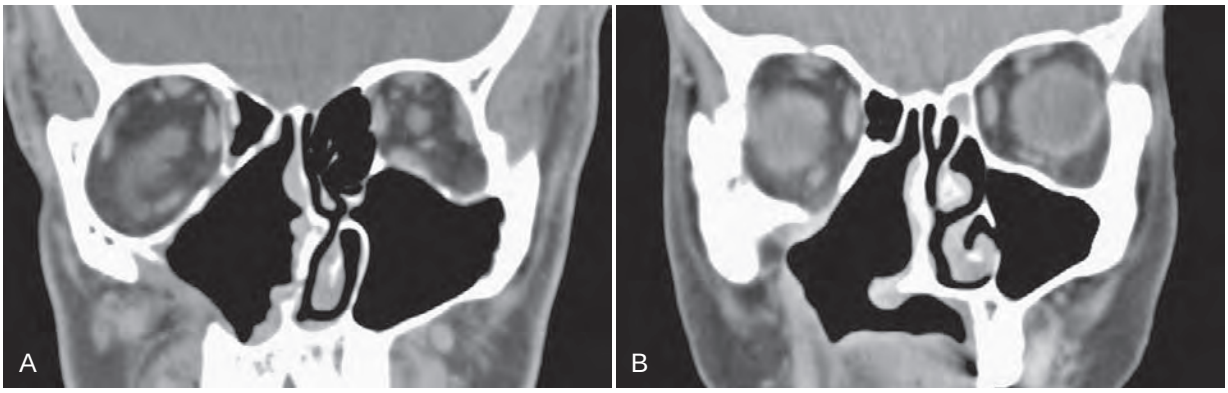

FIGURE 6-50 Coronal CT scans (**A** and **B**) on two different patients who had near-total right maxillectomies. The graft-lined postoperative antral cavities are smooth with uniformly thin soft tissue. In **B**, part of the right palate was resected.

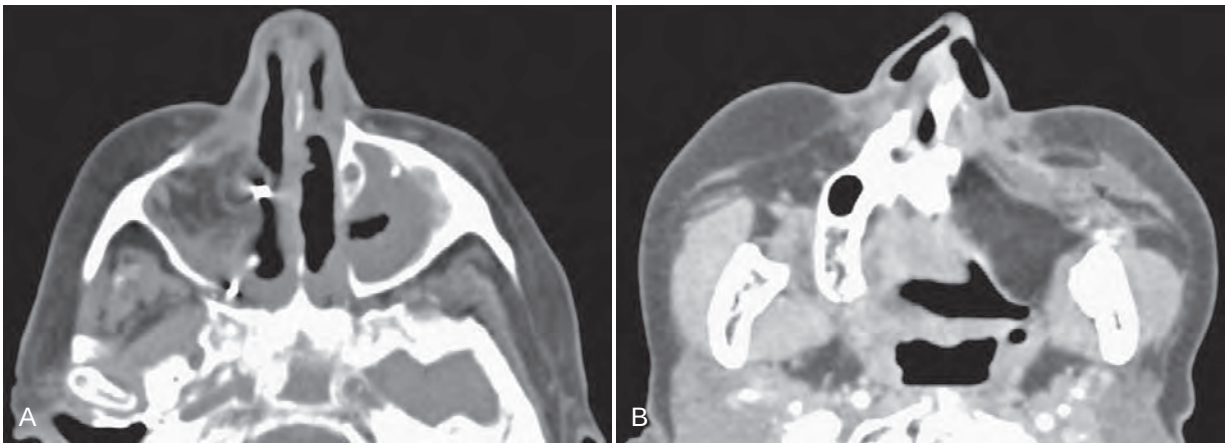

FIGURE 6-51 Axial CT scan (**A**) shows a patient who had a right partial maxillectomy with a flap reconstruction of the defect. Inflammatory mucosal thickening is also present in the left antrum. Axial CT scan (**B**) shows a patient who has had a left total maxillectomy with a graft reconstruction filling the operative defect. In both cases, linear and curvilinear soft tissues within the flap are normal muscle fibers and fibrous strands. No nodule should be seen within the flap or along the flap margins.

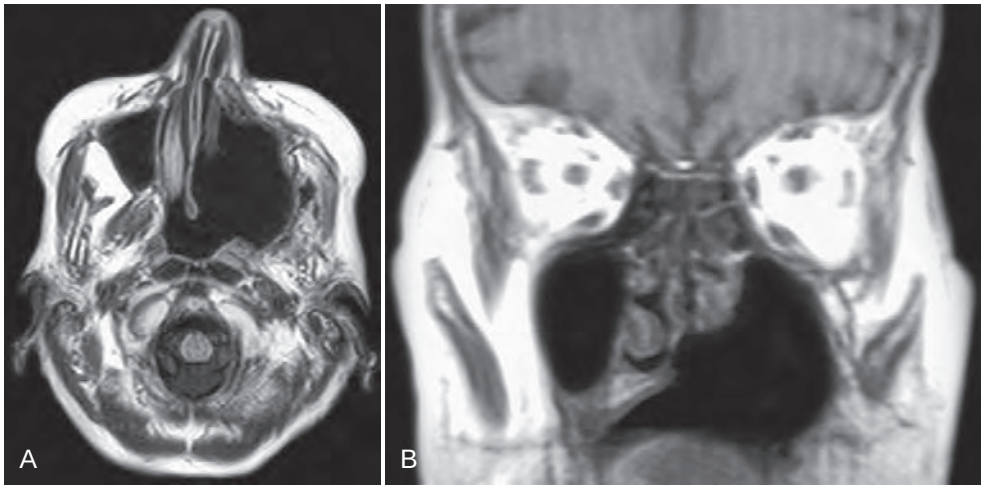

FIGURE 6-52 Axial T1-weighted MR image (**A**) shows a patient who had a radical left maxillectomy. Coronal T1-weighted MR image (**B**) shows a patient who has had a left total maxillectomy. In both cases, the postoperative cavity is smooth and the soft tissues lining the cavity are uniformly thin.

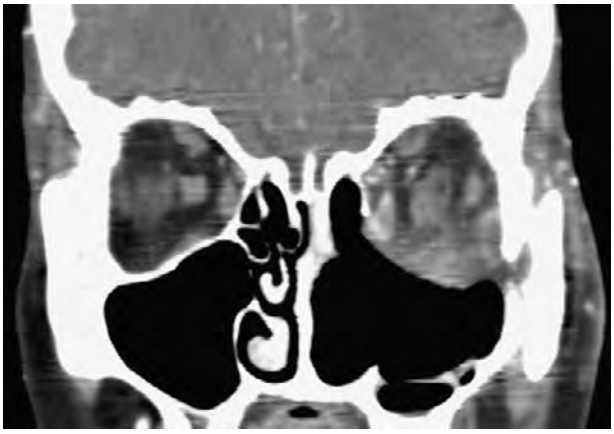

FIGURE 6-53 Coronal CT scan of a patient who had a left suprastructure maxillectomy. The smooth margin of soft tissue supporting the orbital contents is the periorbita of the left orbit.

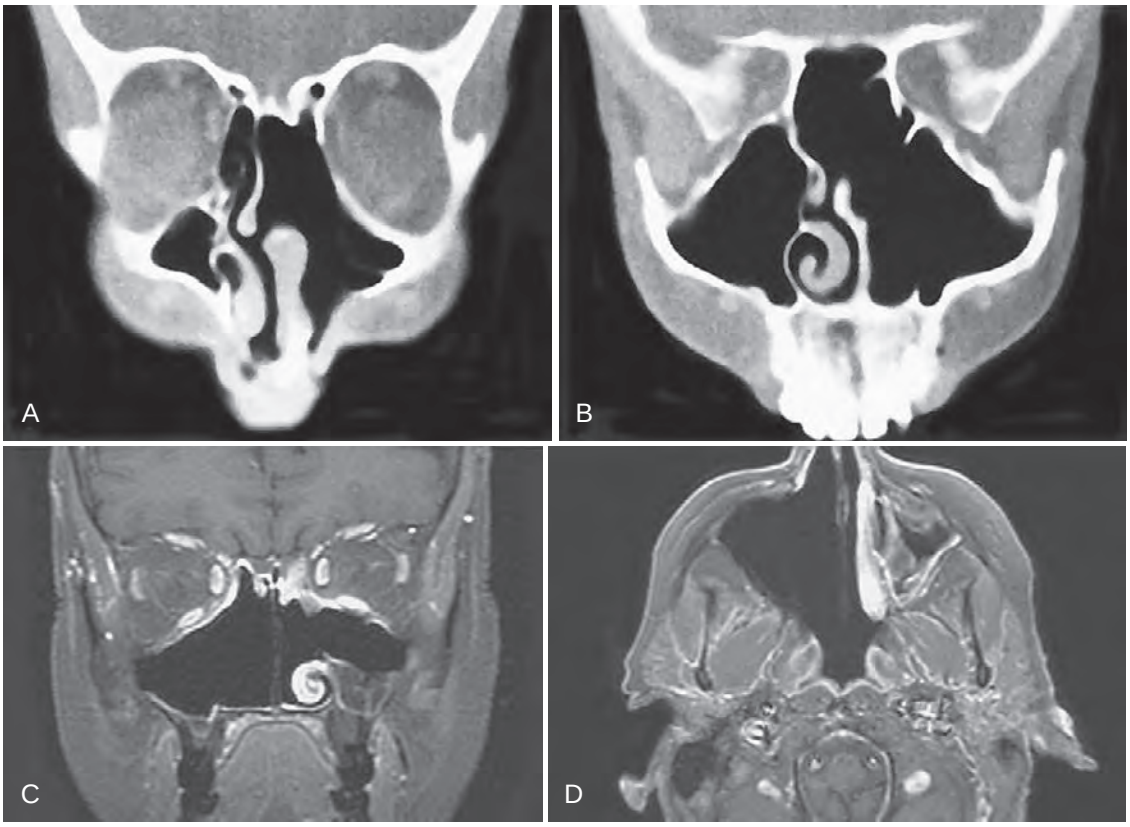

FIGURE 6-54 Coronal CT scan through the anterior antrum (**A**) and posterior antrum and sphenoid sinus (**B**) in a patient who has had a left lateral rhinotomy. There has been a left ethmoidectomy and a medial maxillectomy. The upper nasal septum has also been removed. This is the typical appearance of this operative procedure. Coronal (**C**) and axial (**D**) T1-weighted, fat-suppressed, contrast-enhanced MR images of another patient who has had a lateral rhinotomy, including a right total maxillectomy and ethmoidectomy and a left medial antrostomy and a partial ethmoidectomy. Note the absence of any focal-enhancing nodules.

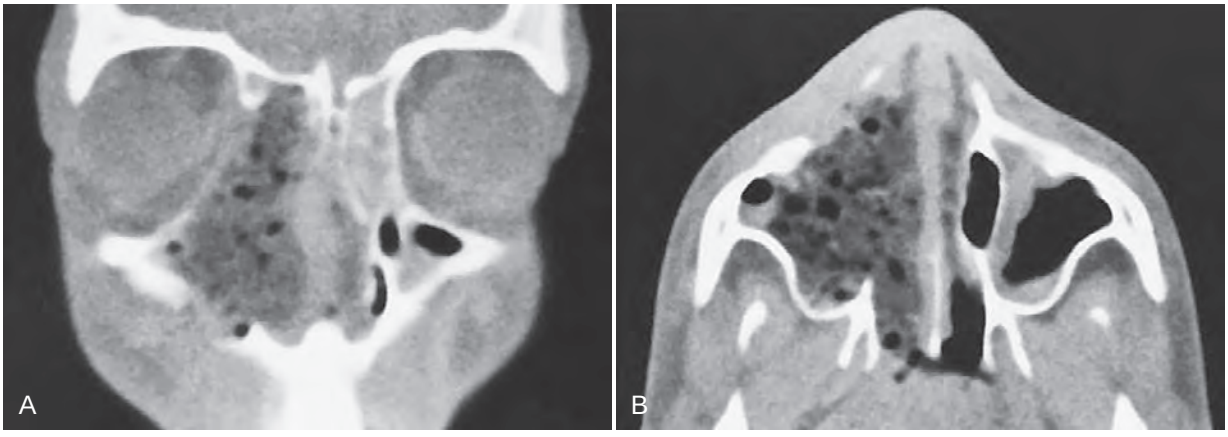

FIGURE 6-55 Coronal (**A**) and axial (**B**) CT scans show a patient who has had a right lateral rhinotomy, ethmoidectomy, and a partial maxillectomy. The postoperative cavity is filled with packing material.

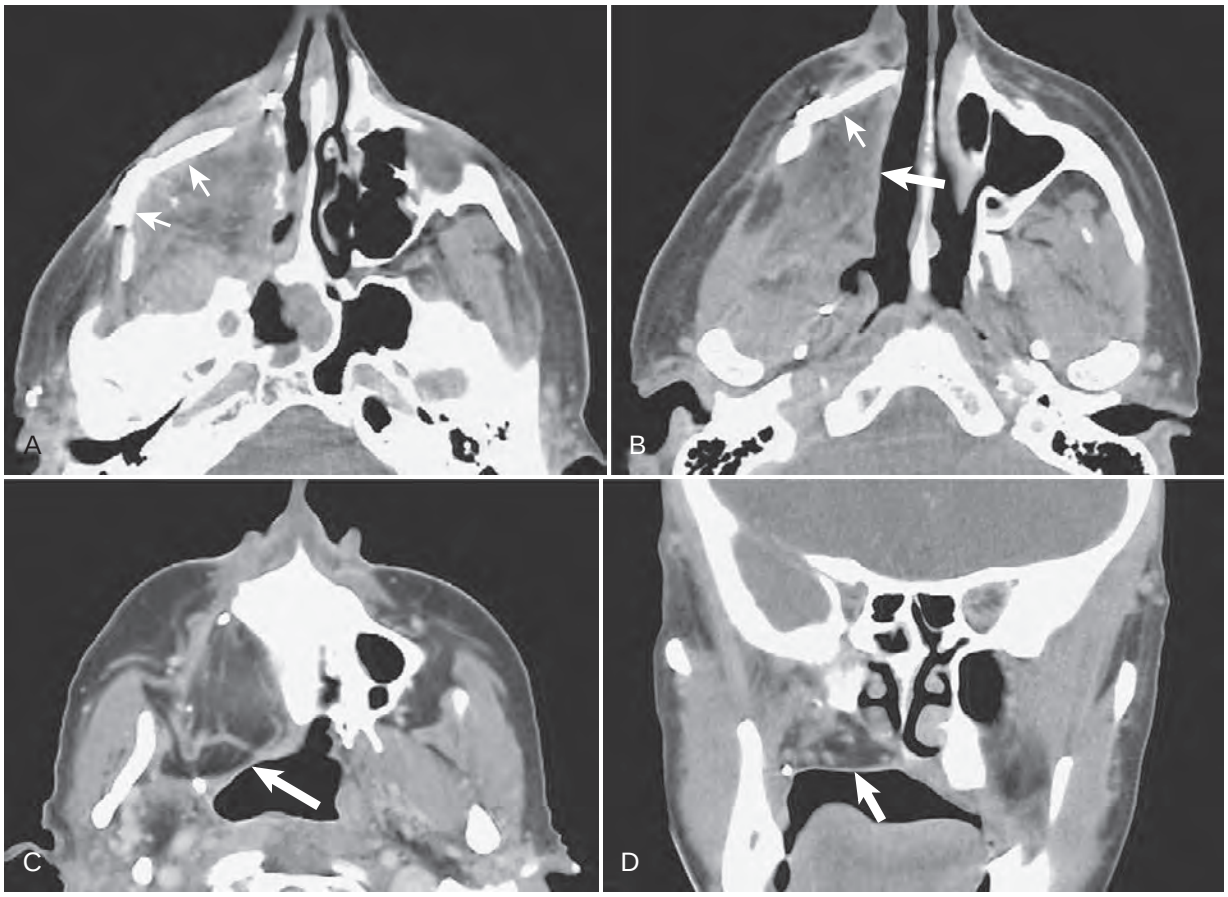

FIGURE 6-56 Serial axial CT scans from cranial (**A**) to caudal (**C**) and a coronal CT scan (**D**) of a patient who has had a right total maxillectomy with a graft reconstruction. Plated bone (*small arrows*) is present superficially to give a better contour to the cheek. The fat of the graft fills most of the postoperative cavity and forms the right side of the reconstructed palate. Notice that the free margins of the graft (*large arrows*) are smooth, with a thin mucosal lining. This is the expected normal postoperative appearance for such an operation.

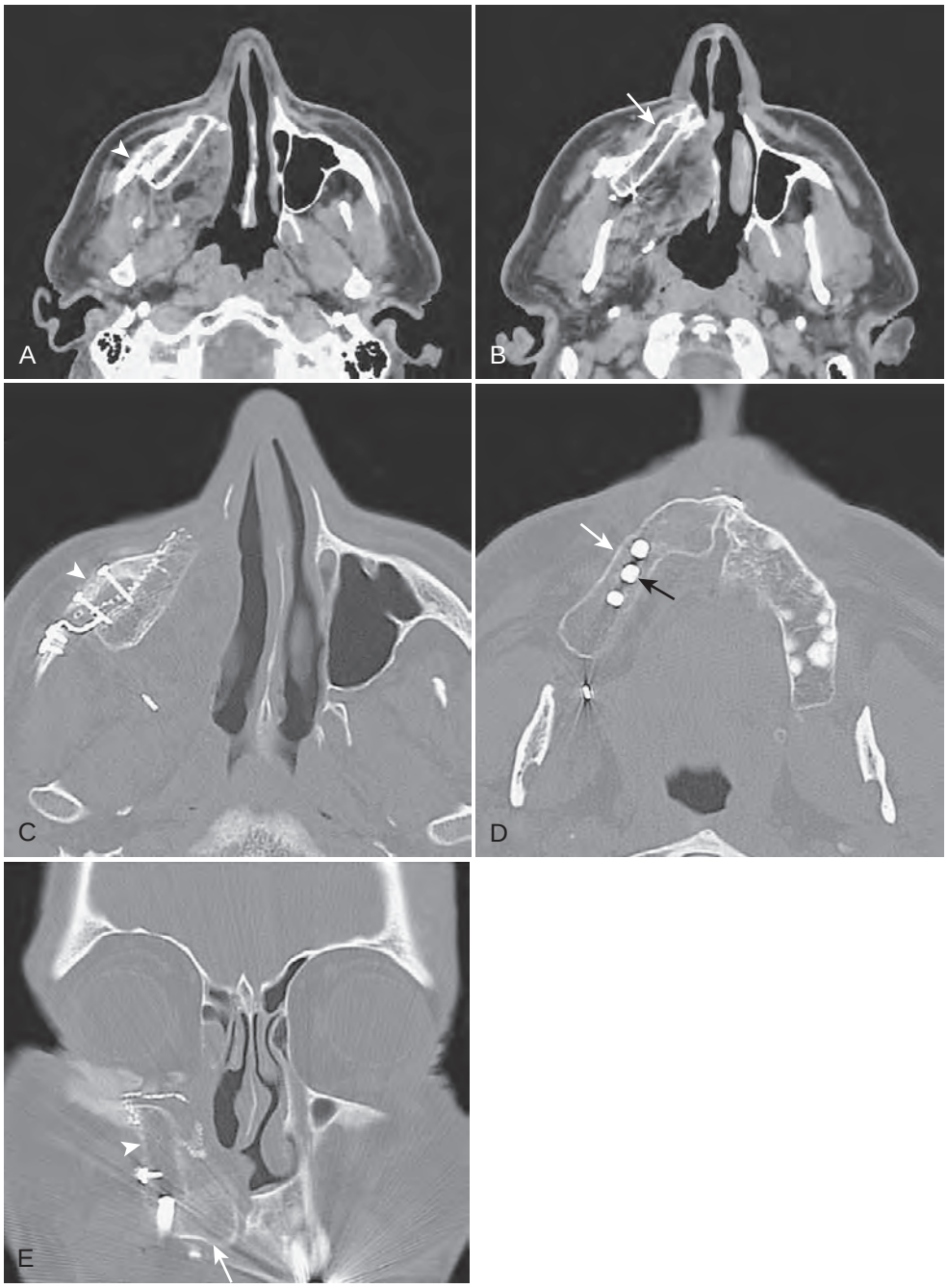

FIGURE 6-57 Axial CT scans (**A** and **B**) at narrow window settings and axial (**C** and **D**) and coronal (**E**) CT scans at wide window settings of a patient who has had a right maxillectomy with an osteomyocutaneous flap reconstruction. Transplanted bone has been used to reconstruct the palate (*white arrows*) and the malar contour (*arrowheads*). Tooth implants (*black arrow*) were then placed in the reconstructed palate/alveolar region.

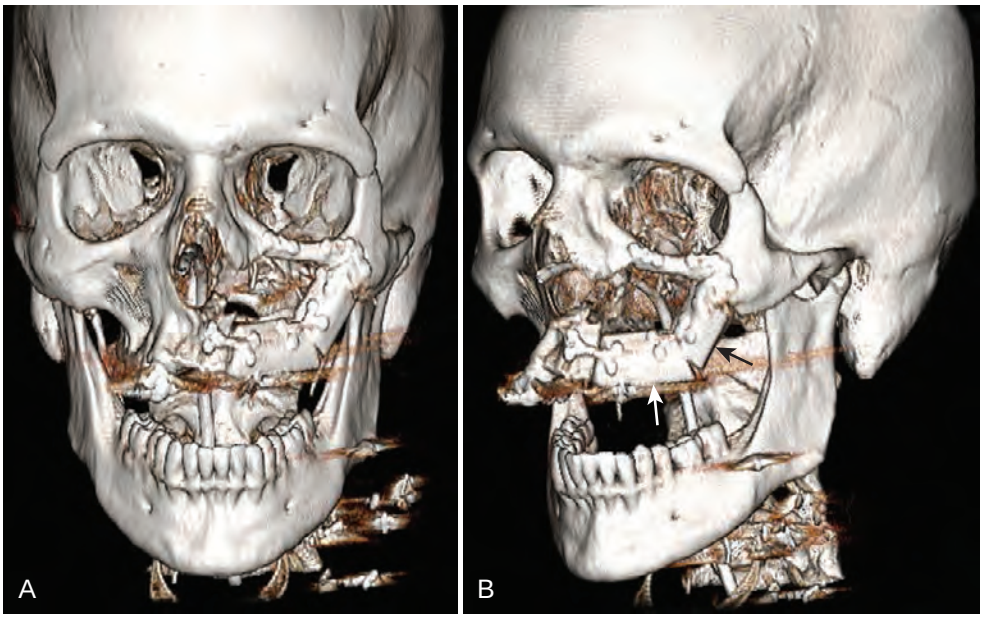

FIGURE 6-58 Frontal (**A**) and left anterior oblique (**B**) 3D reconstructions of a patient who had a left maxillectomy with an osteocutaneous and free flap reconstruction. Portions of rib (*arrows*) were used in the reconstruction to create a new maxillary alveolus and reestablish the facial contour.

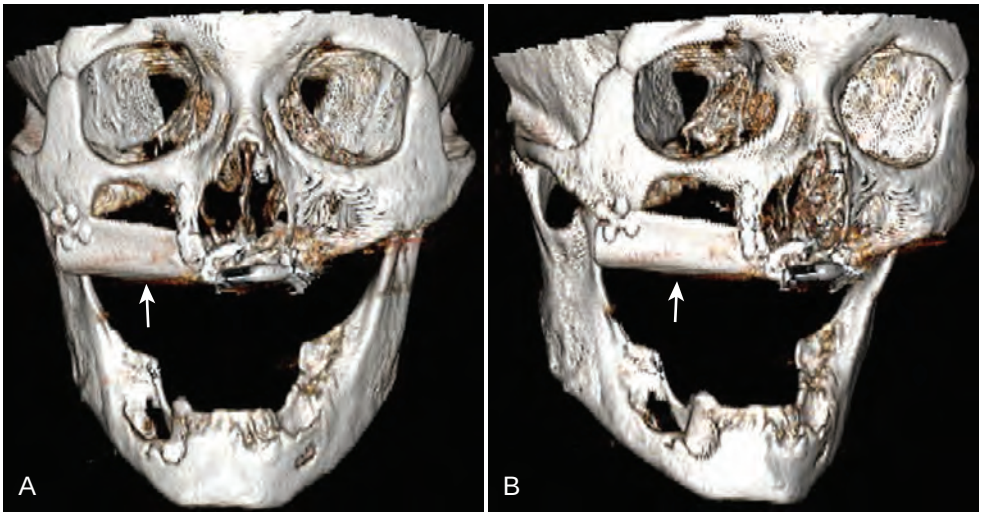

FIGURE 6-59 Frontal (**A**) and a slight right anterior oblique (**B**) 3D reconstruction of a patient who had right infrastructure maxillectomy. Rib (*arrow*) was used to reconstruct a maxillary alveolus. Note the osteosynthesis plates fixing the bone graft.

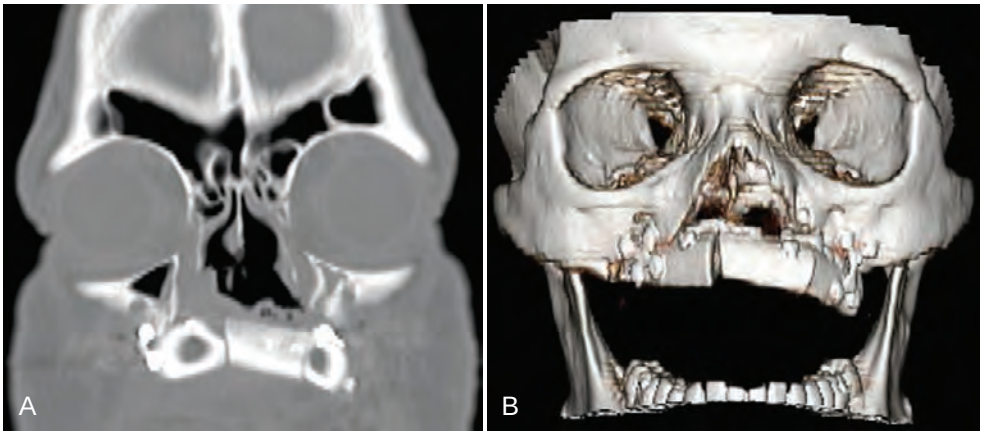

FIGURE 6-60 Coronal CT scan (**A**) and coronal 3D reconstruction (**B**) of a patient who had bilateral infrastructure maxillectomies for a palatal carcinoma. Rib was used to reconstruct the maxillary alveolus. Note the osteosynthesis plates. For most people, the understanding of the surgical procedure is easier to visualize on the 3D reconstruction.

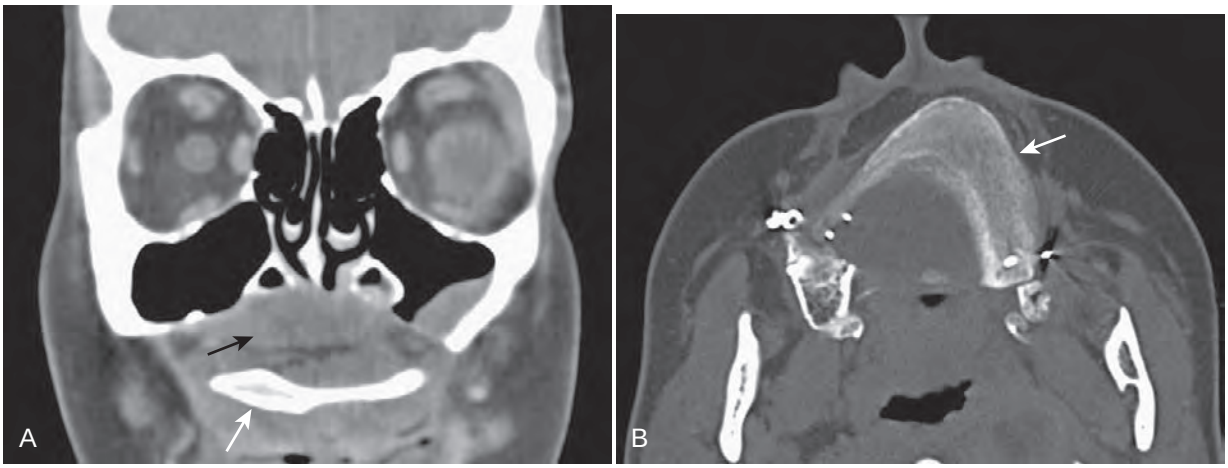

FIGURE 6-61 Coronal (**A**) soft tissue windowed and axial (**B**) bone windowed CT scans a of a patient who had bilateral infrastructure maxillectomies for a palatal carcinoma. Scapula (*white arrows*) was used to reconstruct the palate and alveolar region. In **A**, the soft-tissue component of the osteomucocutaneous free flap can be seen immediately above the scapula graft (*black arrow*).

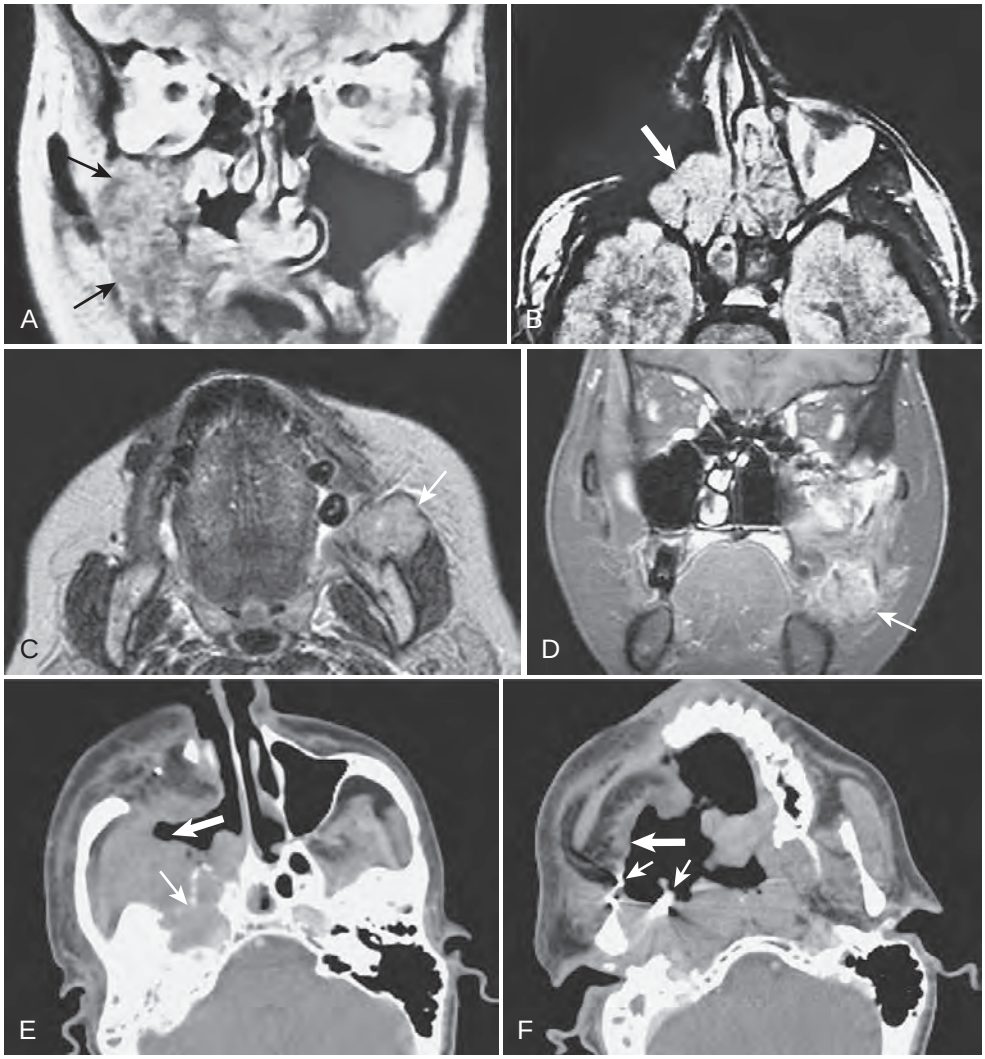

FIGURE 6-62 Coronal proton-density MR image (**A**) shows a large right recurrent tumor with an intermediate signal intensity (*arrows*) in a patient who has had a total right maxillectomy. Axial proton-density MR image (**B**) shows a patient who has had a total right orbital exenteration and a total maxillectomy. Tumor recurrence is seen in the right orbital apex (*arrow*). Axial T2-weighted (**C**) and coronal T1-weighted, fat-suppressed, contrast-enhanced MR image (**D**) on a different patient who has had a left maxillectomy with a graft reconstruction. A tumor nodule is seen at the lower lateral margin of the graft (*arrows*). This was not clinically evident and points out the value of surveillance imaging. Axial CT scans (**E** and **F**) on another patient who has had a right total maxillectomy with a flap reconstruction. Tumor is present along the upper margin of the flap, eroding the skull base (*thin arrow*). Tumor fills the flap, and the medial side of the flap has become thickened, necrotic, and ulcerated (*large arrow*). In **F**, surgical clips that were within the flap are now exposed (*small arrows*) at the necrotic surface of the flap.

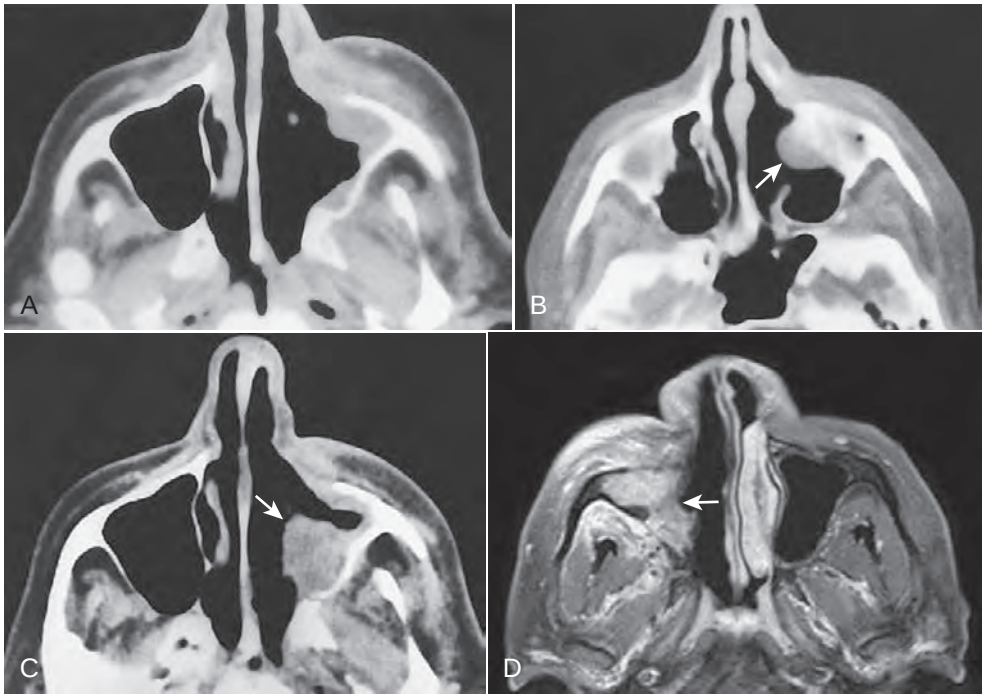

FIGURE 6-63 Axial CT scan (**A**) of a patient after a left medial maxillectomy. There is a nodular fullness in the soft tissues filling the postoperative cavity. This smooth nodule was a retention cyst and not recurrent tumor. Axial CT scan (**B**) of another patient after a partial left maxillectomy with a smooth nodular mass (*arrow*) in the antrum. Although this could be an inflammatory mass, tumor should be suspected until proven otherwise. This patient had tumor recurrence. Axial CT scan (**C**) of a third patient after a partial left maxillectomy with irregularly nodular tumor recurrence (*arrow*) in the antrum. The smooth soft tissues lining the anterior left antrum were scar tissue. Axial T1-weighted, fat-suppressed, contrast-enhanced (**D**) MR imaging of a patient who had a partial right maxillectomy. A moderately enhancing nodular mass (*arrow*) fills the postoperative cavity. This was a tumor recurrence.

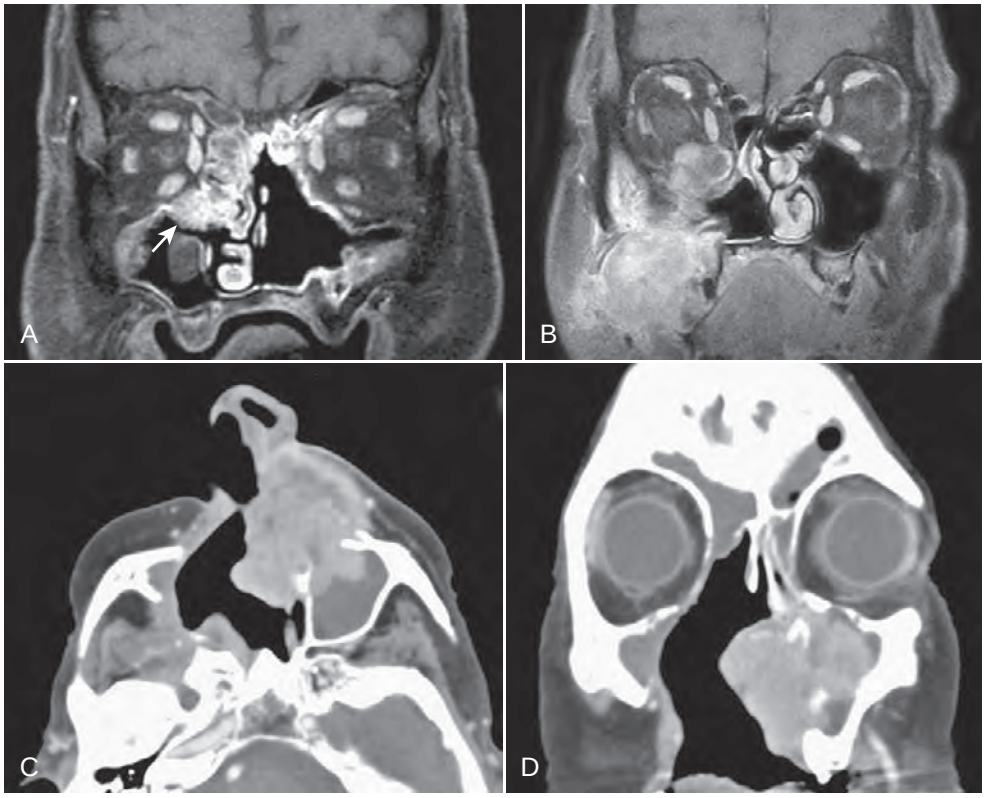

FIGURE 6-64 Coronal T1-weighted, fat-suppressed, contrast-enhanced (**A**) MR image of a patient who had a left lateral rhinotomy with an ethmoidectomy and total maxillectomy. In the roof of the right antrum, there is an irregular, enhancing mass (*arrow*) that was a tumor recurrence along the margin of the operative bed. The remaining soft tissue disease was inflammatory in nature. Coronal T1-weighted, fat-suppressed, contrast-enhanced (**B**) MR image of a patient who had a right maxillectomy. There is tumor recurrence at the lower lateral operative margin and in the lateral wall and orbit. Axial (**C**) and coronal (**D**) CT scans of a patient who had a right medial maxillectomy and ethmoidectomy. There is a large tumor recurrence along the left anterior maxillary wall extending into the nasal cavity, nose, cheek, and antrum. This case illustrates that many recurrences occur at the margins of the surgical bed and not in the immediate site of the primary tumor.

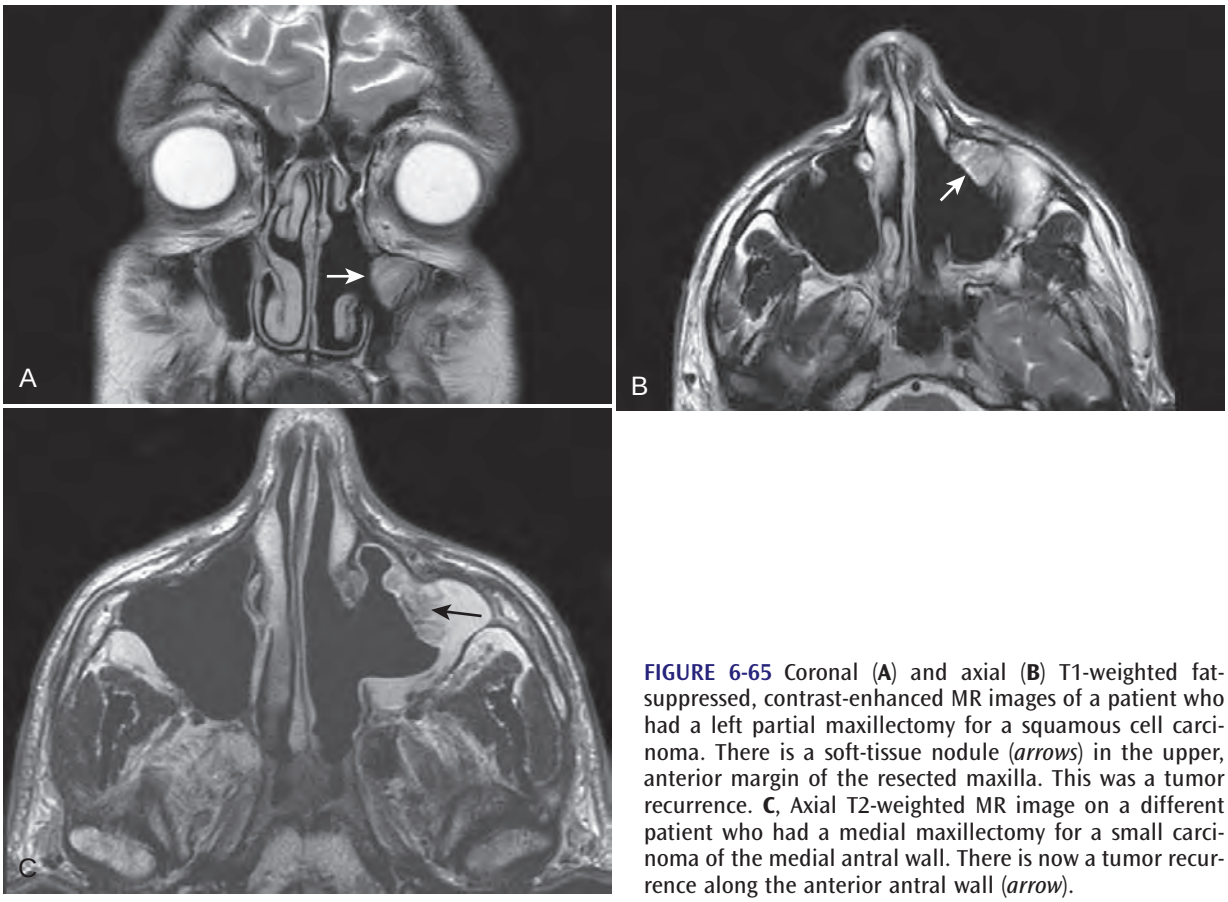

FIGURE 6-65 Coronal (**A**) and axial (**B**) T1-weighted fat-suppressed, contrast-enhanced MR images of a patient who had a left partial maxillectomy for a squamous cell carcinoma. There is a soft-tissue nodule (*arrows*) in the upper, anterior margin of the resected maxilla. This was a tumor recurrence. **C**, Axial T2-weighted MR image on a different patient who had a medial maxillectomy for a small carcinoma of the medial antral wall. There is now a tumor recurrence along the anterior antral wall (*arrow*).

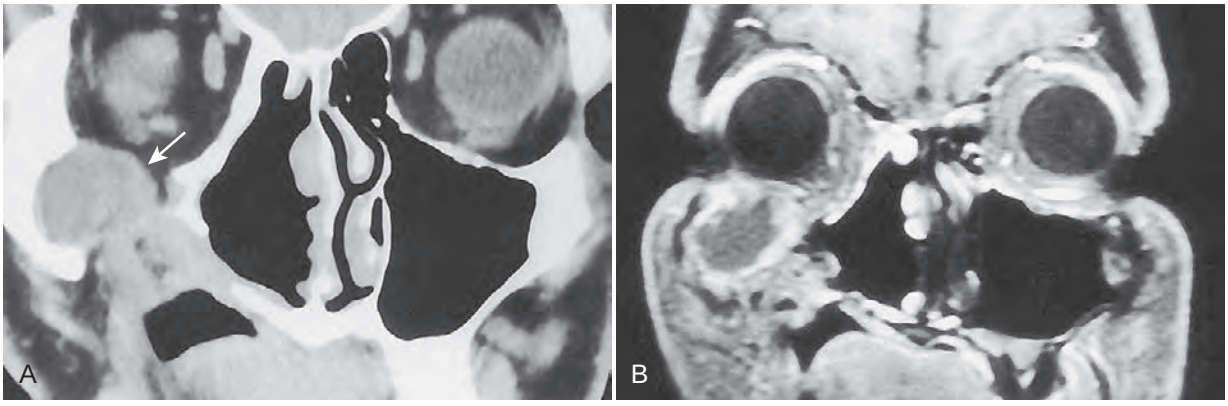

FIGURE 6-66 Coronal CT (**A**) and coronal T1-weighted, contrast-enhanced, fat-suppressed MR (**B**) images show a patient's status after an extended right lateral rhinotomy. No nodularity is present within the postoperative cavity. However, there is a mass (*arrow in* **A**) in the right zygomatic recess of the right antrum, which has broken into the floor of the right orbit. The lesion has surrounding mucosal enhancement, but the secretions within it do not enhance. This patient had a postoperative mucocele.

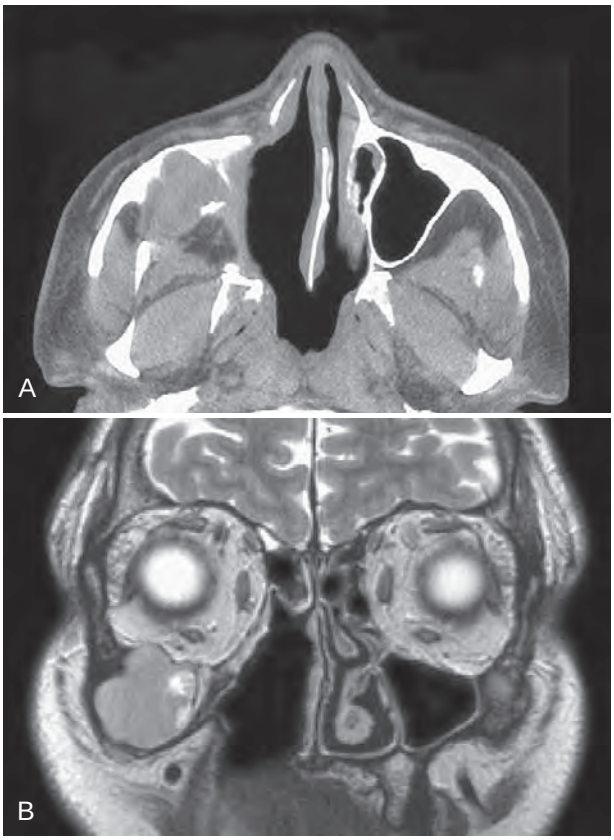

FIGURE 6-67 Axial CT scan (**A**) and a coronal T2-weighted MR image (**B**) of a patient who had a right medial maxillectomy and an ethmoidectomy. There is a soft-tissue, primarily expansile, mass in the zygomatic recess region elevating the orbital floor but not infiltrating into the orbit. There is an intermediate-to-low T2-weighted signal intensity with focal areas of high signal along the medial margin of the mass. This nodularity is not the typical imaging appearance of a postoperative mucocele and this was a tumor recurrence of an ameloblastoma.

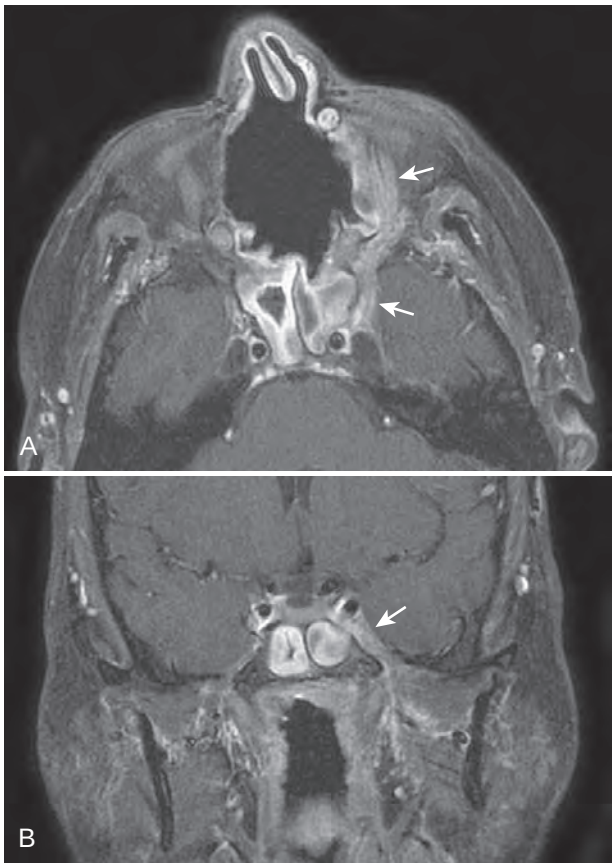

FIGURE 6-68 Axial (**A**) and coronal (**B**) T1-weighted, fat-suppressed, contrast-enhanced MR images of a patient who had a rhinotomy, bilateral medial maxillectomies, and ethmoidectomies. There is thickening and enhancement of the left maxillary and mandibular nerves represent perineural tumor spread. Inflammatory mucosal disease is present in the sphenoid sinuses.

Initially, one of several types of frontal or bifrontal craniotomies is performed, the frontal lobes are elevated, and any tumor extension into the brain is resected. The bone and dura in the floor of the anterior cranial fossa are then incised. The typical resection includes the posterior wall of the frontal sinuses, the cribriform plate, the fovea ethmoidalis on each side, and as much of the orbital roof as is necessary to obtain a margin around the tumor. The posterior incision runs along the posterior roof of the sphenoid sinus and it can extend back to the tuberculum sella. An extended lateral rhinotomy is then performed, and the resection includes one or both ethmoid sinuses (including the corresponding medial orbital wall), the nasal septum, and if necessary a portion of the medial maxilla. Once the osteotomies are completed, the surgeons proceed with an en bloc extirpation. The skull base defects are generally closed with a pericranial flap. With large defects, a free flap may be required. Dural defects are closed with fascial grafts. The lateral rhinotomy is closed separately (Fig. 6-69).[2,22,23] The nasal cavity is generally packed with gauze to support the intracranial repair (Fig. 6-70).

Postoperative CT scans contain several areas that may cause diagnostic difficulties. First, the anterior dura adjacent to the frontal osteotomy becomes thickened and enhances on contrast studies. This appearance may persist indefinitely and relates to a low-grade reactive process that obliterates the dural spaces (Fig. 6-71). There also are areas of subfrontal encephalomalacia caused by the retraction of the brain during surgery. These changes also persist indefinitely. Second, the musculofascial flap that supports the central region of the floor of the anterior cranial fossa can bulge downward into the upper postoperative nasoethmoid cavity (Figs. 6-72 to 6-78). This can simulate a tumor mass on axial CT scans and MR images, but usually can be identified as representing the graft region on coronal images. This is especially true during the period before the free flap becomes completely fibrosed, usually between 2 and 8 months after the surgery. Although the CT appearance is not significantly altered once the flap is completely fibrosed, the MR imaging findings are changed. The initial intermediate T1-weighted and high T2-weighted signal intensities are

Text continued on page 483

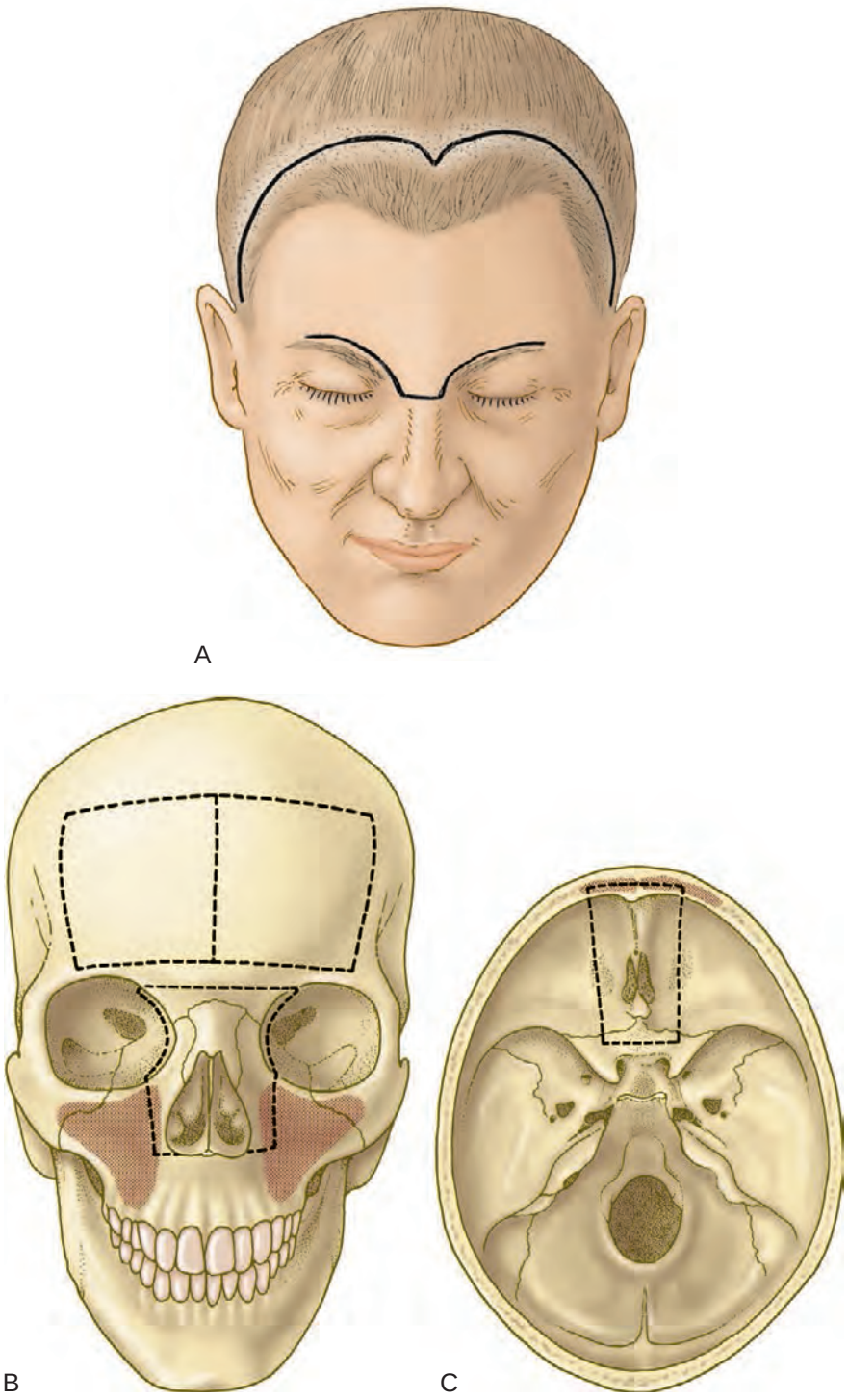

FIGURE 6-69 Frontal drawing of the face (**A**) shows the two main incisions used for craniofacial resections. The bicoronal incision scar is usually well hidden by the hair. The brow incision usually heals with little if any identifiable scar, much of which is hidden by the eyebrows. Drawing of the skull in the frontal view (**B**) and the axial view (**C**) as seen from above with the calvarium removed. The osteotomies typically performed in the craniofacial procedure (*dashed lines*) are outlined.

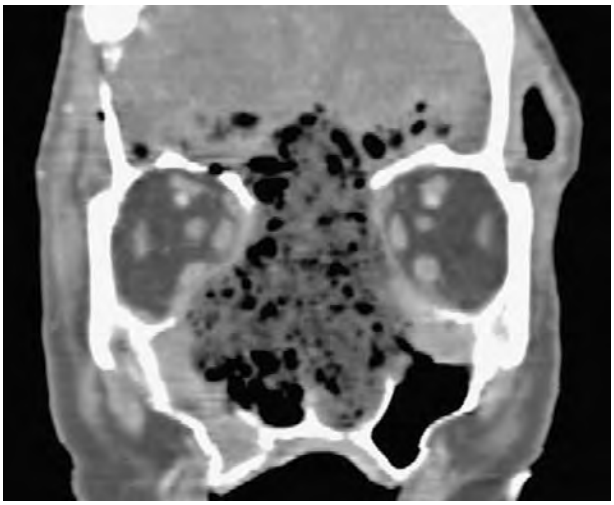

FIGURE 6-70 Coronal CT scan of a patient who had a craniofacial resection. This is an immediate postoperative study showing packing in the operative cavity with some pneumocephalus and subcutaneous emphysema. This is the normal appearance right after surgery.

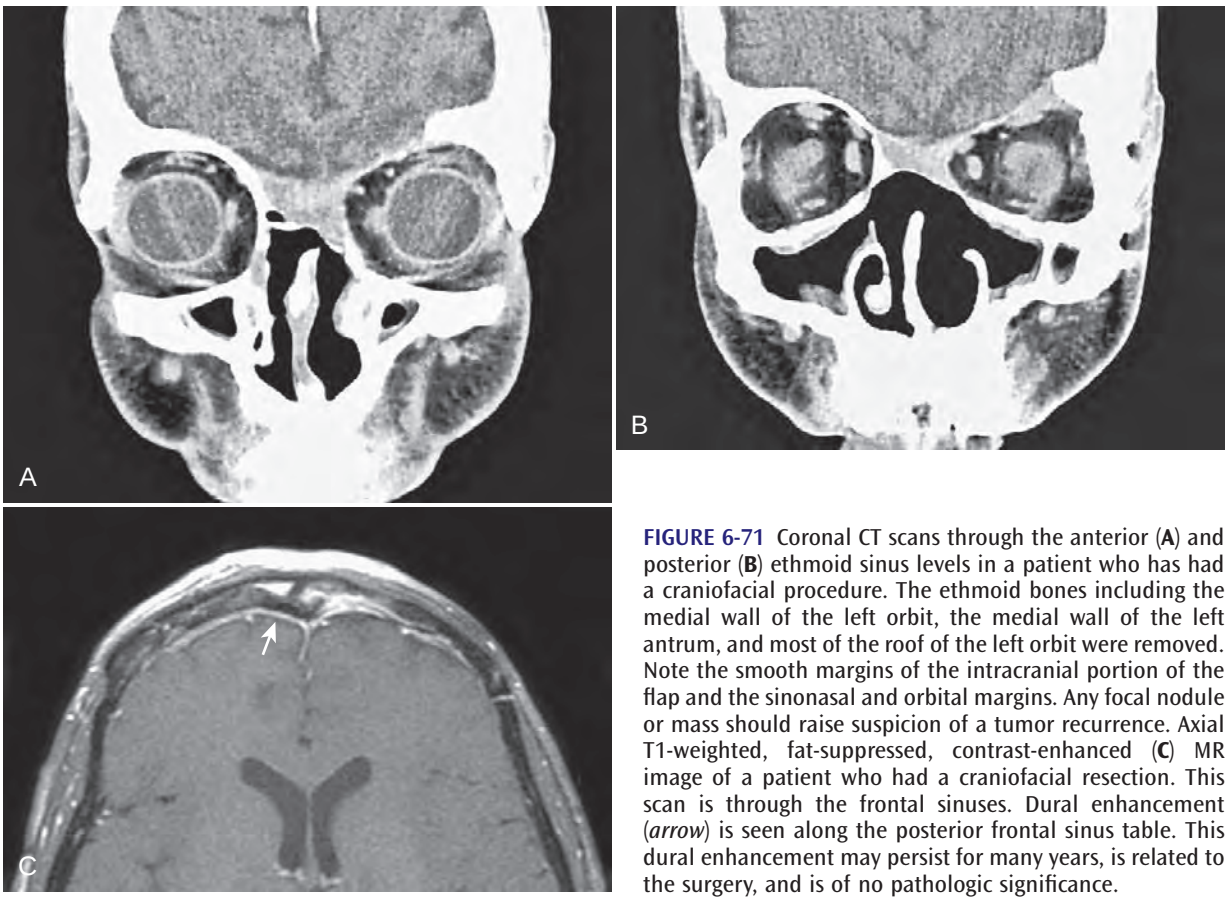

FIGURE 6-71 Coronal CT scans through the anterior (**A**) and posterior (**B**) ethmoid sinus levels in a patient who has had a craniofacial procedure. The ethmoid bones including the medial wall of the left orbit, the medial wall of the left antrum, and most of the roof of the left orbit were removed. Note the smooth margins of the intracranial portion of the flap and the sinonasal and orbital margins. Any focal nodule or mass should raise suspicion of a tumor recurrence. Axial T1-weighted, fat-suppressed, contrast-enhanced (**C**) MR image of a patient who had a craniofacial resection. This scan is through the frontal sinuses. Dural enhancement (*arrow*) is seen along the posterior frontal sinus table. This dural enhancement may persist for many years, is related to the surgery, and is of no pathologic significance.

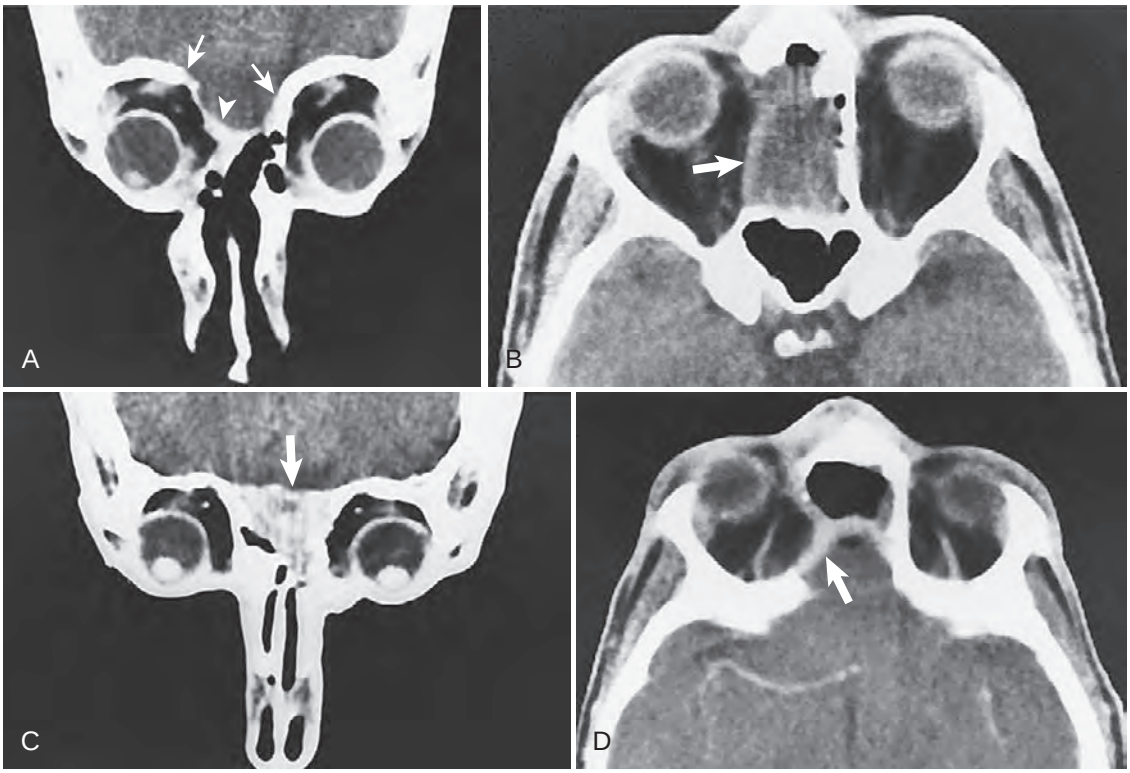

FIGURE 6-72 Coronal contrast-enhanced CT scan (**A**) of a patient who has had a craniofacial procedure. There is enhancement of the muscle fascial graft (*arrowhead*) between the margins of the bony resection (*arrows*). The intracranial and sinonasal contours of the graft are smooth. Axial CT scan (**B**) shows a soft-tissue mass (*arrow*) in the postoperative upper nasoethmoid cavity. This is the fascial–muscle graft of an osteoplastic flap as it prolapses slightly below the level of the anterior skull base. Any confusion regarding this "pseudomass" can be resolved with a coronal study. Coronal contrast-enhanced CT scan (**C**) of a patient who has had a craniofacial resection. The fascial–muscle graft and adjacent dura enhance (*arrow*), filling the surgical defect in the floor of the anterior cranial fossa. The graft hangs down into the postoperative nasoethmoid cavity. Axial contrast-enhanced CT scan (**D**) shows enhancement of dura and granulation tissue (*arrow*) partially below the level of the fascial–muscle graft in a patient who has had a craniofacial resection. The air anteriorly is actually in the upper postoperative nasoethmoid cavity.

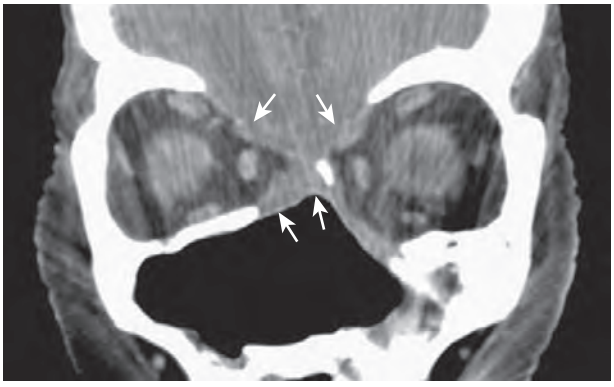

FIGURE 6-73 Coronal CT scan of a patient who had a craniofacial resection. Note the smooth contour of both the intracranial and sinonasal margins of the flap (*arrows*). Also note that the adjacent bone margins are smooth and "clean." This is the normal postoperative appearance of this procedure.

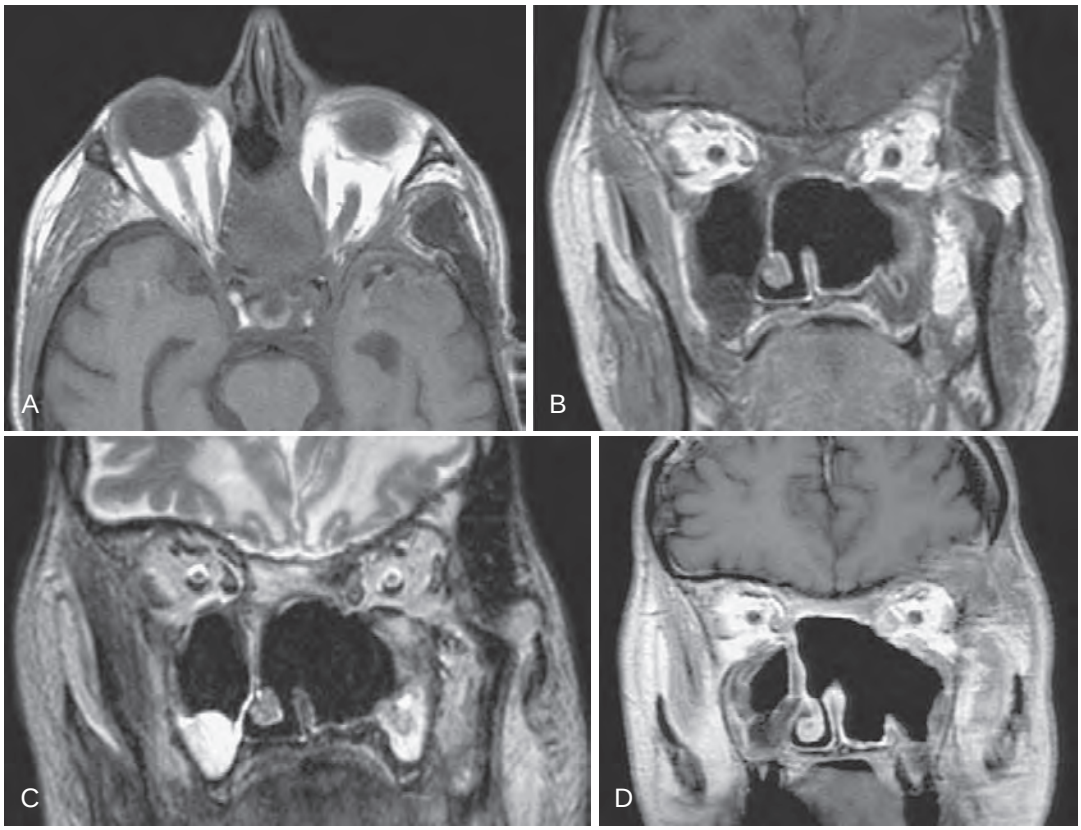

FIGURE 6-74 Axial T1-weighted (**A**) and coronal T1-weighted (**B**), T2-weighted (**C**), and T1-weighted, fat-suppressed, contrast-enhanced (**D**) MR images of a patient who has had a craniofacial procedure. In **A**, a "pseudomass" is seen in the midline upper nasoethmoid region. This is the flap as it hangs down into the upper sinonasal cavity. This is confirmed on the coronal images, where smooth margins are seen along the intracranial, sinonasal, and orbital margins. Incidental inflammatory disease is present in the right maxillary sinus. This is the normal postoperative appearance of a patient who has had a craniofacial procedure.

FIGURE 6-75 Coronal T1-weighted, fat-suppressed, contrast-enhanced MR image of a patient who had a craniofacial resection. Note that the flap is smooth and minimally enhancing (*arrow*). No focal nodule is present. This is the normal postoperative appearance. This patient had surgery 3 months earlier. With time, the flap will thin and not enhance as it becomes fibrotic.

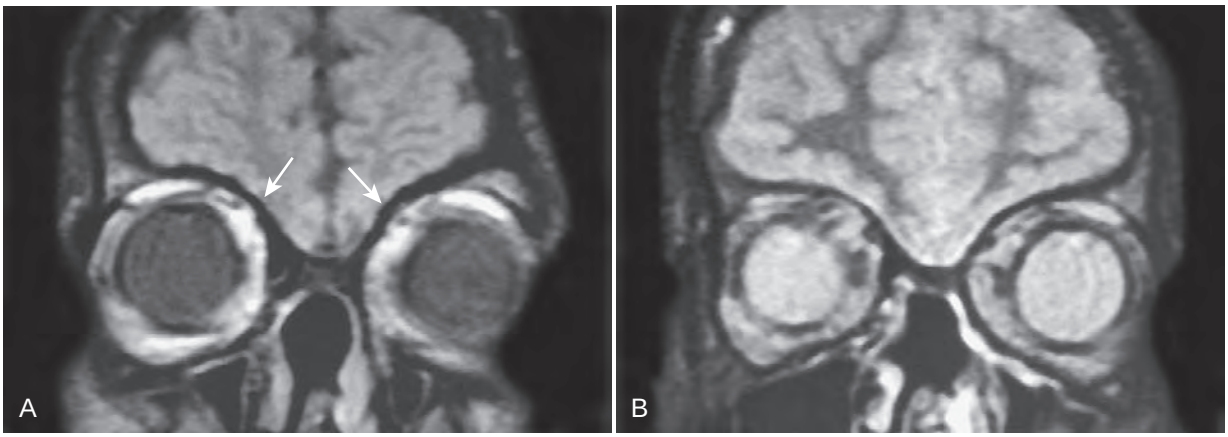

FIGURE 6-76 Coronal T1-weighted (**A**) and proton-density (**B**) MR images of a patient who has had a craniofacial resection. The graft has fibrosed, giving it signal void on all sequences. Because the graft has about the same thickness as the adjacent bone (*arrows* in **A**) in the remaining floor of the anterior cranial fossa, no obvious defect is seen. The imaging key to identifying that this surgery was performed is the absent normal contour of the crista galli and fovea ethmoidalis. Note that the cranial and sinonasal margins of the graft site are smooth.

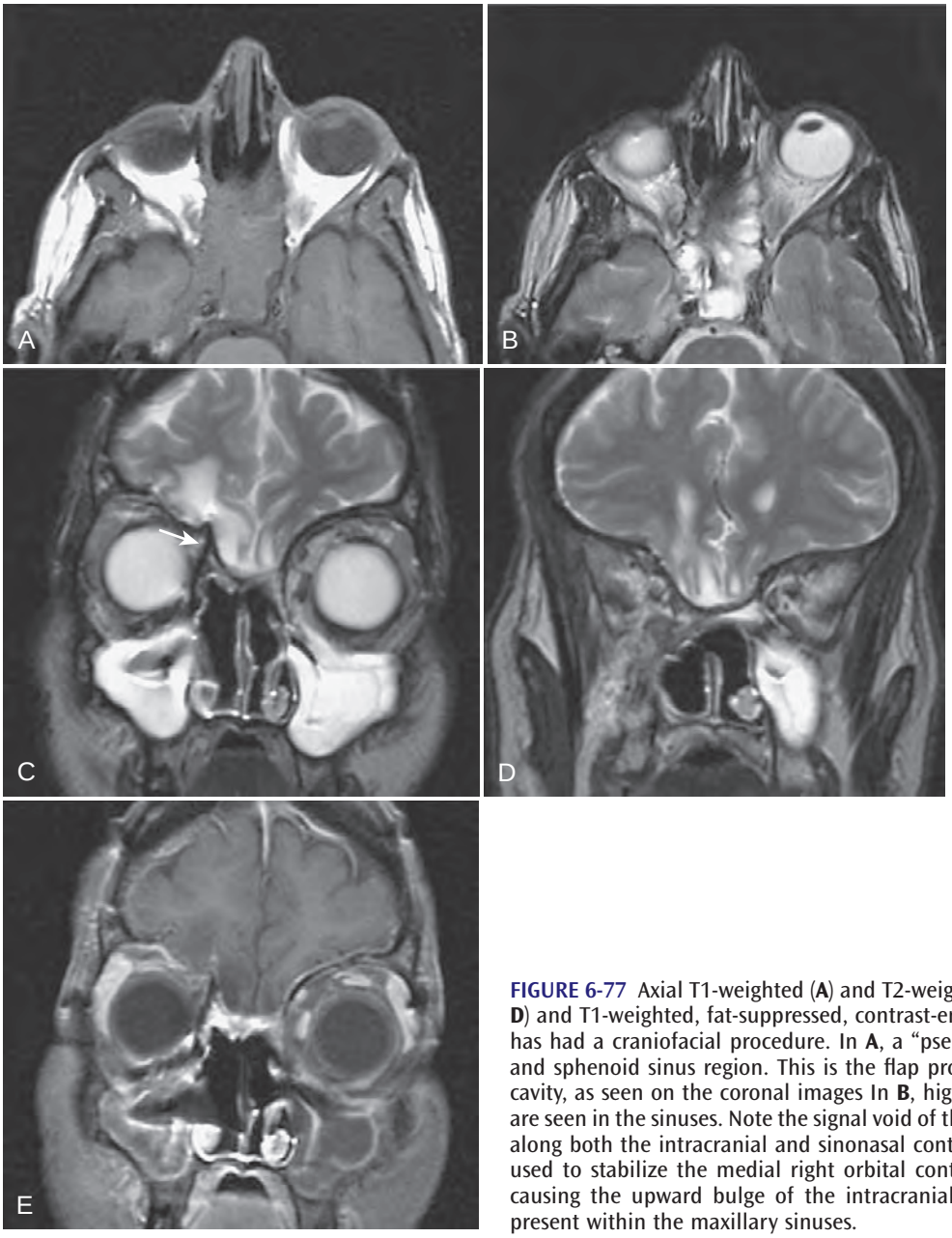

FIGURE 6-77 Axial T1-weighted (**A**) and T2-weighted (**B**) and coronal T2-weighted (**C** and **D**) and T1-weighted, fat-suppressed, contrast-enhanced (**E**) MR images of a patient who has had a craniofacial procedure. In **A**, a "pseudomass" is seen in the upper ethmoid and sphenoid sinus region. This is the flap protruding down into the upper sinonasal cavity, as seen on the coronal images In **B**, high signal intensity inflammatory changes are seen in the sinuses. Note the signal void of the fibrosed flap and the smooth contours along both the intracranial and sinonasal contours of the flap. A thin metal plate was used to stabilize the medial right orbital contour (*arrow* in **C**). It is this plate that is causing the upward bulge of the intracranial contour. Inflammatory disease is also present within the maxillary sinuses.

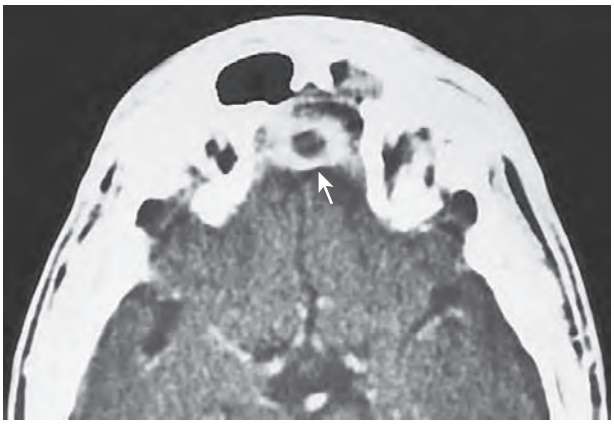

FIGURE 6-78 Axial contrast-enhanced CT scan shows a ring-enhancing mass (*arrow*) just above the fascial–muscle graft in a patient who has had a craniofacial resection. This patient had a postoperative abscess.

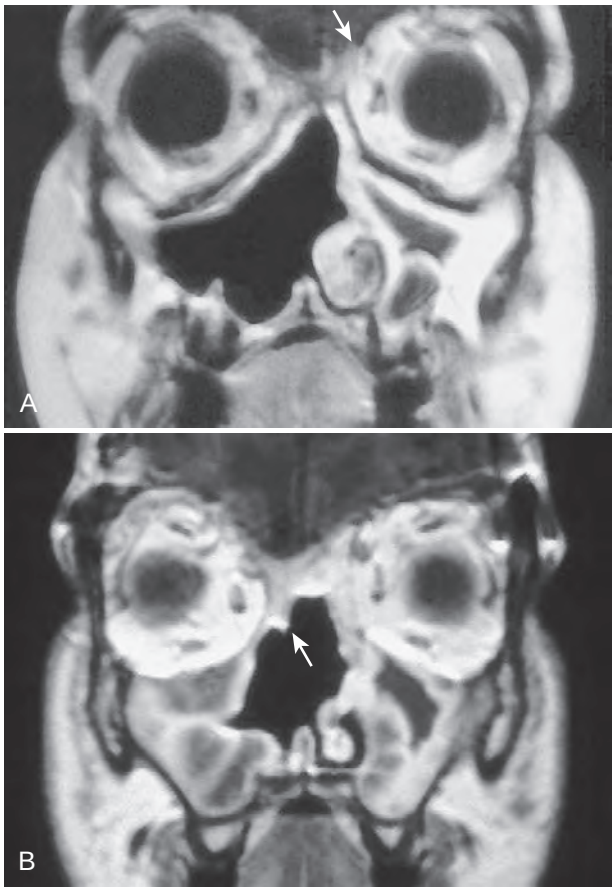

FIGURE 6-79 Coronal T1-weighted, contrast-enhanced MR images of two different patients who have had craniofacial procedures. In **A**, the mucosa lining the postoperative nasal cavity and the right maxillectomy cavity is smooth and normal. There is a sinusitis with entrapped secretions in the left antrum. The graft in the floor of the anterior cranial fossa enhances minimally, and if one is not careful, one may overlook the extent of the removed bone, especially in the skull base. A focal area of nodularity is seen (*arrow*) along the intracranial margin near the left attachment of the graft to the bone. This remained stable in appearance over several postoperative years. In this patient, this was a postoperative variant, and it points out the value of obtaining baseline postoperative images. In **B**, the intracranial margin is smooth, but there is a focal nodule along the right sinonasal margin (*arrow*). Although this area is easily accessible to clinical observation, it was also present on the baseline scan and remained unchanged. There is also bilateral antral inflammatory disease.

gradually replaced by low signal intensities or signal voids on all imaging sequences. This change corresponds to replacement of the graft by scar. The thickness of the fibrosed graft or flap may occasionally be sufficiently similar to that of the remaining bony floor of the adjacent anterior cranial fossa that on coronal MR images the radiologist may not detect that bone has been removed (Figs. 6-75 to 6-78). Only the altered contour of the bony floor of the anterior cranial fossa (absence of the crista galli and fovea ethmoidalis) may signify that the surgery included the bone in this region. Such bone defects are seen easily on coronal CT. There are slight variations in the imaging appearance of patients who have had craniofacial procedures, primarily reflecting variations in the surgical approach.

Any nodularity along the cranial or nasal margin of the graft or postoperative sinonasal cavity must be suspected of representing tumor (Figs. 6-79 to 6-83). Progressive thickening of the graft or an upward convexity along the cranial margin of the graft are possible signs of tumor recurrence. Unfortunately, vascularized scar tissue develops postoperatively that has imaging findings similar to those of recurrent tumor on both CT and MR imaging, with or without contrast. However, this tissue will not progressively grow on serial imaging studies. Thus, tumor recurrence in these patients is best detected by a change in the mucosal or graft surface contour or thickness.[2] Occasionally, inflammatory disease, including abscess formation, may be seen after surgery. However, in these cases, the clinical presentation usually suggests the correct diagnosis.

In contrast, the transnasal endoscopic skull base approach (closed craniofacial resection) is performed entirely through the nose or through a sublabial incision, thus eliminating a facial incision as well as bifrontal craniotomy incisions. The aim of this approach is to achieve complete tumor resection without subjecting the patient to the morbidity associated with the frontal lobe retraction required in the traditional open approach. Endoscopic craniofacial resection is traditionally indicated for neoplasms located medial to the optic nerves. Contraindications include neoplasms that extend lateral to the optic nerves or lesions associated with enhancement of the dura lateral to the optic nerves. Although the goals of the open and endoscopic approaches are similar, overall the bony defect associated with the endoscopic approach is generally more limited as compared to the traditional approach. The endoscopic approach is achieved by performing a craniotomy in the floor of the anterior cranial fossa. Because this approach is performed without a bifrontal craniotomy, access to reconstructing the cranial base defect is more limited and the reconstruction is performed via a combination of vascularized septal flaps, nonvascularized fascia, polyglycolic acid mesh, fibrin glue, and nonvascularized fat. Thus, although the anterior cranial base defect may be similar in both approaches, the imaging appearance of the reconstruction site in the floor of the anterior cranial fossa differs. In addition, there are few, if any, imaging changes in the frontal lobes associated with the

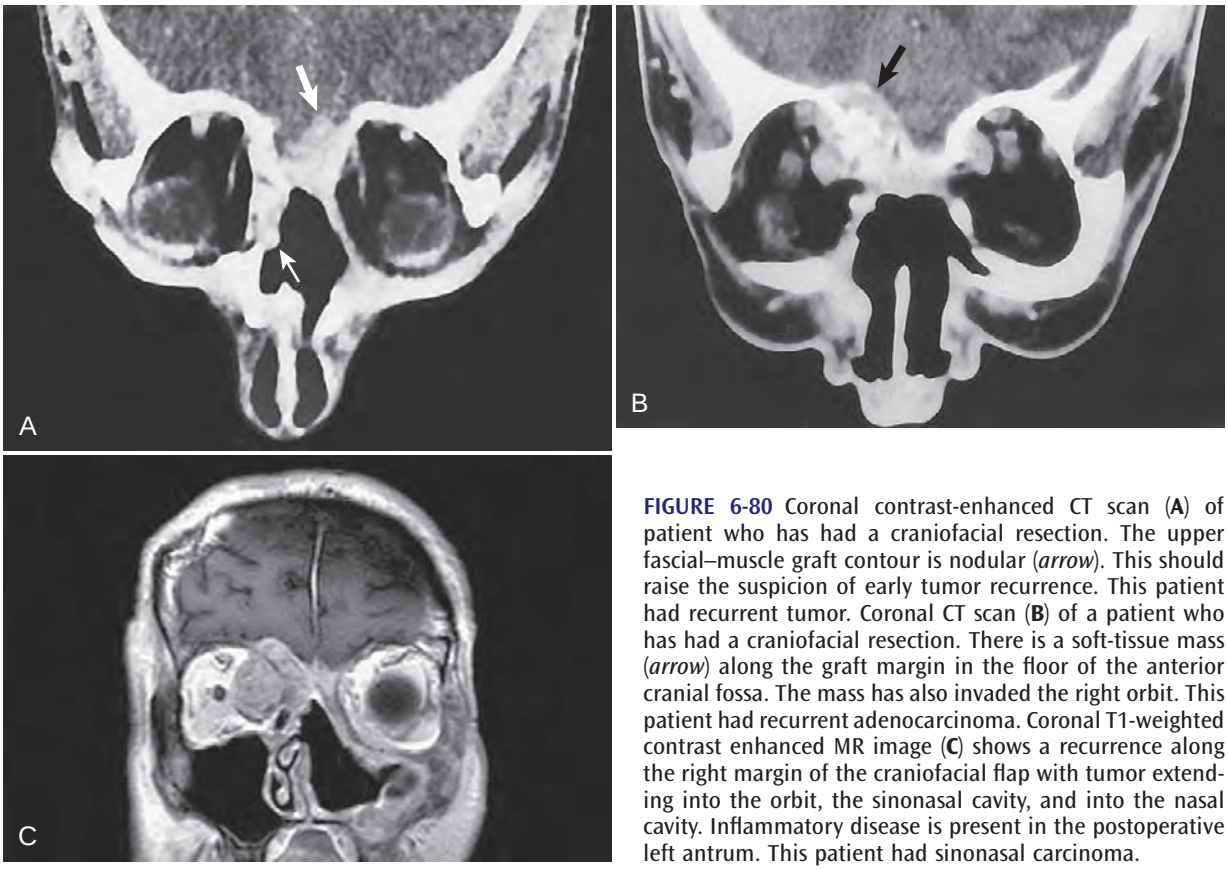

FIGURE 6-80 Coronal contrast-enhanced CT scan (**A**) of patient who has had a craniofacial resection. The upper fascial–muscle graft contour is nodular (*arrow*). This should raise the suspicion of early tumor recurrence. This patient had recurrent tumor. Coronal CT scan (**B**) of a patient who has had a craniofacial resection. There is a soft-tissue mass (*arrow*) along the graft margin in the floor of the anterior cranial fossa. The mass has also invaded the right orbit. This patient had recurrent adenocarcinoma. Coronal T1-weighted contrast enhanced MR image (**C**) shows a recurrence along the right margin of the craniofacial flap with tumor extending into the orbit, the sinonasal cavity, and into the nasal cavity. Inflammatory disease is present in the postoperative left antrum. This patient had sinonasal carcinoma.

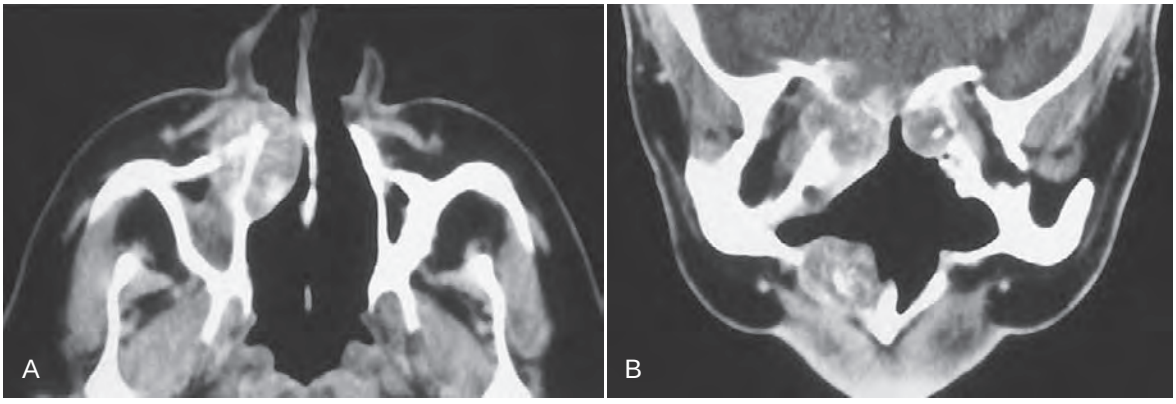

FIGURE 6-81 Axial (**A**) and coronal (**B**) CT scans of a patient who has had a craniofacial procedure. There are tumor nodules along the upper sinonasal cavity, in the right orbit, and along the right intracranial graft margin. There is also tumor in the right anterior maxilla. Speckled calcifications are seen within each tumor nodule. This patient had recurrent adenocarcinoma.

endoscopic approach because frontal lobe retraction is not required.

The transnasal endoscopic resection of olfactory neuroblastoma was first described in 1997.[21] In this original paper, an endoscopic transnasal resection was combined with a transcranial approach, thus eliminating any facial incisions. To date, the limitations of assessing the success of the endoscopic studies are the small number of patients and short followup time. Future studies will better be able to assess the oncologic cure rate of endoscopic procedure as compared to the classical open resection.

For the endoscopic surgical procedure, as compared to the "open" procedure, on imaging there usually is more limited resection of the sinonasal bones and soft tissues, although defects as extensive with the classical approach can be seen. There is usually a more limited defect in the floor of the anterior cranial fossa, at most extending to the medial thirds of the orbital roofs. The major imaging difference between the

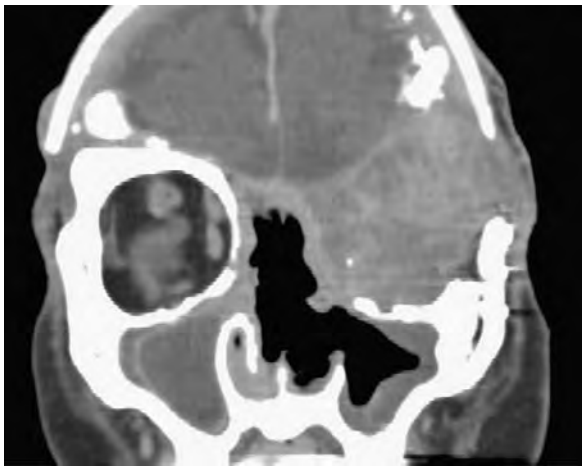

FIGURE 6-82 Coronal contrast-enhanced CT scan of a patient who had a craniofacial resection with a left orbital exenteration. There is a large tumor recurrence within the orbital flap, crawling along the sinonasal margin of the craniofacial flap and extending to the right nasal cavity.

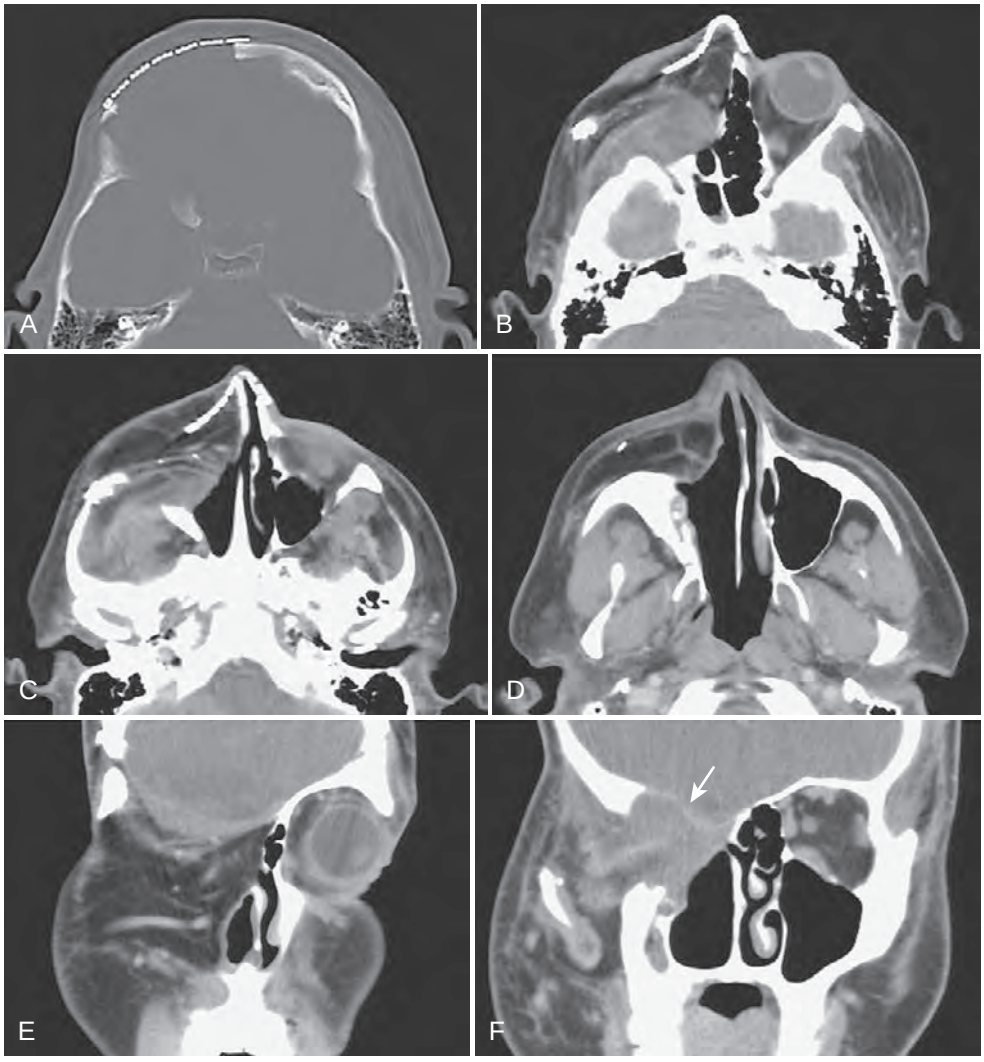

FIGURE 6-83 Serial axial CT scans from cranial (**A**) to caudal (**D**) and coronal CT scans from anterior (**E**) to posterior (**F**) of a patient who has had a craniofacial procedure, with a myocutaneous graft replacing the right orbit and face. Metal plates have been used to form a nasal contour. Although soft-tissue attenuation is seen near the cranial margin of the craniofacial graft, the intracranial margin (*arrow*) is smooth, as is the sinonasal margin. No recurrence is present.

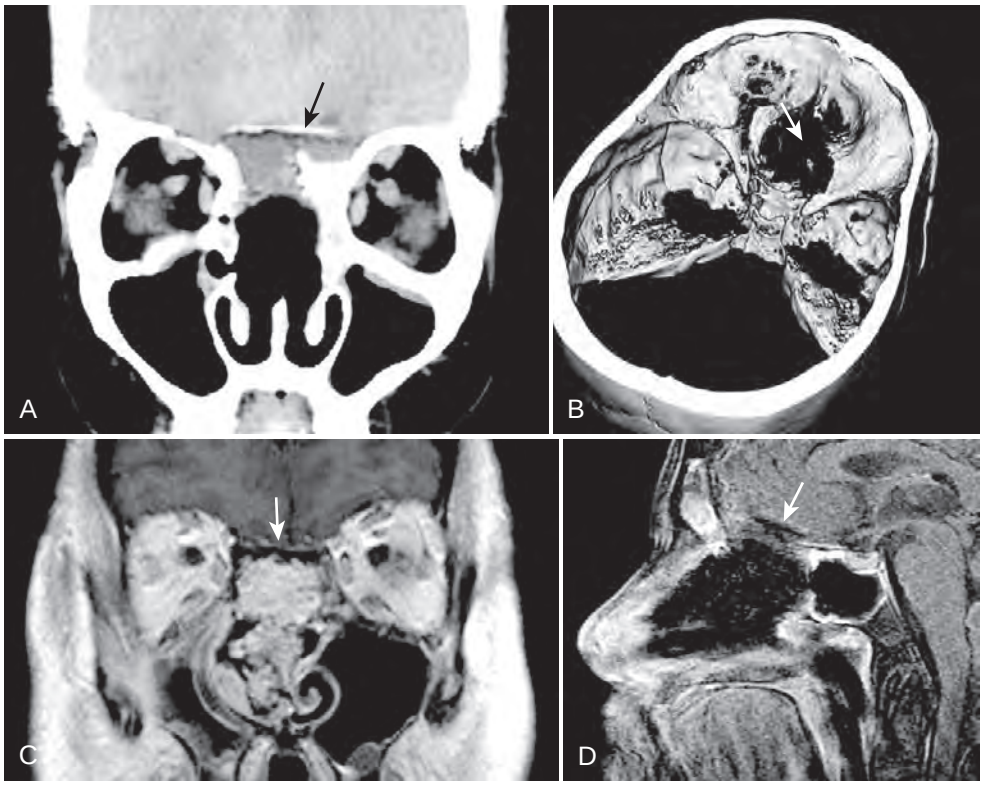

FIGURE 6-84 Coronal CT scan (**A**) of a patient who has had a recent endoscopic craniofacial resection. Mesh (*arrow*) has been placed in the surgical defect and a graft has been placed in the roof of the nasal cavity. The surgical defect, in general, is smaller than that seen with a conventional external craniofacial procedure. A 3D bone reconstruction (**B**) seen from above of a patient who has had an endoscopic craniofacial resection. Note the relatively small surgical defect in the floor of the anterior cranial fossa (*arrow*) and that unlike the external approach, the posterior wall of the frontal sinus remains intact and there is no craniotomy. Coronal T1-weighted MR image (**C**) of a patient who had an endoscopic craniofacial resection shows the mesh (*arrow*) in place with limited surgical defects. A flap has also been placed in the nasal cavity. Sagittal T1-weighted MR image (**D**) on another patient who had an endoscopic craniofacial resection shows the mesh (*arrow*) in place with limited surgical defects.

two procedures is that the polyglycolic acid mesh can be seen on CT as a slightly radiodense mesh along the uniformly thin flap. On MR imaging, this mesh has low signal intensity on all sequences. Although initially, there may be some edema and air in the subfrontal region, this subsides within weeks. The persistent dural enhancement and edema in the frontal lobes seen in the "open" procedure are not seen in the "closed" operation. Again, normally there should be no focal mass either along the intracranial or sinonasal margins of the operative bed.

As the endoscopic approach to craniofacial resection is growing in acceptance, one should be familiar with its imaging appearance so that on imaging the type of surgery is not underestimated and the approach can be confidently differentiated from the "open" procedure (Fig. 6-84).

Although technically large graft replacements of the facial area can be performed, the cure rate of such major surgery is often disappointing. Tumor recurrences can occur either deep within the graft or adjacent to the surgical bed (Figs. 6-85 and 6-86).

NONSURGICAL TREATMENT OF EPISTAXIS

For minor cases of epistaxis, focal cautery with silver nitrate solution is usually sufficient to stop the bleeding. In more severe cases, nasal packing may be used and this can be either an anterior or posterior packing or both (the use of a Foley-type balloon for the posterior packing is effective in most cases; Fig. 6-87). If these approaches are still insufficient to stop the bleeding, either catheter placement of coils in the internal maxillary artery (Fig. 6-88) (and/or other source vessels) can be performed or the internal maxillary artery can be ligated through a Caldwell-Luc approach, then going through the posterior antral wall and using a vascular staple to ligate this vessel (Fig. 6-89).

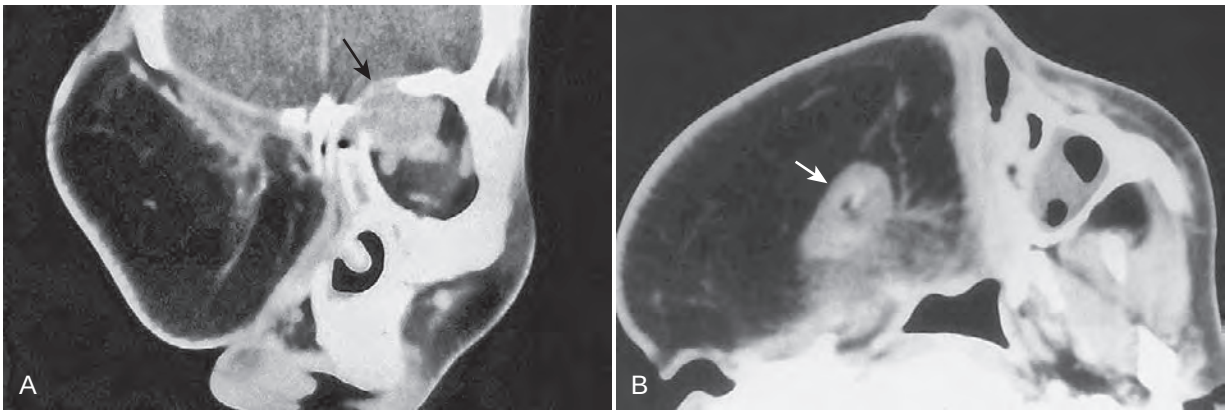

FIGURE 6-85 Coronal (**A**) and axial (**B**) CT scans of a patient who has had multiple recurrences of a rhabdomyosarcoma after chemotherapy, irradiation, and numerous operations. Finally, a large myocutaneous graft was used to replace her entire right facial region. The bulk of this graft makes clinical detection of a recurrence within it extremely difficult. Imaging shows the muscle (*arrow* in **B**) within the graft and no evidence of tumor recurrence, However, tumor has now recurred on the left side of the craniofacial graft and in the upper left orbit (*arrow* in **A**).

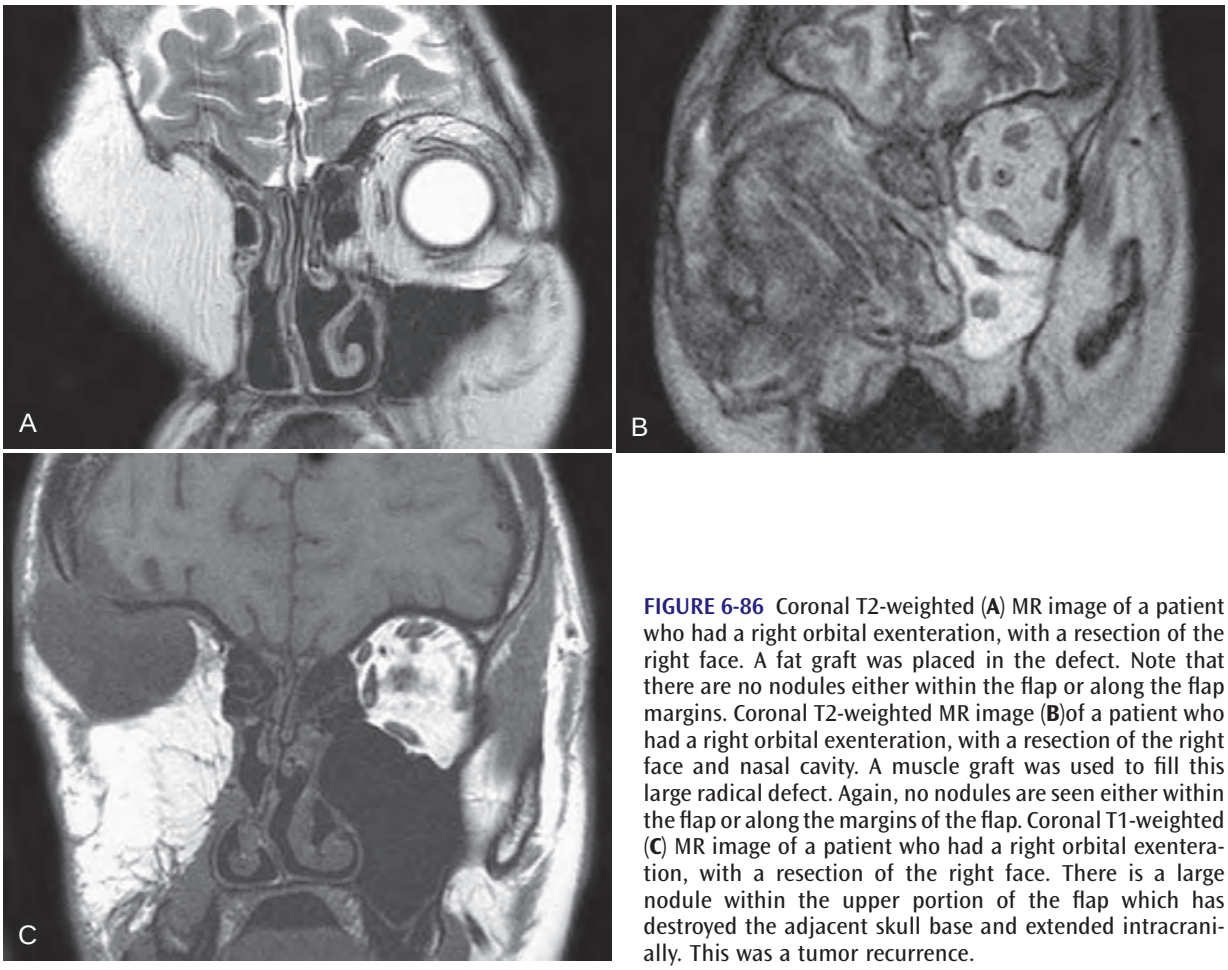

FIGURE 6-86 Coronal T2-weighted (**A**) MR image of a patient who had a right orbital exenteration, with a resection of the right face. A fat graft was placed in the defect. Note that there are no nodules either within the flap or along the flap margins. Coronal T2-weighted MR image (**B**)of a patient who had a right orbital exenteration, with a resection of the right face and nasal cavity. A muscle graft was used to fill this large radical defect. Again, no nodules are seen either within the flap or along the margins of the flap. Coronal T1-weighted (**C**) MR image of a patient who had a right orbital exenteration, with a resection of the right face. There is a large nodule within the upper portion of the flap which has destroyed the adjacent skull base and extended intracranially. This was a tumor recurrence.

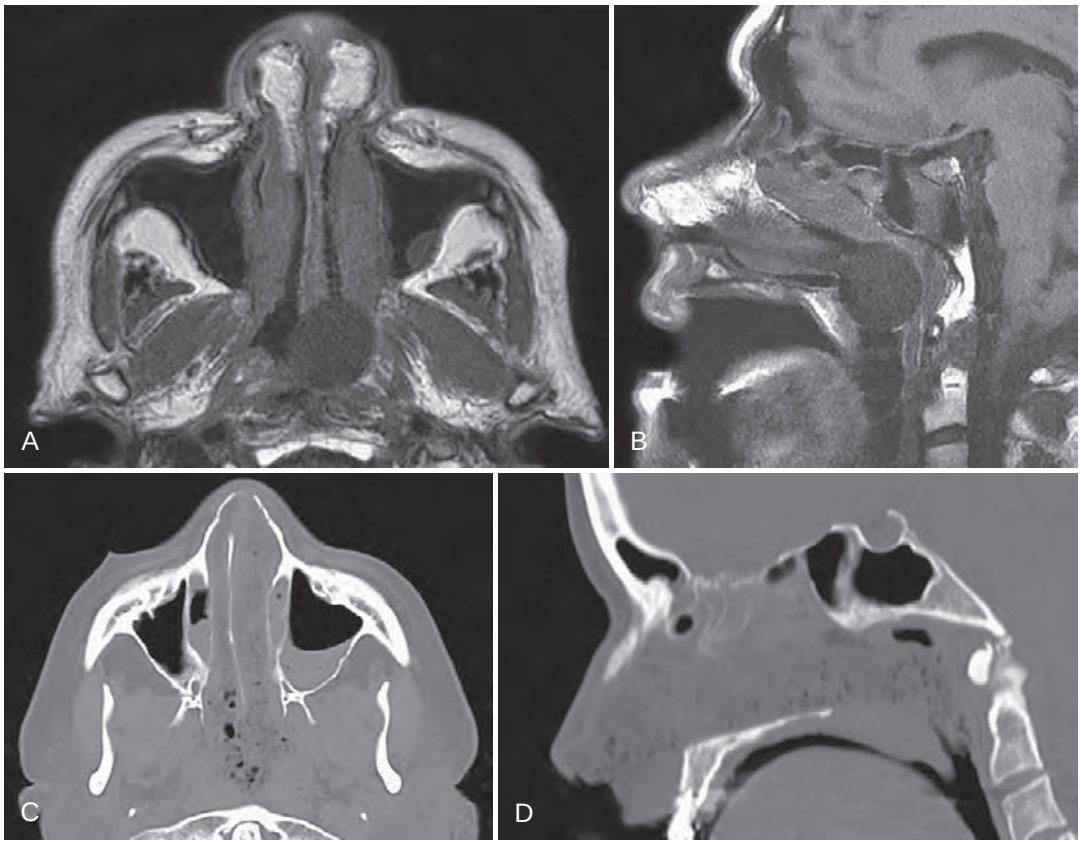

FIGURE 6-87 Axial (**A**) and sagittal (**B**) T1-weighted MR images show bilateral anterior nasal packing that has absorbed blood. There is Foley balloon in the posterior nares and nasopharynx which acts as a posterior nasal pack. Axial (**C**) and sagittal (**D**) CT scans of a patient with epistaxis show anterior and posterior nasal packings in place.

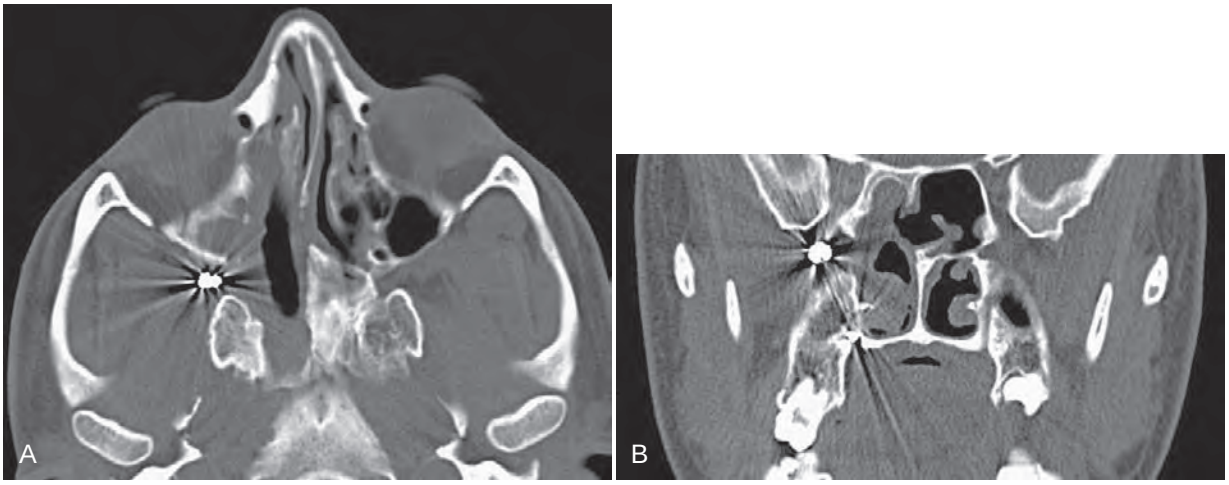

FIGURE 6-88 Axial (**A**) and coronal (**B**) non–contrast-enhanced CT scans of a patient who had a right internal ethmoidectomy and sphenoid sinusotomy for inflammatory disease. Postoperative bleeding occurred which could not be controlled by packing. A coil was then placed in the right internal maxillary artery. The coil is larger and causes a greater artefact than a vascular staple (see Fig. 6-89).

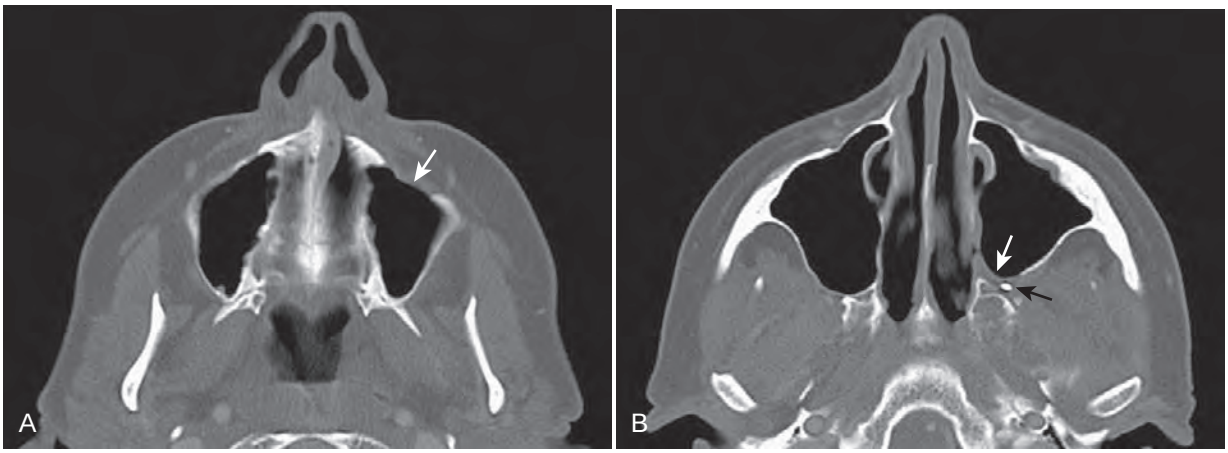

FIGURE 6-89 Axial CT scan through the lower maxilla (**A**) and the upper maxilla (**B**) of a patient with intractable epistaxis. A Caldwell-Luc procedure was performed (*arrow* in **A**) and the upper, medial antral wall was removed (*white arrow* in **B**). The internal maxillary artery was then exposed and a vascular staple (*black arrow*) was placed on it to occlude the vessel.

REFERENCES

1. Som PM, Lawson W, Biller HF, et al. Ethmoid sinus disease: CT evaluation in 400 cases. Part II. Postoperative findings. Radiology 1986;159:599-604.
2. Som PM, Lawson W, Biller HF, et al. Ethmoid sinus disease: CT evaluation in 400 cases. Part III. Craniofacial resection. Radiology 1986;159:605-609.
3. Som PM, Urken ML, Biller H, et al. Imaging the postoperative neck. Radiology 1993;187:593-603.
4. Som PM , Shapiro MD, Biller HF, et al. Sinonasal tumors and inflammatory tissues: differentiation with MR imaging. Radiology 1988;167:803-808.
5. Naumann HH, Buckingham RA. Head and Neck Surgery: Indications, Techniques, Pitfalls, vol. 1. Philadelphia: WB Saunders; 1980.
6. Lore JM, Medina JE. The sinuses and maxilla. In: Lore JM, Medina JE, editors. An Atlas of Head and Neck Surgery. 4th ed. Philadelphia: Elsevier Saunders; 2005. p. 214-266.
7. Ballantyne JC, Harrison DFN. Operative Surgery: Nose and Throat. London, UK: Butterworth Publishers; 1986.
8. Hellmich S. Surgical treatment of sinusitis. Acta Otorhinolaryngol Belg 1983;37:624-634.
9. Hwang PH, Han JK, Bilstrom EJ, et al. Surgical revision of the failed obliterated frontal sinus. Am J Rhinol 2005;19:425-429.
10. Urken ML , Som PM, Lawson W, et al. The abnormally large frontal sinus. Part I: a practical method for its determination based upon an analysis of 100 normal patients. Laryngoscope 1987;97:602-605.
11. Loevner LA, Yousem DM, Lanza DC, et al. MR evaluation of frontal sinus osteoplastic flaps with autogenous fat grafts. AJNR Am J Neuroradiol 1995;16:1721-1726.
12. Som PM, Shugar JMA. The CT classification of ethmoid mucoceles. J Comput Assist Tomogr 1980;4:199-203.
13. Unger JM, Dennison BF, Duncavage JA, et al. The radiological appearance of the post-Caldwell-Luc maxillary sinus. Clin Radiol 1986;37:77-81.
14. Goldberg RA, Weinberg DA, Shorr N, et al. Maximal, three-wall, orbital decompression through a coronal approach. Ophthalmic Surg Lasers 1997;28:832-843.
15. Graham SM, Brown CL, Carter KD, et al. Medial and lateral orbital wall surgery for balanced decompression in thyroid eye disease. Laryngoscope 2003;113:1206-1209.
16. Johnson DM, Hopkins RJ, Hanafee WN. The unprotected parasphenoidal carotid artery studied by high resolution computed tomography. Radiology 1985;155:137-141.
17. Pedersen RA, Troost BT, Schramm VL. Carotid-cavernous sinus fistula after external ethmoid-sphenoid surgery. Arch Otolaryngol 1981;107:307-309.
18. Yanagisawa E, Smith HW. Normal radiographic anatomy of the paranasal sinuses. Otolaryngol Clin North Am 1973;6:429-457.
19. Baredes S, Cho HT, Som ML. Total maxillectomy. In: Blitzer A, Lawson W, Friedman WH, editors. Surgery of the Paranasal Sinuses. Philadelphia: WB Saunders; 1985.
20. Som PM, Shugar JMA, Biller HF. The early detection of antral malignancy in the post-maxillectomy patient. Radiology 1982;143:509-512.
21. Yuen AP, Fung CF, Hung KN. Endoscopic cranionasal resection of anterior skull base tumor. Am J Otolaryngol 1997;18:431-433.
22. Lund VJ, Howard DJ, Lloyd GAS. CT evaluation of paranasal sinus tumors for craniofacial resection. Br J Radiol 1983;56:439-446.
23. Nuss DW, Janecka IP. Surgery of the anterior and middle cranial base. In: Cummings CW, Fredrickson JM, Harker LA, et al, editors. Otolaryngology-Head and Neck Surgery, vol. 4. St. Louis: Mosby; 1993.
24. Casiano RR, Numa WA, Falquez AM. Endoscopic resection of esthesioneuroblastoma. Am J Rhinol 2001;15:271-279.